ADDIS ABABA UNIVERSITY

COLEGE OF NATURAL SCIENCES

SCHOOL OF EARTH AND PLANETARY SCIENCES

DEPARTMENT OF EARTH SCIENCES

Geochemistry of lower sandstone in Blue Nile Gorge Mesozoic sedimentary sequences: Implication for provenance composition and paleoclimate

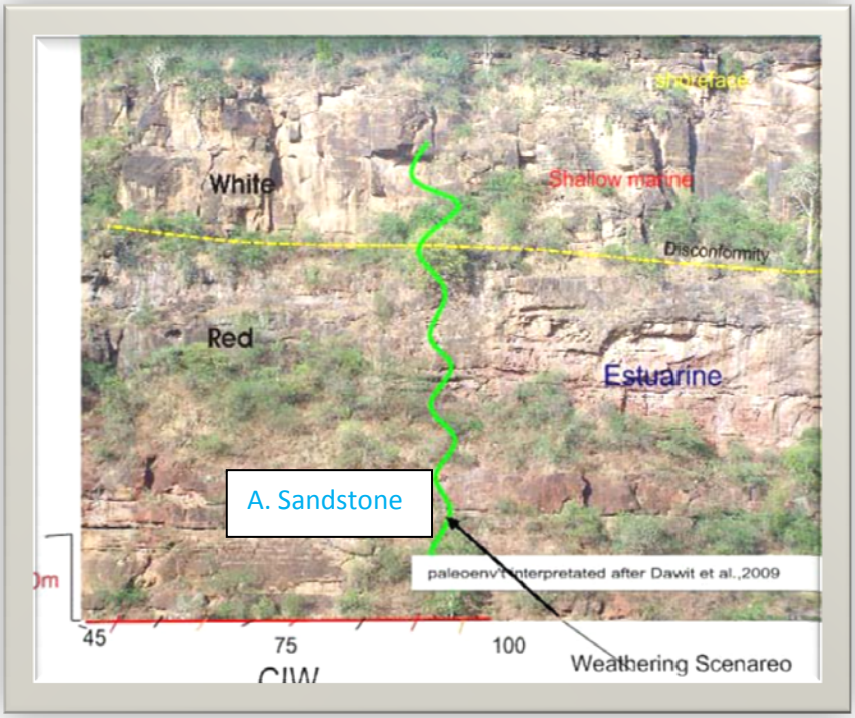

A Thesis Submitted to School of Graduate Studies in Partial Fulfillment of the Requirements for the Degree of Masters of Sciences in geochemistry

By: Barsisa Bekele

June 2011

ADDIS ABABA UNIVERSITY

COLEGE OF NATURAL SCIENCES

SCHOOL OF EARTH AND PLANETARY SCIENCES

Department of earth sciences

Geochemistry of lower sandstone in Blue Nile Gorge Mesozoic sedimentary sequences: Implication for provenance composition and paleoclimate

Barsisa Bekele

Approval by board of examiners

Dr. Tigistu Hayile _____ (Chairman)

Dr. Dereje Ayalew _____ (Advisor)

Dr. Balemwal Atnafu _____ (Advisor)

Dr. Mohammed Umer _____ (Examiner)

Dr. Gilamikael Kidaneariyam_____ (Examiner)

Date_____

Declaration

This thesis is my original work and has not been presented for a degree in any other University, and that all sources of material used for the thesis have been dully acknowledged.

Barsisa Bekele

_____

Approved by : Dr. Dereje Ayalew (Advisor)

_____

Dr. Balemwal Atnafu (Advisor)

_____

Date: 01/07/2011

ABSTRACT

Mineralogy, major, traces, and rare earth elements geochemistry of Adigrat Sandstones Formation from the Blue Nile Basin (BNB), NW Ethiopian plateau have been analyzed to determine their provenance composition, paleoweathering and paleoclimaice scenarios. Samples of this sandstone are slightly variable in composition. Mineralogically the framework grains are quartz (Q), feldspar (F) and lithic fragments (L) and on QFL diagram; most o the samples are plotted in subarkose and lithic subarkose fields. Geochemically, Adigrat sandstones are classified as arkose, subarkose, litharenite, and sublitharenite. The CIA, PIA and CIW values for this sandstone and the A–CN–K diagram agreeably suggest that source rocks experienced intense chemical weathering under hot and humid tropical to sub-tropical climate. Mineralogical evidence suggests that plutonic and metamorphic rocks were major contributing source rocks. Perhaps, multi-cyclic processes reworked the sediment. Relatively immobile elements have been selected for provenance studies. Ratios and plots of relatively immobile elements consistently suggest that the Adigrat Sandstone is derived from compositionally mixed source between mafic and intermediate igneous rocks. Discriminant function diagram constructed from major oxides, the Chondrite normalized REE plot, Cr/V vs. Y/Ni ratios, La vs. Th plot and Th-Hf-Co ternary diagram all suggest that the Adigrat Sandstone is derived from compositionally mixed source. Significant contributions of intermediate supply are also confirmed by Al_2O_3/TiO_2 *ratios and lower* ***Eu/Eu* (0.****552) values than that of PAAS (0.65). Provenance composition and degree of sorting between Adigrat Sandstone in BNB vs. Mekele Basin (MB) have been compared. The result shows that sediment of the former were highly sorted and compositionally derived from mafic and intermediate input, where as that of the later was mainly derived from felsic rocks.*

Keywords*: Adigrat sandstones, provenance, paleoweathering, paleoclimate and Discriminant function diagram*

ACKNOWLEDGEMENTS

Foremost, I thank the Almighty **GOD** by the name of **Jesus Christ** for his mercy and grace upon me during my works and in all my life.

Very special thanks to my supervisor **Dr. Daraje Ayalew**, for giving me priceless guidance, facilitation and for his friendly approach throughout my research. I am also indebted to my co-supervisor, **Dr. Balemwal Atnafu** for his support, encouragement, and valuable comments in my thesis. I have greatly benefited from their encouragement to develop independent thinking and to critically evaluate conventional wisdom on the geochemistry and geology of the study theme respectively. Their thorough work on the thesis is most gratefully acknowledged. I am grateful to have had them as my teachers. I will rely upon these traits in my future geochemistry studies.

My heartfelt gratitude goes to **Dr. Gilamichael Kidanemariam**, Ministry of Mines, for his generous advice and field support, posting his luxurious time.

My special thanks extend to **Dr. Raphael Pik, CRPG** Nancy, France. All chemical laboratories are virtually covered and performed by him and his organization and hence by no means his support has been second to none. Without him, this work would not have been realized.

I would like to thank to **Dr. Dawit Enkurie** and **Adise Mokonnen** because of their significant and helpful contribution.

I would also like to articulate my appreciation to all academic staff of Earth Science Department, **AAU** for they candidly shared innumerable and valuable knowledge.

Finally, I would like to thank my MSc colleagues and families for immeasurable reasons.

CONTENTS

LIST OF FIGURES

LIST OF TABLES

1. Introduction

1.1. Preface

Clastic sedimentary rocks are rock materials by which can decipher a lot about the past geologic processes. These rock types mainly comprise conglomerates, sandstones and Mudrock. Sandstones are useful as economic resources: abrasives; raw materials in the chemical, glass, and metallurgical industries; construction materials, both building stone and as ingredient of plaster and concrete, molding sand, paper filler, and so forth. Sandstones are one of the important known reservoir rocks for natural gas, oil, and artesian water. Some placer sands are a source of ore materials and gems. Sandstones have immense potential, probably more than any other sediment in contributing to our understanding of geological history. Their composition is a clue to the provenance and paleoclimate, their directional structures are clue to the paleocurrent direction and their geometry as well as internal structures is a guideline for understanding of depositional environments. Despite this and countless importance of sedimentary rocks, the study of geochemistry of sedimentary rocks in the country is yet at its incipient position as compared to other rocks. These facts have made Adigrat Sandstone the target rock types of this research for understanding the paleoweathering profile, the paleoclimate and the source rocks.

Clastic rocks are not precipitated from a solution; rather they are deposited from a transporting agent with a sediment load. The sediment in turn is the result of physical, chemical or physicochemical, biological or biochemical processes acting on preexisting rocks. For a chemical, physical or biological processes to take place there must be some driving force behind. Changes in natural condition should play an important role in determining the mentioned driving force. The changing natural condition may be the change in temperature, pressure or composition. Therefore, the preexisting rocks may encounter one or more of these variables.

The preexisting rocks have its own P-T-X (pressure-Temperature-concentration) assemblage in which the constituting minerals are under stable or matastable condition. This assemblage is

kwon as equilibrium assemblage. The change in P-T-X, therefore result in disequilibrium condition. Consequently, minerals need to tolerate that new condition by doing their internal structural rearrangement. Not all minerals are expected to being weather at a given P-T-X condition, for they are formed at different conditions. Rather they follow the Goldfinch's series, which is roughly the inverse of Bowen's reaction series. The latter predicts order in which minerals will crystallize from a cooling silicate melt.

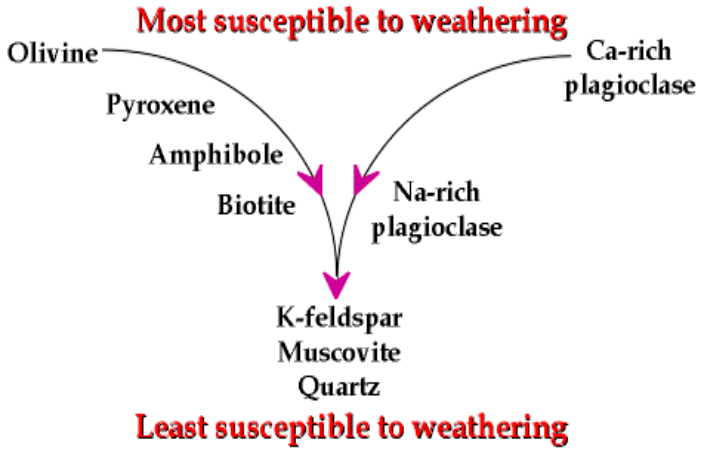

The above-mentioned processes in particular form clastic sedimentary rocks. Therefore, their mineralogical and/or chemical composition must mimic the prevailing condition.

1.2. Previous work

The pioneering works on the sedimentary succession within the Blue Nile Basin include that of Aubry (1886), Dainelli (1943), Mohr (1963) and Beauchamp (1977). Later works on the Mesozoic succession of the basin include that of Getaneh Assefa (1980, 1981, 1991); Russo et al. (1994), Wolela (1997), Dawit & Bussert (2009). An excellent recent study, which focused on the paleoenviroment and facies architecture of the Adigrat Sandstone in the Blue Nile Basin, is that of Dawit & Bussert (2009). These workers interpreted this sandstone unit as being a result of a marine transgression (estuarine infilling, followed by the landward migration of a coastal barrier-strand plain complex) that came from the southeast. This is an interpretation consistent with that of Danielli (1943). Although numerous research has been done in the Blue Nile Basin, the source

composition for these rocks and the climatic conditions that triggered the weathering of these source rocks have not yet been elucidated.

1.2.1. Study site description

Location, climate, and topography

The study area is located in the Blue Nile River Basin, which is located in the Northwestern Ethiopian highlands and is about 210km from Addis Ababa (fig 1.1). The climate of the study area varies from humid to semiarid. Most precipitation occurs in the wet Karemt season (June through September) when the ITCZ moves north, and the southwest airstream extends over the entire Ethiopian highlands. Annual rainfall varies between 1000 mm, in the lowland to 2000 mm, in the highland (Daniel, 1977; Conway, 1997; UNESCO, 2004; etc). The Atlantic Ocean is the main source of rainfall in summer i.e. June, July, August and September (Daniel, 1977; Conway, 1997; UNESCO, 2004; Seifu *et al*., 2005). The eastern mountainous region of the basin receives rainfall originating from the Indian Ocean in April and March (e.g. Seifu Kebede et al., 2005). Spatial variation in rainfall amount is controlled by topography.

The mean annual temperature from 1961 to 1990 was estimated to be 18.3 °C with a seasonal variation of less than 2°C. The annual potential evapotranspiration was found to be about 1100 mm (Kim et al., 2008).

More than 80% of annual flow in the Blue Nile results from the summer monsoon and is concentrated between July and October (Soleiman et al., 2009). This runoff flows directly to downstream countries due to the absence of storage capacity in Ethiopia. The basin has an elevation ranging from 500 m in the western lowland to over 4000 m in the east and northeast.

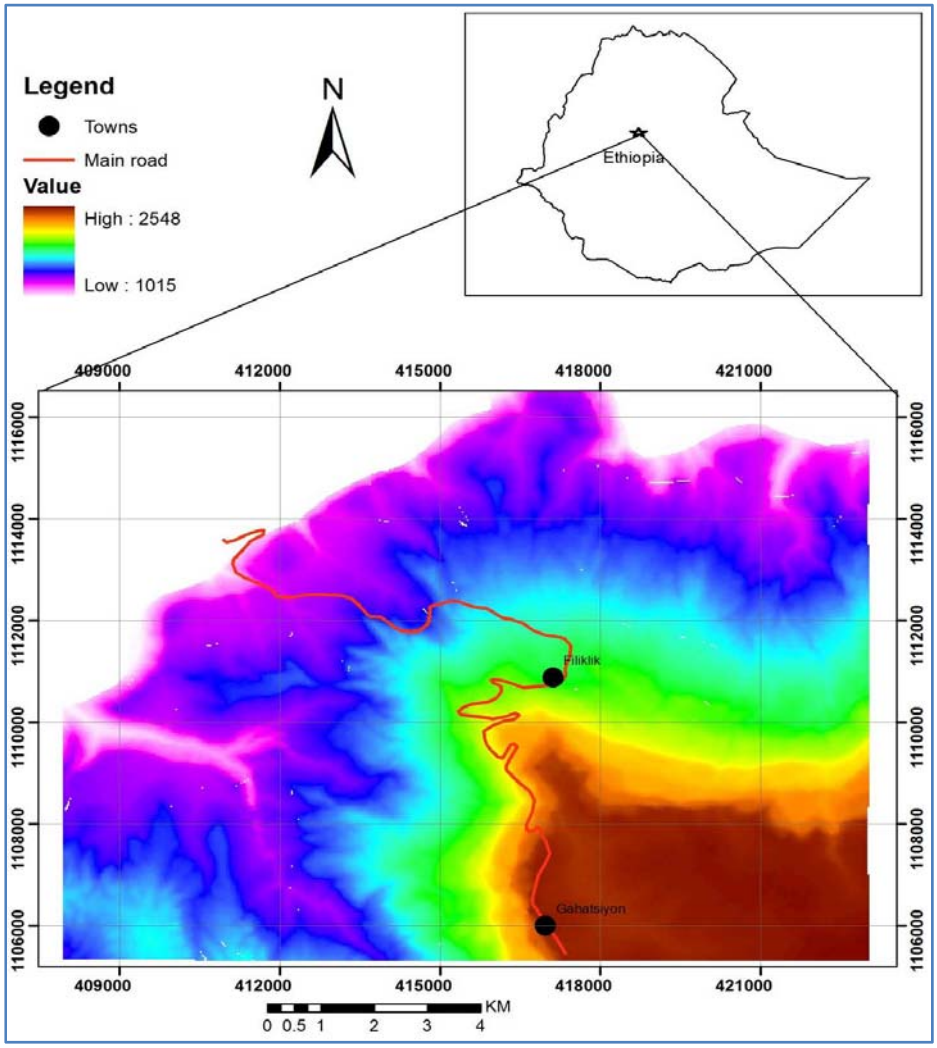

Figure 1. 1 Location map of the study area.

1.2.2. Age

The age of the Adigrat Sandstone unit has been inferred from two lines of evidence. Palynological* data from fosilifereous sediments within the Adigrat Sandstone Formation of the

* **palynology is** also called pollen dating. The unit of the calendar is the pollen zone. A pollen zone is a period of time in which a particular species is much more abundant than any other species of the time. Pollen zones are translated into absolute dates by the use of radiocarbon dating. In addition, pollen dating provides relative dates beyond the limits of radiocarbon (40,000 years), and can be used in some places where radiocarbon dates are unobtainable.

Blue Nile Basin indicate an age range of Middle Triassic–Early Jurassic (Wolela, 1997); an Early Jurassic to Middle Jurassic age in the Mekele Basin (Dawit, 2009) and a Late-Triassic to Early-Jurassic age in the Ogaden Basin (Worku, 1987).

The Apatite Fission track Analysis (AFTA) is another method that has been applied on the sediments of the Blue Nile Basin. Based on AFTA the age of the Adigrat Sandstone in the Blue Nile Basin is in the range of 237-197 Ma years (Wolela, 1997), which is equivalent to Anisian to Pliensbachian age (table 1.1).

Table 1.1: Age and depositional environment of Adigrat Sandstone unit

Period	Age[1]	Lithostratigraphy	Mineralogical composition	Depositional environment[2]
Early Jurassic	Pliensbachian	Upper (White) Adigrat unit	-High porosity, Quartz-Arenite, calcite and quartz cement.	Barrier/inlet and wave-dominated shore face
Middle Triassic	Anisian	Lower(Reddish) Adigrat unit	-Subarkose to Lithic subarkose calcite/hematite/clay cemented -intercalated paleosol	Estuarine and storm - dominated shore face

1.2.3. Environment of deposition

In view of depositional environment, there are two contradicting ideas. Based on minerals, texture and sedimentary structures Wolela (1997) has concluded that the depositional environment of the Adigrat Sandstone is dominated by a mixture of alluvial fan, meandering river, and lacustrine deposits. However, Dawit (2010) has found additional tidal sedimentary structures (e.g. herringbone, mud-drapes on foresets, flaser bedding, etc); hummoky cross-stratification which indicates storm influence; as well as trace fossils (e.g. *Thalassinoids*, *Rosselia*, *Paleophycus*, etc) that does not show the above depositional environment. As a result, he concluded that the environment of deposition of the Upper (White) and the Lower (red)

[1] Wolela, 1997

[2] Dawit, 2009

Adigrat Sandstone are barrier lagoon to wave dominated shoreface and estuarine to storm dominated shoreface respectively.

1.3. Present works

Having previously outlined the importance of sandstones in their contribution to the understanding of geological history in general and paleoclimate and source rock identification in particular, the present study is concerned with these aspects from the study of the Adigrat Sandstone Unit in the Blue Nile Basin (Ethiopia), which is exposed along the Dejen - Gohatsion road (Fig. 1).

1.3.1. Objective

1.3.2. Main objectives

The main objective of this research is to assess the provenance composition of the Adigrat Sandstone and the paleoclimatic scenario from Middle Triassic to Early Jurassic period.

1.3.2.1. Specific objectives

- To identify the intensity of chemical weathering that the source rocks of the Adigrat Sandstone had experienced.
- To investigate the trend in climate change from Middle Triassic to Early Jurassic time in the area.
- To justify the cause for the difference in color of the upper and lower part of the Adigrat Sandstone unit in the study area.
- To chemically and mineralogically classify these sandstone, which in turn would help in further investigation and inferences of sedimentary processes.
- To geochemically correlate the Adigrat Sandstone in the Blue Nile Basin with equivalent Sandstone in the Mekele Basin

1.3.3. Research question

The Middle Triassic-Early Jurassic weathering profile and its related paleoclimate during the deposition of the Lower Sandstone unit (Adigrat Sandstone unit) of the Blue Nile Mesozoic sedimentary sequence has not been yet fully verified. For this reason, the regional climatic fluctuation from the Triassic to Early Jurassic period has not been precisely calibrated on a large scale (temporal/spatial) because of the absence of other full paleoclimate markers such as fossil remnants. This is in contrast to the relatively adequate calibration of paleoclimate for the Quaternary sediments of Ethiopia, which have been investigated by numerous researchers.

Furthermore, field studies show that the Adigrat Sandstone Formation in the Blue Nile Gorge is characterized by two distinctly colored intervals, the lower red color and the upper white color, with an unconformity between them (Dawit & Bussert, 2010). This physical distinction may either be the result of differences in climate during weathering and deposition or an effect of post depositional alteration/diagenesis. The cause of this clear difference in color is still open to interpretation.

In addition to the above questions, the source composition, from which the sediments of the Adigrat Sandstone unit in the Blue Nile Mesozoic sedimentary sequence were derived, has not yet been geochemically studied.

1.3.4. Methodology

This research has been conducted using whole rock geochemistry, mineralogy and petrographic analysis. Field investigation of outcrops of the Unit, which included detailed descriptions of sampled horizons, preceded the petrographic and analytical stages. These steps have been deemed essential for the objectives outlined previously. Fresh representative rock samples were collected and stored in plastic bags. Thin sections of 13 rock samples were made for petrographic analysis (Appendix). The rock samples were trimmed into rectangular blocks and one side polished so that a smooth, flat surface was obtained for adherence to glass specimen plates. After the samples were glued to the glass specimen plates, the sample blocks were then trimmed and polished again, until an even surface (~0.3mm thickness) was obtained allowing maximum light distribution through the specimen plates. Petrographic study of these thin sections was then undertaken. Thin-section point counting model was used for quantitative compositional analysis.

The modal analysis was performed by counting more than 300 points per thin section, using the Gazzi–Dickinson point-counting method (Dickinson, 1970).

Part of representative rocks samples (12 samples) is prepared for geochemical purpose. The Samples were crushed and grinded, and reduced to a mass of 250 g by coning and quartering. The samples were then dried at 60°C for 12 hours. Aliquots of 20–30 g of each dried sample were powdered in an agate mill at Central Geological Laboratory of the Geological Survey of Ethiopia (G.S.E) and partly at Department of Earth Sciences, Addis Ababa University. Powdered rock samples were shipped to France for whole rock geochemical analysis. Samples were prepared for chemical analysis using standard method. Then the samples were analyzed for major oxides by ICP-AES (Inductively Coupled Plasma Atomic Emission Spectrometry) and trace elements including REE elements by ICP-MS (Inductively Coupled Plasma mass Spectrometer) at **CRPG** (Centre des recherches geochimique et petrologique) in Nancy, France. The analytical procedure for the ICP-MS analysis is fully described by Qi *et al*., (2000). The precision and accuracy of the analyzed data are within the permissible limits. After mineralogical and geochemical analysis, the A-CN-K diagram, the CIA, PIA, and CIW and elemental ratios were calculated to quantitatively measure the degree of weathering. From the degree of weathering, the paleoclimatic scenario during the sedimentation of the Adigrat Sandstone has been interpreted. Similarly, the pattern of REE, major and minor element abundance and/or their ratios coupled with petrographic data have been used for the interpretation of the provenance.

The relative mobility of certain oxides has helped many researchers in developing some paleoweathering and paleoclimate proxies such as the CIA (Chemical Index of Alteration), PIA (Plagioclase Index of Alteration), CIW (Chemical Index of Weathering), A-CN-K ternary diagram and elemental ratios. In addition to this, the pattern in REE could give some clue to the weathering intensity. These paleoclimate proxies have been adopted for this study.

1.3.5. Limitation of the study

Ideal geochemical works with such objectives would inevitably involve undertaking laboratory analysis, to determine elemental concentration of field samples; and conducting experiments in the lab for small scale visualization and simulation of the geological processes that took place at a much larger scale (both temporal and spatial).

Immense limitations occur in this sense because of the absence of a standard geochemical laboratory at the Department of Earth Sciences, Addis Ababa University, where this research undertaking is based. This has meant that the exposure to the real practical environment has been very limited.

Attempts have been made to use the Central Geological Laboratory, Geological Survey of Ethiopia to counter these limitations to some extent. The major laboratory work (geochemical analysis) was done at CRPG (Centre des recherches geochimique et petrologique) in Nancy, France, with the help and coordination of Dr. Dereje Ayalew(Advisor). Seeking solutions for the major limitation described above has taken much time that time limitations for the thesis work in general have been a consequence.

1.3.6. Thesis outline

This thesis contains six chapters, which are organized as follows. After a general introduction where the relevant works, methodology, objectives and research questions are presented, the geological setting of the study area is described. A review of literature related to the studied area is then presented separately. Discussions on investigation of source rocks and paleoclimatic scenario for the Adigrat Sandstone, with data analysis are separately provided in two chapters. The results and recommendations of the research output are summarized in the final chapter.

2. Geological setting

2.1. General

The intra-plate deformation of NE Africa, the formation of a number of transtensional basins and local to regional uplifts were the result of two events that occurred in the late Permian and late Jurassic. These two events are the inception of the Gondwana rift and the formation of NeoTethyan passive margin, which introduced the fundamental plate reorganization. These events are associated with the Mesozoic break-up of Pangaea (Ziegler, 1989); which is the second stage of the dismemberment of Pangaea II.

The Mesozoic sedimentary basins in Ethiopia in general and the NW trending, fault controlled intracratonic Blue Nile Basin in particular was formed as the result of these events (Russo et al., 1994; Wolela, 1997; Dawit & Bussert, 2009). Thus, the Ogaden, Blue Nile and Mekele basins are presumed to be cratonic rift basins formed because of stress induced by the break-up of Gondwanaland, which is presumed to be extensional geodynamic tectonics. The Blue Nile Basin is part of these sedimentary basins covering an area of about 120,000 $km^{2.}$ (Wolela, 2008)

The Blue Nile Basin has evolved in three main phases (Getaneh (1981); Gani *et al*., (2008): (1) pre-sedimentation phase, include pre-rift peneplanation of the Neoproterozoic basement rocks, possibly during Paleozoic time. (2) The Triassic to Early Cretaceous sedimentation phase. (3) The post-sedimentation phase, including Early–Late Oligocene eruption of 500–2000m thick Lower volcanic rocks, related to the Afar Mantle Plume and emplacement of 300m thick Quaternary Upper volcanic rocks (Gani *et al*., 2008).

The Late Triassic- Earliest Jurassic was the time of rifting between Gondwana and Laurasia; initiation of ocean basin formations, rifts and microplates in the western Tethys region and rapid northward drift of the Cimmerian continent, by active seafloor spreading within the Neotethys Ocean (Sengör, 1984) that occurred during this time. The late Triassic (Norian super sequence) corresponds with a low first-order sea level stand and a time of high continental emergence. The Early Jurassic (Pliensbachian- Toarcian super sequence) was the time of the initiation of the first-order sea level rise in the mid-Mesozoic (Golonka, 2000, 2002). The regression of the sea from the region began in the upper Jurassic (and continued throughout this period) as the result of

arching and doming of the Arabian-Somalian massif (Getaneh, 1991; Russo et al., 1994; Wolela, 1997; Mongelli et al., 2006). The transition from icehouse to greenhouse conditions continued in this time (Frakes et al., 1992). In the early-Late Jurassic time, the carbonate sedimentation predominated along all Neotethyan margins (Dercourt et al., 1993; Fourcade et al., 1996). By the early Cretaceous, the sea completely withdrew leaving behind regressive continental clastics, mainly consisting of sandstones belonging to the Cretaceous Ambaradom Formation.

Large portion of the country (about 40 percent), Ethiopia, is covered by sedimentary rocks and comprises five distinct sedimentary basins: These are Blue Nile Basin, Ogaden Basin, Mekele Basin, Gambella Basin and Southern Rift Basin.

The Adigrat sandstone is part of Mesozoic sedimentary succession in the Blue Nile Basin. These sedimentary beds are nearly horizontal, but a general, slight southeasterly deep causes progressively older beds to disappear beneath the lavas in a westerly or downstream direction (Getaneh, 1991). The Adigrat Sandstone in this sedimentary basin is formed partly as the result of the Jurassic transgression (Coffin & Rabinowitz, 1988) and global rise in sea level (Haq et al, 1987).

The Adigrat Sandstone Formation is extensively distributed in the Blue Nile Basin, Ogaden Basin and Mekele outlier as pointed up in the correlation diagram (Table 1). It covers wide area and forms vertical cliffs with paleosoil (mudstone) intercalation at its bottom part at Gohatsion-Dejen area (e.g. Wolela, 2008, Dawit & Bussert, 2009). The formation is largely composed of continental clastics (conglomerates, gravely sandstone, mudstone, siltstone and carbonaceous materials). The geological map of the Blue Nile Basin (Gohastion to Abay River) is illustrated in Figure-1.

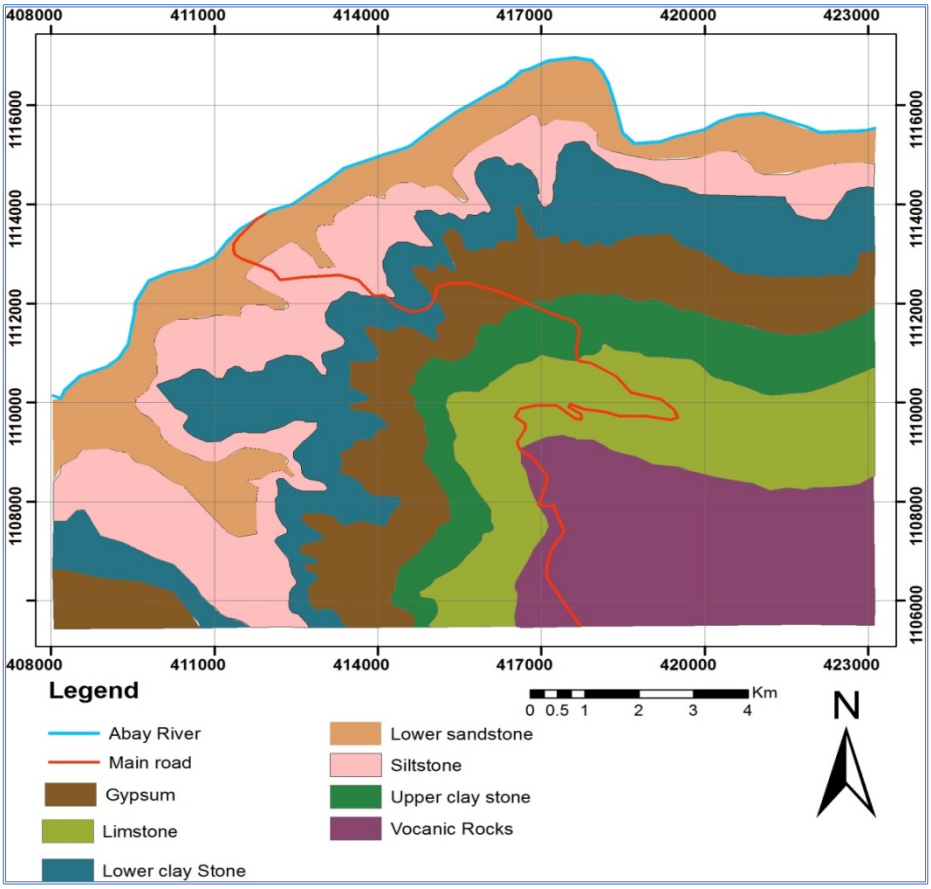

Figure 2. 1 Geological map of the Study area (Adopted from Kazmin, 1975)

At the central part of the Blue Nile Basin (Gohatsion-Dejen area), the sedimentary succession reaches a maximum thickness of 3000m (Mohr,1963; Getaneh, 1991; Russo et al, 1994; Wolela, 1997). This Mesozoic sedimentary section is overlain unconformably by Late Oligocene volcanic rocks (Hofmann et al.,1997) and in turn, underlain unconformably by the Neoproterozoic basement rocks.

Five sedimentary formations are found in the Blue Nile basin (Getaneh, 1981; Getaneh, 1991; Wolela, 1997). Accordingly, from bottom to top the sequences are as follows: lower sandstone unit, limestone unit, gypsum unit, shaly sandstone unit and upper sandstone unit. However, recent study classified the succession in to eight stratigraphic unit (Dawit and Bussert, 2009), with additional unit of pre-Adigrat I, II and III.

2.2. Lithology of the Blue Nile Basin

2.2.1. The basement

The age of the basement rocks is considered to be Neoproterozoic, ranging from 850 to 550 Ma as documented from U-Pb and Rb-Sr geochronologic studies by Ayalew et al., 1990. These rocks are made-up of variably metamorphosed quartzofeldspathic schists and gneisses, migmatites and plutonic rocks. Neoproterozoic penetrative NNE-trending sub-vertical ductile planar fabrics are associated with NNE- to NE-trending upright tight folds (Gani et al., 2008) are its' tectonic structure.

2.2.2. The pre-Adigrat I, II, III

Prior to Dawit (2009), the pre-Adigrat has been simply considered as single unit. As assumed by Kazimin (1975) the age of pre-Adigrat I is a broad interval of Carboniferous-Mesozoic age and is made up of sandstone siltstone and shales filling north-south trending channels that are carved in to basement gneiss (Mohr, 1963, Jespen & Athearn, 1964). However, Dawit classified the pre-Adigrat unit in to three distinct units. From bottom to top, they are the Pre-Adigrat I, II and III.

The Pre-Adigrat II is a 800m thick unit that unconformably overlies either the Precambrian basement or pre-Adigrat I. Lateral accretion deposit, floodplain fine and playa-lake mudstone characterizes its lower part (Dawit and Bussert, 2009).

The pre-Adigrat III reaches a thickness of 400m, and is composed of three successive cycles of stacked, multi-story sheet sandstone bodies. It is dominated by horizontal bedding and low angle cross-bedding (Dawit and Bussert, 2009).

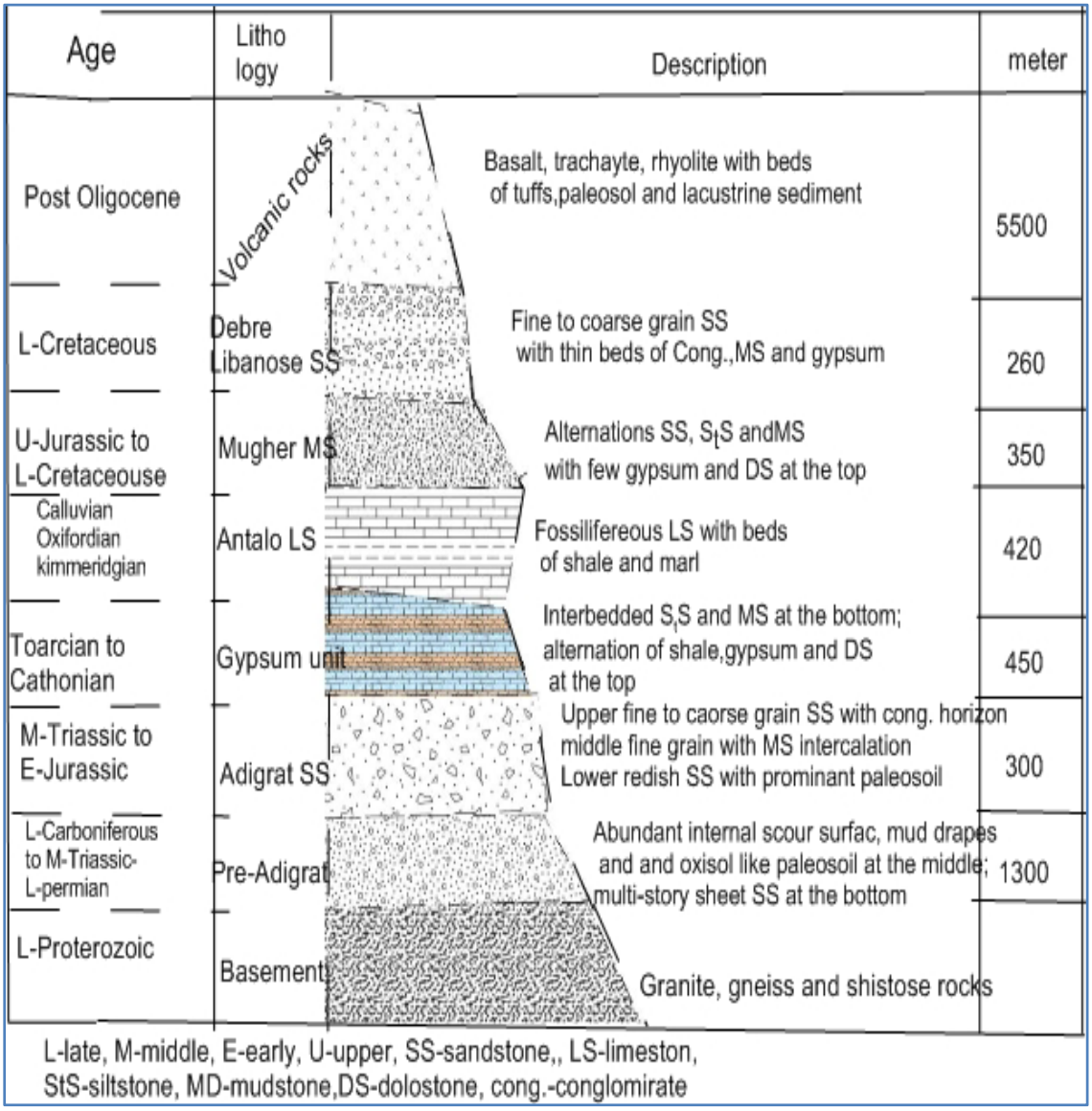

Figure 2. 2 Lithostratigraphic unit of Blue Nile Basin (after Getaneh, 1991; Russo et al.,1994; wolela, 1997; Dawit & Bussert, 2009).

2.2.3. The lower sandstone (Adigrat sandstone)

The lower sandstone (also known as adigrat sandstone) is formed because of jurassic marine transgression came from the south-east (Daniell, 1974). This unit is generally underlain either by the pre-Adigrat unit or by the basement rocks (Getaneh, 1991; Wolela 1997; Dawit and Bussert, 2009). The unit boundary with overlying shale and gypsum is transitional (Getaneh, 1991).

The Lower Sandstone (also known as Adigrat Sandstone) is the primary concern of this research, It formed as a result of Jurassic marine transgression came from the south-east (Danielli, 1943). However, some researchers consider the Adigrat Formation as purely continental siliciclastic sediment (Russo et al., 1994; Bosellini, 2001). This unit is generally underlain either by the pre-Adigrat unit or by the basement rocks (Getaneh, 1991; Wolela 1997; Dawit and Bussert, 2009). The unit boundary with overlying shale and gypsum is transitional (Getaneh, 1991). The unit mostly intercalated with layers of siltstone, mudstone, paleosoils, occasional beds of conglomerates and shales (Getaneh, 1991; Russo et al., 1994; Wolela 1997; Dawit and Bussert, 2009). Detailed lithological section of the Adigrat Sandstone unit in the Blue Nile canyon, with sample numbers and description of beds is shown in figure 2.3.

Wolela, 1997, described detailed facies analysis for this unit. Based on sedimentary structures, grain size and lithofacies association, Wolela classified Adigrat sandstone formation in the Blue Nile Basin in to six major facies (Wolela, 2008). From bottom to top, the facies are the mudstone, finely laminated siltstone, very fine-grained cross-bedded sandstone, coarse to medium-grained sandstone, massive to crudly cross- bedded sandstone and massive to crudely cross-bedded conglomerate. In broader sense however, Adigrat sandstone in the Blue Nile Basin is divided in to two facies architecture (Dawit and Bussert, 2009). These are the lower Red part and the Upper white part.

At Blue Nile canyon the unit is about 300m thick (Russo et al., 1994). Incised-valley –estuarine system and barrier-beach – strand plain systems are its two inferred depositional paleoenviroments (Dawit & Bussert, 2009). The unit is lithostratigraphic equivalent of Adigrat sandstone (Getaneh,et al., 1991). The distributions of Adigrat Sandstone at different localities are shown in Table 2.1.

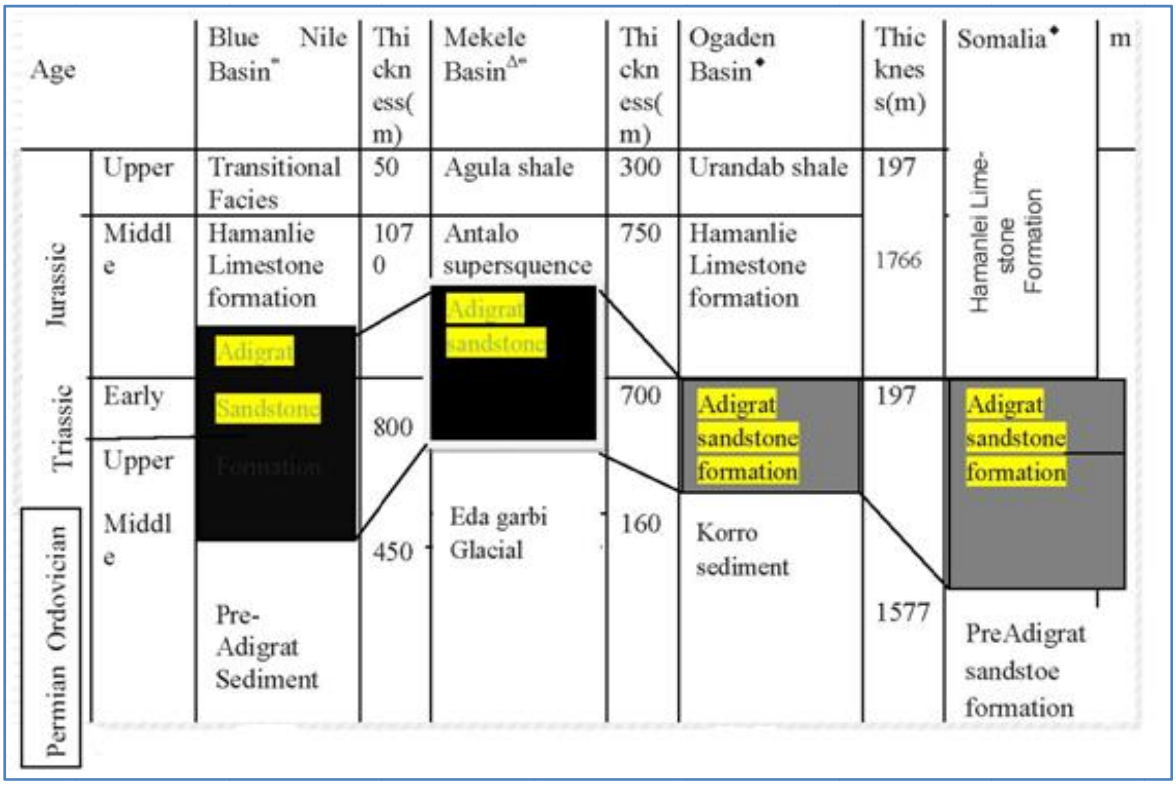

Table 2.1 correlation diagram of Adigrat sandstone found at different localities (After Wolela, 2008 and references there in))

2.2.4. Gohatsion Formation

The age of lower and upper boundary of the shale and gypsum unit is considered as Toarcian to Bathonian during which marine transgression begun in the Abay River Basin. The thickness of this unit is about 450m (Russo *et al.,* 1994). At its lower part the formation is characterized by dolostone and shale comprising of 50-80m thickness. The middle part of the formation consists of several cycles (Russo *et al*., 1991); non-fossiliferous shale, marlstone or dolostone, with few scattered small bivalves, fine grained cross-laminated sandstone, and thick beds of gypsum. The upper part of this unit contains varicolored clay and siltstone. Generally, the unit is 350m thick consisting of interbedded sandstone siltstone, mudstone and shale in the lower part, and alternation of gypsum, dolomite, limestone and shale in its upper part. The increment of deposition for the terrigenous clastics is interpreted as deltaic, and shallow lagoonal for non

terrigenous one (dolomite, gypsum, limestone and shale) the environment of deposition is interpreted as supratidal (Getaneh 1981).

2.2.5. The Limestone unit (The Antalo Limestone)

This unit conformably overlies the Gohatsion Formation and consists of the Hamanlei Formation at the bottom and the Urandab formation on top. It is approximately 600m thick and is characterized by shallow water oolitic and reefal limestone, fossiliferous carbonates interbedded with marl, shale, and mudstone. overlain by a more massive limestone bearing corals, Nerineids, and stromatoporoids and small pebbles in an ascending order (Russo, et al., 1994). The top most part of this unit (ca. 170m thick) is oolitic, massive and cliff-forming limestone. The middle upper Antalo limestone is 200m thick succession, which comprises of marly limestone, marls, and silty limestone. In its middle and lower part, marly limestone and marls dominate, however the frequency of silty limestone has increased upward. In addition recent study by Gilamichael (2010) indicates that marls and coquinoid limestones (oyster- rich) form cyclic alternations in the Blue Nile, and this sequence is overlain by cliff forming turbidites or tempestites. The latter comprise of skeletal packstones, mudstones and oolitic grainstones.

According to Russo et al., (1994), this carbonate succession formed as a result of a sea level highstand from Oxfordian-Kimmeridgian most probably bout 155Ma years ago. This unit is the product of a major transgression caused both by the formation of African continental margin and eustatic sea level rise (Hallam, 2001). Similarly Gilamichael (2010) indicated that the sequence represents upward- deepening of the sea-level of the second order that consists of a number of transgressive- regressive cycles of the third order. These cycles are results of an inter play of tectonics, global sea- level change and climate. Recent age determination done by Kurita et al., (2009) based on dinoflagellate cysts and ammonites, foraminifers, green algae and other fossils (Gilamichael, 2010) showed that carbonate deposition (excluding the Gohatsion Formation) in the Blue Nile Basin lasted from the Lower Callovian up to the Kimmeridgian.

2.2.6. The Mugher Mudstone unit

The 260m thick Mugher Mudstone unit (Getaneh, 1991) is the result of withdrawal of the sea from east African Craton during late Late Jurassic. The unit does not crop out in the Abay gorge however it is confined to the canyon of (e.g. Mugher, Zega wedam, etc) the Blue Nile Basin. This unit has two distinctive features. The lower part consists of 15m of alternating gypsum, dolomite and shales. The upper part constitutes 240m thick mudstone. This part of the Mugher mudstone unit consists of mudstone, fine to medium-grained siltstone.

2.2.7. The Debre Libanos Sandstone unit

This sandstone has variable thickness with maximum value of 280m near Lemi and lithologically it comprises of pebbly sandstone, conglomerate and claystone (Getaneh, 1991).

The AFTA method was applied to determine absolute age of Upper Sandstone formation. Accordingly, its age ranges from 120-94Ma years, which is equivalent to Barremian to Cenomanian (Wolela, 1997). This unit also does not outcrop in the Abay canyon; however, it is exposed in the Zega Wodem river and its tributaries.

The major sedimentary structures within this sandstone bodies are large scale planar-tabular and asymmetrical trough cross-beds, small scale trough and planar tabular beds, convolute beds , flat beds , scoured and channel surface , and massive beds (Getaneh,1991) .

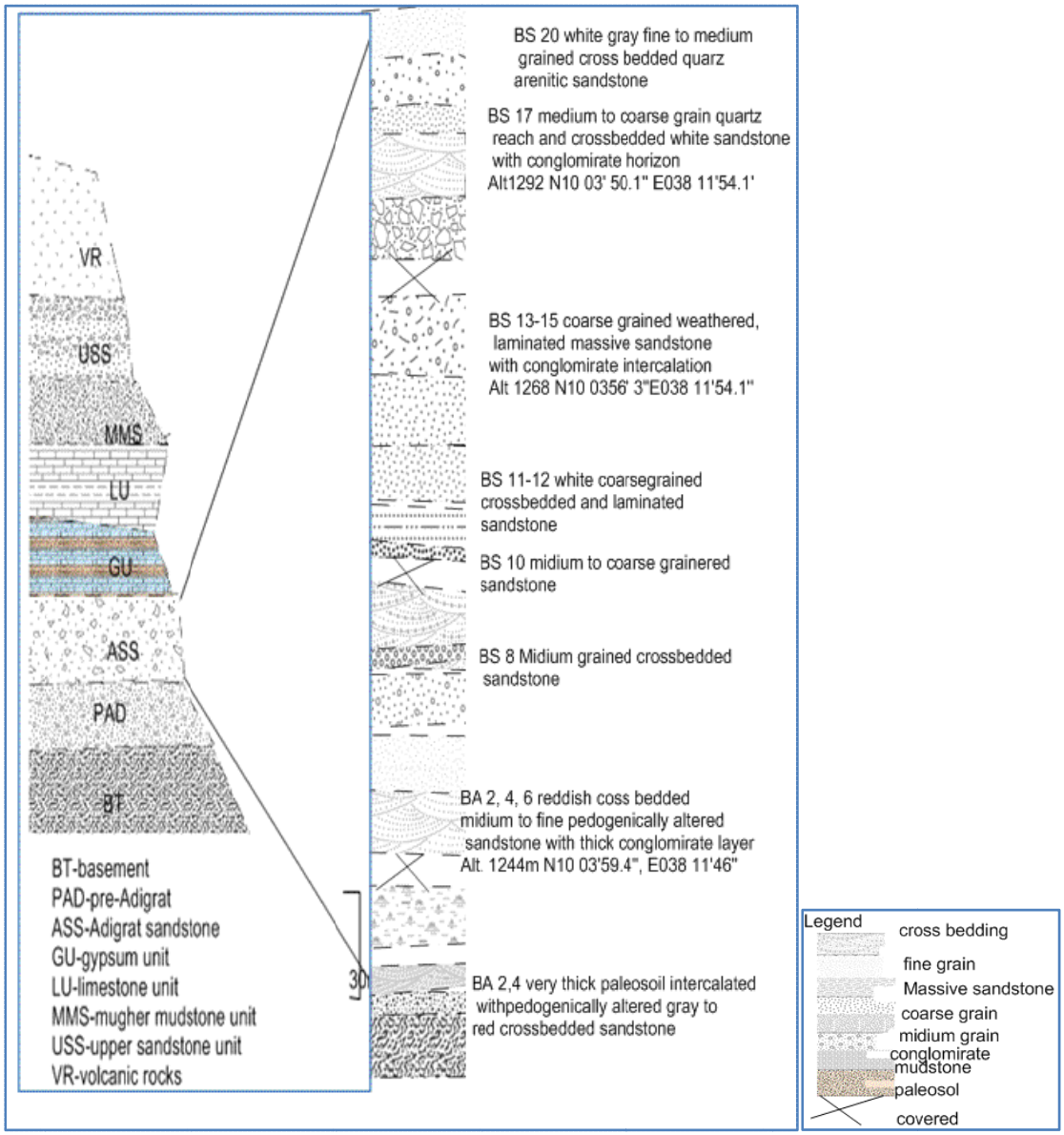

Figure 2. 3 Lithological log of Adigrat sandstone at Blue Nile Basin with sample point.

1.1.1. The Volcanic rocks

The volcanic rocks are generally post Oligocene (Hofmann, et al., 1997) and reach a maximum thickness of 5500 meters (Getaneh, 1991). This unit uncoformably overlies the Antalo limestone unit at Gohastion Dejen main road. These volcanic rocks mainly comprises of basalt, trachyte, rhyolite with beds of tuff, paleosols and lacustrine sediment (Getaneh, 1991).

3 Literature review

3.1 Preface

Igneous and metamorphic rocks are formed within the earth's crust, where the temperature and pressure is relatively high. When these rocks are exposed by erosion, or tectonically brought/uplifted to the surface, where T-P condition is entirely different from that within the earth, its constituent minerals are so unstable that they tend to reorganize themselves to a new mineral in order to tolerate the new condition. The term for the collection of processes by which these minerals re-equilibrate and readjust to surface conditions is *weathering.* This could easily be explained by Le chatlier principle. Which states, 'If a dynamic equilibrium is disturbed by changing the conditions, the position of equilibrium moves to counteract the change'. For instance, decreasing the temperature of a system in dynamic equilibrium favors the exothermic reaction. The system counteracts the change have made in temperature by producing more heat. Increase in pressure shifts the reaction towards the smaller number of phases. Similarly, if certain components are added to a reaction at equilibrium, the equilibrium will shift in a direction that remains the added component.

The new formed minerals in such processes are minerals of sedimentary rocks in general. In order to achieve such new minerals the pre-existing source rocks must pass through certain processes. These processes may include weathering, transportation, deposition, diagenesis and so forth. From these processes, weathering is the principal attributing element in forming clastic sedimentary rocks and therefore its brief discussion using and investigation interims of Adigrat Sandstone have been discussed using tools of geochemistry under chapter 5.

Sedimentary rocks are formed in three different processes. Accordingly, they are classified in to clastic, chemical and biogenic sedimentary rocks. This research concerned on clastic sedimentary rocks exclusively sandstone. Based on chemical and mineralogical composition of sandstone, an attempt has been made to deduce the provenance composition (source rocks) from which this sandstone was derived and to determine the extent of weathering to infer the paleoclimate scenarios from late Triassic to Middle Jurassic at regional scale. Provenance, climate, transport, tectonic-setting, sorting, relief and diagenesis determine the chemical composition of clastic sedimentary rocks to lesser or greater extent (Middle- ton 1960; Piper

1974; Bhatia 1983; McLennan 1989; Cox and Lowe 1995; Johnsson, 1993). However, type of source rock and climate are the major contributing factors in determining the chemical composition of the sandstone (E.g. Nesbitt and Young, 1982; Fedo et al., 1997, etc) Classification.

3.1.1 Mineralogical classification

Sandstone is best classified based on textural and mineralogical composition. The principal components of any sandstone are quartz, feldspar, and rock fragment. The later constituting sand sized particles of fine-grained igneous, sedimentary and metamorphic origin. The framework composition therefore, can be expressed in terms of those three components and the proportion of these three major constituents can define the principal sandstone classes Pettijohn et al. (1972)

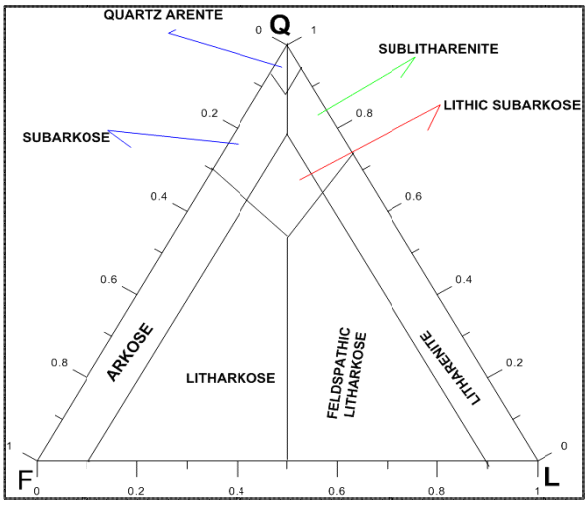

Figure 3.1 Ternary diagram for mineralogical classification of the sandstone fields (after Okada, 1971), Where Q=quartz, F=Feldspar, R= lithic fragment

3.1.2 Chemical Classification

Various workers (e.g., Crook, 1974; Pettijohn et al., 1972; Blatt et al., 1980) have devised plots to chemically classify sedimentary rocks. The chemical classification of Blatt et al., (1980), the Fe_2O_3/K_2O vs. SiO_2/Al_2O_3 diagram of Herron, 1988 and the Na_2O - K_2O diagram of Crook (1974) are among geochemical methods used to classify sandstone into different sub classes.

According to Pettijohn et al. (1972) and crook et al., 1974 we may have four common types of sandstone.

Quartz arenite – is sandstone with at least 95% quartz grain and is texturally and/or compositionally very mature.

Arkose: - is sandstone containing significant feldspar, much quartz and some rock fragment. The texture is typically poorly sorted to well sorted, with very angular to sub rounded gains.

Litharenite: - characterized by rock fragments in excess of feldspar and have variable composition.

Graywackes:-characterized by fine-grained matrix, which consists of an intergrowth of chlorite, sericite and silt-sized grain of quartz and feldspar. In contrast to arkose, it is compositionally uniform.

Each type of sandstone has some implication about its depositional history - quartz sandstone implies a long time in the depositional basin; arkose implies a short time in the depositional basin and also implies rapid erosion, arid climate, tectonic activity, steep slopes; litharenite implies rapid erosion, temperate or arid (not humid) climate (crook et al., 1974).

3.2 The provenance identification

The term provenance (French, provenoir, to originate or come forth) refers to the source rock from which the rock materials were derived. Particular type of source rock tends to yield distinctive suite of minerals, which is the guideline for source identification. However, the composition of the sediment is not solely determined by the nature of the source rock, rather it is also the complex utility of other factors (such as climate etc) within the source region (Bhatia 1983; McLennan 1989; Nesbitt and Young, 1982; Fedo et al., 1997).

3.2.1 Mineralogy

The optical property of framework grains of sandstone can potentially help us to infer the source rock from which these detrital materials were derived. The presence of rare rounded detrital quartz grains, sedimentary lithic fragments, such as quartz arenite, and rounded grains of zircon and tourmaline, suggest that a component of the provenance is older (pre-existing) sedimentary rocks (e.g. Shiloh et al., 2005).

If the quartz grains are strained then it could in part may be due to post depositional effect of folding and metamorphism, and the occurrence of strained and unstrained quartz in the sandstone sample therefore suggest that some of the strain were inherited from the metamorphic and/ or plutonic source area(e.g., Young 1976).

The presence of rare rounded detrital quartz grains, sedimentary lithic fragments, such as quartz arenite and rounded grains of zircon and tourmaline, suggest that a component of the provenance is older (pre-existing) sedimentary rocks (Shiloh et al., 2005).

Presence of undulatory extinction in another case shows distinctive source rocks i.e. detrital material were probably derived from exposed gneisses, schist, and granitic rocks. In some grain derived from metamorphic rocks, sharp boundaries separate sectors each differing in extinction by a few degrees with respect to its neighbors. In petrographic studies, different varieties of feldspar must be differentiated for they vary in chemical composition and are among the reliable indicator of provenances.

Detrital grain of perthite, microcline and orthoclase usually indicate source areas were granitic rocks and high-grade gneisses and schist are exposed. Sanidine implies a silicic or alkaline

volcanic source, while detrital albite chiefly comes from low-grade regionally metamorphosed terrain. More Calc-plagioclase is abundant in basic igneous rocks and some high-grade metamorphic rocks. The presence of euhedral or subhedral phenocryst, usually of feldspar, indicates intermediate and basic volcanic origin. Volcanic grains of highly felsic composition, in contrast, are essentially may be microfibrous or microgranular (felsitic).

Lithic grains also help us in source rock identification for they are fragments of preexisting rocks and are compositionally and/or mineralogically less or unaltered. Most lithic grains derived from sedimentary source rocks are restricted to fine grain, firmly lithified types that are not readily disintegrated during erosion. Metamorphic rock fragments are usually recognized by schistose or semi schistose fabric.

3.2.2 Geochemistry

3.2.2.1 Major element Geochemistry

Before we begin to understand how the chemical composition monitors the provenance, we must first know the question which element derived from which mineral. For example; if TiO_2 shows strong correlation with the Al_2O_3 contents this correlation suggests that Ti is mainly contained in phyllosilicates, possibly biotite (Asiedu et al., 2000; Condie et al., 1992).

Major and trace oxides coupled with REE pattern help quantitatively to understand the source rocks (provenance) from which siliciclasitc sedimentary rocks were derived. Discriminant function (DF) analysis using major element compositions is classical method for determining the provenance of sandstones (Roser and Korsch, 1988). The discriminant functions of Roser and Korsch (1988) were designed to discriminate between four sedimentary provenance fields. These are mafic (P1), intermediate (P2), felsic (P3) and recycled (P4). The descriminant functions are determined from major oxide constituting the rocks and are calculated according to the following equations:

Discriminant function 1=30.638 TiO_2/Al_2O_3 -12.541Fe_2O_3/Al_2O_3+ 7.329MgO/Al_2O_3+ 2.031Na_2O/Al_2O_3 + 35.40$_2K_2O/Al_2O_3$-6.382

Discriminant function 2=56.500 TiO_2/Al_2O_3-10879Fe_2O_3T/Al_2O_3+30.875MgO/Al_2O_3-5.404Na_2O/Al_2O_3 +11.112K2O/Al203-3.89

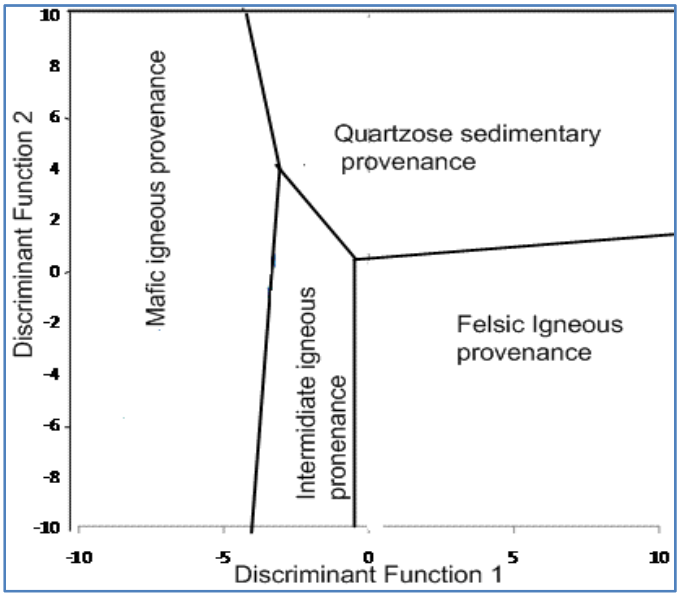

Figure 3. 2 Discriminant function diagram for the provenance signature of sandstone (after Roser and Korsch, 1988).

3.2.2.2 Using trace and REE geochemistry

The name "rare earth" has its origin in the history of the discovery of these elements. The 'rare' part of the name refers to the difficulty in obtaining the pure elements.

The rare earths are a group of metallic elements consisting of the lanthanide series on the periodic table as well as the element yttrium. This grouping is based on the similarity in chemical behavior between the elements. In the periodic table, these lanthanide elements have atomic numbers 57 through 71.

The REE, Th and Sc are generally accepted as among the most reliable indicators of sediment provenance because their distribution is less affected by heavy-mineral fractionation than that of elements such as Zr, Hf, and Sn (Cullers et al., 1979; Taylor and McLennan, 1985).[3]

♥ In geochemistry, Eu anomaly is defined as the phenomenon whereby Europium (Eu) concentration is either depleted or enriched in a rock relative to the other (REEs). An Eu anomaly is said to be "negative" if Eu is depleted relative to the other REEs and is said to be "positive" if Eu is enriched relative to the other REEs and is calculated by the equation $Eu/Eu^* = Eu_{cn}/ [(Sm_{cn})(Gd_{cn})]$.

The Th/Sc ratio is a reliable provenance indicator, as both elements are immobile under surface conditions and therefore preserve the characteristics of their source (Taylor and McLennan, 1985). Sc is compatible trace mafic component where as Th is incompatible enriched in felsic rocks. Average upper continental crust has a Th/Sc ratio of 0.79 (McLennan, 2001). In general, REE and Th abundances are higher in felsic igneous rocks and in their weathering products, whereas Co, Sc, Ni, and Cr are more concentrated in mafic than in felsic igneous rocks. Therefore, low concentrations of ferromagnesian trace elements such as Cr, Ni, Sc and V in the sandstones indicate insignificant mafic rocks were exposed in the source area. The unusual Co enrichment with respect to average upper continental crust may suggest some input of mafic materials from the source terrain.

On the other hand, the Eu/Eu*, $(La/Lu)_N$, La/Sc, Th/Sc,and Cr/Th ratios of the sandstones are either similar to sediments derived from felsic source rocks or to mafic source rocks from which they may derived (e.g., McLennan *et al*., 1993; Mongelli *et al*., 1998). Because they are significantly different in mafic and felsic source rocks and can, therefore, provide information about the provenance of sedimentary rocks (Amstrong-Altrin et al., 2004).

Absence or presence of Eu-anomaly and HREE patterns shows the source is either a granodiorite or a granite source (Condie, 1993; Cullers, 2000). However, the appreciably high Eu/Eu* values and the overall flat HREEs may suggest a component of mafic volcanic rocks (Fedo et al., 1996). Enrichments of normally incompatible over compatible elements (e.g., LREE enrichment, high Th/Sc, La/Sc, and high Rb/Sr ratios suggest that the sandstones are derived from old upper continental crust (e.g., McLennan et al., 1990). The La-Th-Sc plot has been used to discriminate sediments from felsic sources to progressively more mafic sources (Bhatia and Crook, 1986; Cullers, 1994). Mafic and ultramfic supply can also be identified based on mixing curve between granite and mafic-ultramafic end-member in the Y/Ni vs. Cr/V diagram.

3.3 The weathering profile and paleoclimate interpretation

Chemical weathering in continents is controlled by many factors including source rock type, climate regime, tectonic and topographic settings, vegetation, soil development, and human activities as well (Nesbitt and Young, 1982; Fedo et al., 1997; Bhatia 1983; McLennan 1989). Many previous studies suggest that rock type plays an important role on chemical denudation (Price and Velbel, 2003).

Various geochemical proxies have been proposed to estimate the intensity of chemical weathering in continents. Some of them are based on dissolved loads while others depend on solid phase.

Grain morphology, clay minerals and geochemistry are the best paleoclimatic proxies especially when they are complemented. Mineralogical and chemical compositions of siliciclastic deposits depend on the intensity of chemical weathering linked to the climate in provenance terrains (Nesbitt and Young, 1982; Fedo et al., 1997).

Therefore, changes in the mineralogical and chemical compositions of sedimentary rocks (particularly fine-grained siliciclastic rocks), can potentially be used as a proxy for climate changes (Detian Yan et al., 2010).

3.3.1 Major element Geochemistry

The Chemical Index of Alteration (CIA) was pioneered by Nesbitt and Young (1982) to quantitatively evaluate weathering history recorded in sediments and sedimentary rocks. Accordingly, the chemical index of alteration is proposed to evaluate the climate changes (Nesbitt and Young, 1982; Fedo *et al.,* 1995, 1997; Young and Nesbitt, 1999; Rieu *et al., 2007).*

The chemical index of alteration is defined as:

$$CIA = \frac{Al2O3}{Al2O_3 + CaO^* + Na_2O} \times 100$$

Where oxides are in their molar contents and the CaO* used in the calculation of CIA refers to the amount of CaO incorporated in silicate fraction only (Nesbitt and Young, 1982; McLennan, 1993).

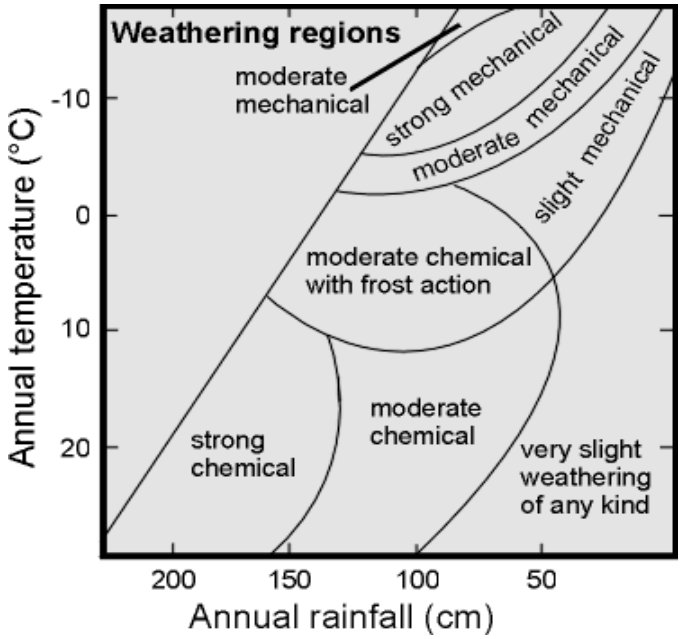

Figure 3. 3 Temperature versus rainfall to characterize the dominant weathering type

In such a case, it is necessary to make a correction to the measured CaO content for the presence of carbonates (calcite, dolomite) and apatite according to correction method proposed by Mclennan, (1993). In this methods, CaO was initially corrected for phosphate using available P_2O_5 data (CaO* =mole CaO − mole P_2O_5 × 10/3). If the remaining number of moles is less than that of Na_2O, the CaO value was adopted as the CaO*. Otherwise, the CaO* was assumed to be equivalent to Na_2O (McLennan, 1993).

The CIA actually reflects changes in the proportion of feldspar and various clay minerals in the weathering product (Nesbitt and Young, 1982).

It is well known that aluminous minerals such as kaolinite and gibbsite are secondarily formed while Na- and Ca-bearing silicate minerals are significantly removed from the weathering profile during intense chemical weathering, resulting in high CIA values in the weathered sediments.

Sediments (especially fine-grained argillites) deposited in a hot and humid tropic climate generally have CIA values from 80 to 100, those in a warm and humid climate have values from

70 to 80 or above, and those in a cold and arid climate have values from 50 to 70 (Nesbitt and Young, 1982; 1989).

Consequently, CIA values of about 45 to 55 indicate virtually no weathering (Fig. 3.5), whereas the value of 100 indicates intense weathering with complete removal of alkali and alkaline earth elements (McLennan, 1993). This, on the other hand, reflects the substantial removal of mobile cations (e.g., Ca^{2+}, N^{a+}, K^{+}) relative to stable residual constituents (Al^{3+},Ti^{4+}) through intensive chemical weathering, likely under warm and humid conditions (Fig 3.4). Low CIA values, however, indicate the near absence of chemical weathering, thereby reflecting cool and/or arid conditions (Nesbitt and Young, 1982, 1989; Detian *et al*., 2010).

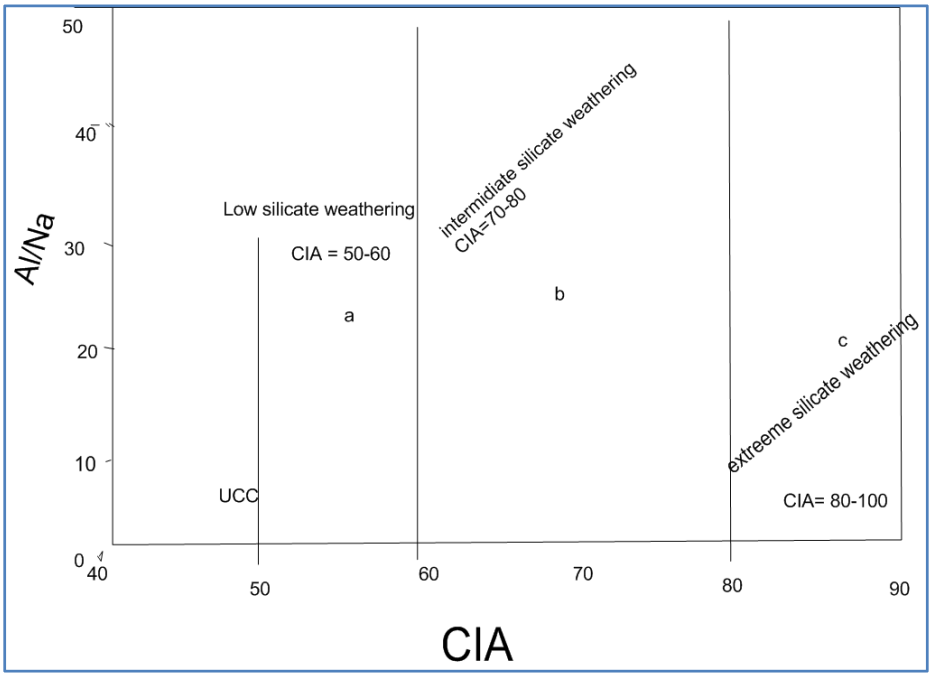

Figure 3. 4 Scatter plot of Al/Na ratio versus chemical index of alteration (CIA). Note the interrelation between both indexes, which reflects the silicate weathering intensity (After Kandasamy and Chen-Tung Chen, 2004).

When plotted in the A-CN-K (Al_2O_3-(CaO^* + Na_2O)-K_2O) ternary diagram(Fig. 3.6), sediments produced by intense chemical weathering were plotted in positions matching with high CIA

values (80−100), where as incipiently weathered sediments were plotted near the feldspar join (CIA of 50−70). Theoretically, products of progressive weathering usually yield a series of CIA values distributed along a straight-line (ideal weathering trend) parallel to the A-CN sideline (Nisbett and Young, 1982; Mclennan, 1993) as attempt is made to show as in the figure below. However, if our data points lie on a line deviating from the theoretical trend, then this condition may be due to K_2O addition because of diagenetic K-metasomatism (conversion of kaolinite to illite) Fedo et al., 1995, 1997; Rieu et al., 2007. Therefore, it is necessary to make correction for K- metasomatism.

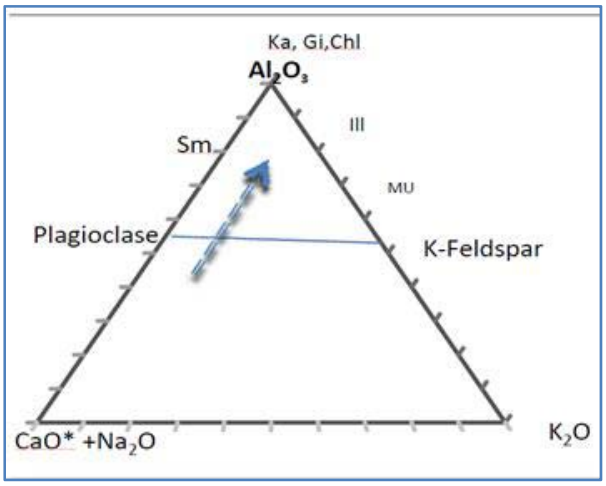

Figure 3. 5 The A-CN-K(Al2O3-(CaO + Na2O) K2O)diagrams to show weathering trend is parallel with the A-CN line (after Nesbitt and Young, 1982, 1984, 1989, 1996; Nesbitt et al., 1996; Fedo et al., 1997). Where Kaol—kaolinite; Chl—chlorite; Gib—Gibbsite;Sm—smectite;Mu—muscovite, arrow indicates ideal weathering trend of fresh rocks with UCC compositions

The Chemical index of weathering is defined as

$$\mathbf{CIW = [Al_2O_3/ (Al_2O_3 + CaO^* + Na_2O)] \times 100}$$

Where CaO* is the amount of CaO incorporated in the silicate fraction only. Phanerozoic shales have CIW values close to 85 and higher values are indicative of intense weathering (e.g., Fedo et al., 1995).The principal difference between CIA and CIW is that the former treats K strictly as mobile component where as the latter does not. The degree of chemical weathering can also be estimated using the Plagioclase Index of Alteration, PIA (Fedo et al., 1995), and is defined as:

$$\mathbf{PIA = [(Al_2O_3\text{-}K_2O)/ (Al_2O_3 + CaO^* + Na_2O\text{-}K_2O)] \times 100}$$

Where oxides are in molecular proportions and CaO* is the CaO residing only in the silicate fraction. The concept of PIA generated by Fedo et al., 1995, is that on weathering plagioclase is transformed in to clay minerals according to the reaction below. Since on silicates weathering, not all ions stay in solution, rather some may react with water to form secondary minerals by incongruent dissolution process.

$2NaAlSi_3O_8 + 1H+ + H_2O \rightarrow Al_2Si_2O_5\ (0H)_4 + 2Na+ + 4SiO_2$ Or most accurately

$2NaAlSi_3O_8 + 2H_2CO_30 + 9H_2O\ (l) \rightarrow 2Na^+ + 2HCO_3^- + Al2Si_2O_5(OH)_4$ (kaolinite) $+ 4H_4SiO_4^0$

Un weathered plagioclase has PIA value of 50 whereas the PAAS(Post Archean Australian Shale) has PIA value of 79, very high PIA values indicating that most of the plagioclase has been converted to clay minerals and the source experienced very intense weathering.

3.3.2 The REE

In addition to the weathering indexes discussed above, other weathering indexes incorporate trace elements such as lanthanides, rare earth elements and isotope including Nd and Sm(Brown et al ., 2003). Elemental, ratios have long been used to characterize weathering intensity (Merrill, 1906; Jerry, 1941).Such ratios most commonly compare the concentration of one or more mobile element ($\sum_{k=0}^{n} C\ j, w$) against one or more immobile element ($\sum_{k=0}^{n} C\ i, w$). The general form of such a relationship is termed the weathering index, Iw.[1]

$$\mathbf{Iw = \sum_{k=0}^{n} C\ j, w / \sum_{k=0}^{n} C\ i, w}$$

Where $\sum_{k=0}^{n} C\ j, w$ = mobile elements; $\sum_{k=0}^{n} C\ i, w$ = immobile elements

Although the REE are quantitatively transferred from the source to the sediment (McLennan et al., 1993), intense weathering produces Light to heavy REE (LREE/HREE) fractionation (Mongelli, *et al.*,1998), possibly due to preferential HREE retention in solution (Cantrell and Byrne, 1987). To facilitate the interpretation of sedimentary rocks other important reference REE compositions such as upper continental crust (UCC), post- Archean Australian shale (from

both Taylor and McLennan 1985), and North American shale composite from Haskin et al., 1966, will have also been included for comparison.

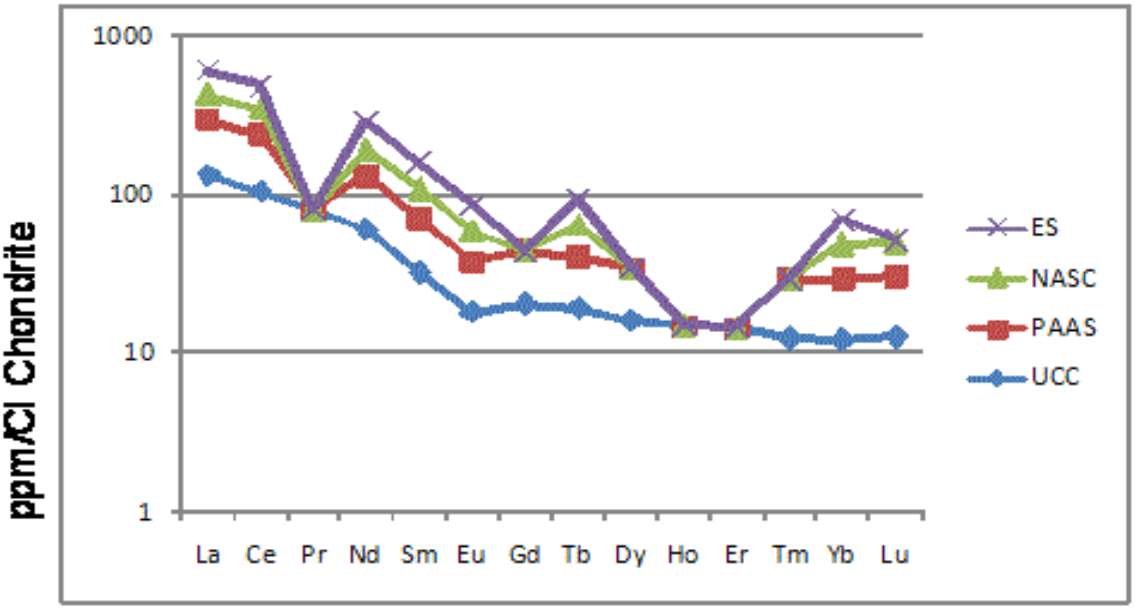

Figure 3. 6 Chondrite normalized value of average PAAS, NASC, UCC and ES. Data for PAAS (post-Archean Australian Shale) is from Taylor and McLennan, 1985; and for NASC (North American shale composite) is from Gromet et al., 1984; Chondrite values are from Anders and Grevesse, 1989. ES (European Shale) from Haskin and Haskin, 1966; UCC (Upper Continental Crust) from Rudnick and Gao, 2003.

3.4 Effect of other parameters

3.4.1 Geographic and topographic effect

There is no consensus, whether geographic and topographic parameters have distinct effect on triggering chemical weathering. Chao and Yang, 2010; Gallardet *et al.*, 1999 found that there is poor correlation between average elevation and chemical denudation. However , Raymo and Ruddiman, 1992; Hren *et al.*, 2007 argue that the regions with rapid tectonic uplift, steep channel slopes, high stream power and exhumation result in frequent exposure of fresh rocks and thus, increase chemical weathering rates. Nevertheless, topographic/tectonic effect on chemical weathering is only regional, rather than a global pattern (Nesbitt and Young, 1982, 1989).

3.4.2 Transportation, Sorting and recycling effect

It is well known that transport and deposition of clastic sediments involves mechanical sorting. Its effect on the chemical composition of terrigeneous sediments is important and may affect the distribution of paleoweathering and provenance proxies (Bauluz et al., 2000). The distribution of the chemical components within a suite is mainly determined by the mechanical properties of the host minerals. The process fractionates Al_2O_3 (clay minerals) from SiO_2 (quartz and feldspars). Sorting also fractionates TiO_2, mostly present in clay minerals and Ti-oxides, from Zr, present in zircon, and sorted with quartz. Ternary plots based on Al_2O_3, TiO_2, and Zr may illustrate the presence of sorting-related fractionations that are recognizable by simple mixing trends on a ternary Al_2O_3-TiO_2-Zr diagram (Fig. 3.8).

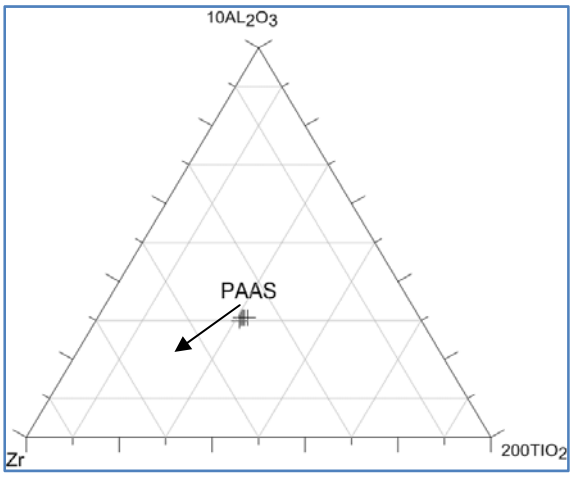

Figure 3. 7 The Al_2O_3-TiO_2-Zr ternary plots. Arrow indicates zircon addition suggestive of a sorting effect (after McLennan et al., 1993; Mongelli *et al*., 2006)

Moreover, the distance to the provenance may also influence the weathering intensity; the shorter the distance (shorter transport and timing of weathering), the lower the CIA value, and vice versa (Carson and Kirkby, 1972; Stallard and Edmond, 1983). This could easily be corrected by considering the relative abundance or ratios of rare earth element (REE) and using textural study under petrography.

3.4.3 K-metasomatic effect

Metasomaitsm is a metamorphic process by which the chemical composition of a rock or rock portion is altered in a pervasive manner and which involves the introduction and/or removal of chemical components because of the interaction of the rock with aqueous fluids (solutions). The presence of K metasomatism can be observed in A-CN-K diagram where data point shift toward K apex. Correction for K-metasomatism is made by projecting data points back onto the ideal weathering pathway from K-apex on the A-CN-K (Al_2O_3-(CaO + Na_2O) -K_2O) diagrams (Detian *et al.*, 2010)

To finalize the chapter, various tools of geochemistry and mineralogy were developed which quarry the rock to investigate geological processes that happened within or on the earth surface. Hence, Adigrat Sandstone source composition and its paleoweathering history, which is mainly the function of climatic condition, could easily be scrutinized under the light of these tools.

4 PROVENANCE COMPOSITIONS

4.1 Classification

Before an attempt is made on surveying of source rock composition, geochemical and mineralogical classifications for Adigrat Sandstone have been verified. Then on this foundation, the main objective of the chapter has been discussed impending by relying on tools of geochemistry and mineralogy. This classification is important for further discussion on source rock investigation, because the effect of various sedimentary processes results in one or more distinct sandstone type, which by in turn controls the inference of these sedimentary processes.

Composition of sandstones does bear some relationship to the action of one process or another. For example, the effects of prolonged weathering and transport are most evident in the formation of quartz arenite; and provenance is a major factor in the formation of arkose and lithic arenite (David, 1999). The effect of diagenesis is on the other hand probably most evident in production of graywacke matrix (Cummins, 1962)

The classes' quartz arenite, graywacke, and arkose can be defined by chemical composition. The enrichment of SiO_2 over Al_2O_3 by mechanical and chemical processes produces quartz arenites. Silica (quartz) enrichment is a measure of sandstone maturity, and is a reflection of the duration and intensity of weathering and destruction of other minerals during transport. Silica enrichment also occurs by addition of silica cement, as quartz and opal. Abundant alkalis (Na_2O and K_2O) characterize immature sandstones such as arkoses and graywackes. The ratio K_2O/Na_2O reflects the relative abundance of potassic feldspar and plagioclase. The ratio K_2O/Na_2O has been used to discriminate between arkose ($K_2O>Na_2O$) and graywacke ($Na_2O>K_2O$) (Pettijohn, 1963). Arkoses are immature sandstones with abundant feldspar (both potassic feldspar and plagioclase). Greywacke contain abundant plagioclase (Huckenholz, 1963). Using the geochemical classification diagram of Herron, 1988 the Adigrat Sandstone is plotted in the arkose, sublithic arenite and quartz arenite field (Fig. 4.1).

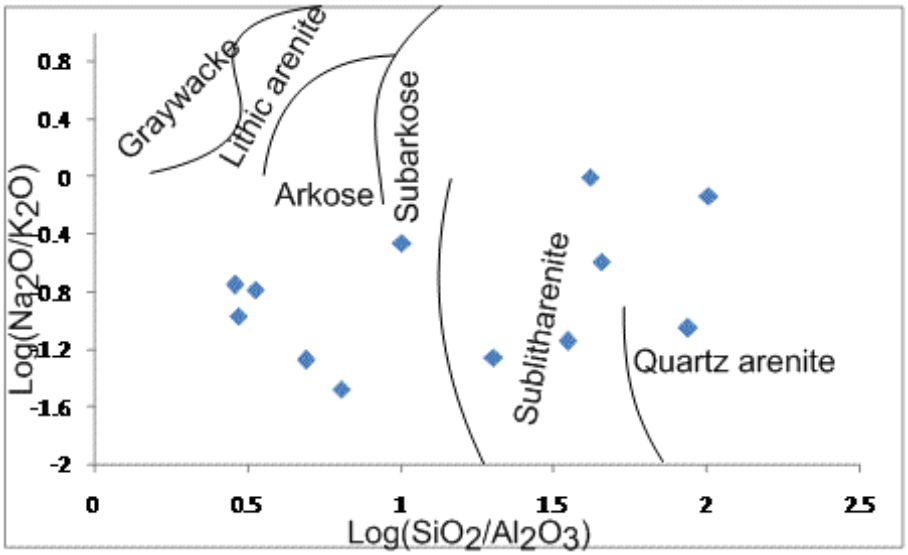

Figure 4. 1 The $LogNa_2O/K_2O$ vs. $Log(SiO_2/Al_2O_3)$ classification of Adigrat Sandstone after (fields are after Herron, 1988).

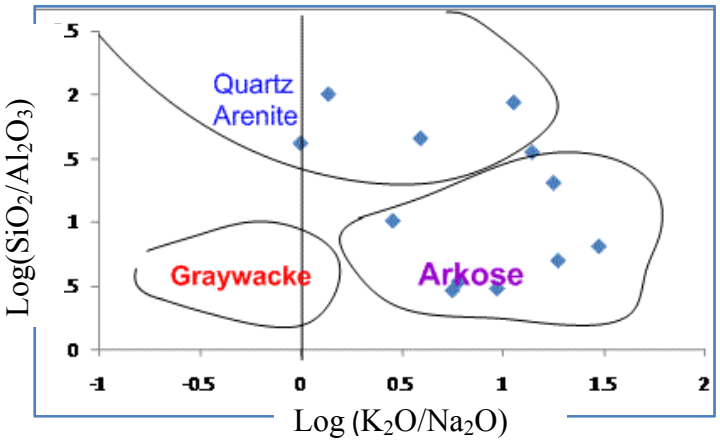

Figure 4. 2 $Log(K_2O/Na_2O)$vs. $Log(SiO_2/Al_2O_3)$ classification of Adigrat Sandstone (fields are after Pettijohn et al., 1972)

Slight enrichment of SiO_2 (wt %) is being attributed to variation in quartz in this sandstone. The depletion of Na_2O in all samples of sandstone is credited to a relatively small amount of Na-rich

plagioclase in them, consistent with the petrographic data.

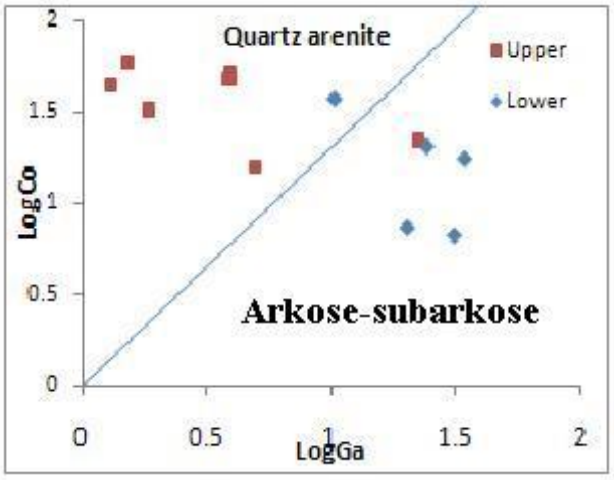

Figure 4. 3 LogCo vs. LogGa sandstone classification between Quartz Arenite and Arkose (after David, 1999). According to this classification, upper part of this unit are characterized by quartz arenite.

K_2O, Na2O content, and their ratios are also consistent with petrographic observation; according to which K-spar dominate over Plagioclase. According to classification proposed by Crook et al, 1974, the Adigrat sandstone plotted within the field of arkose to ferromagnesian-potassic sandstone fig. 4.3

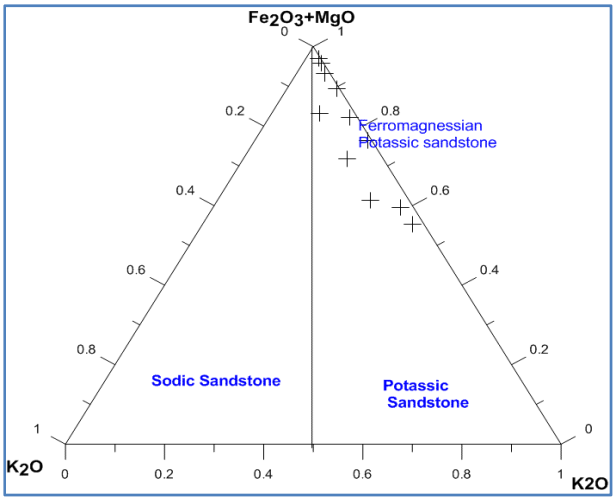

Figure 4. 4 The Na_2O-(MgO+Fe_2O_3)-K_2O (N-(M+F)-K) classification of Adigrat Sandstone(After crook et al., 1974).

In our suite of sandstone samples containing trace element, gallium is highly correlated with SiO_2/Al_2O_3 and cobalt is moderately correlated with $(Fe_TO_3+MgO)/(K_2O+Na_2O)$ trace elements, notably Ga and Co, show promise for use in chemical classification (David, 1999). LogCo vs. logGa has been used to distinguish arkosic sandstones from quartz arenites. In this diagram, most of the sandstone samples plot within the arkose to subarkose field and minor in quartz arenite field (Fig. 4.3). This is consistent with major oxide sandstone classification of Pettijohn et al., 1972 (Fig. 4.2)

4.2 Source rocks (Provenance composition)

4.2.1 Mineralogical interpretation

A textural study was carried out for the Adigrat Sandstone to characterize grain size, shape, degree of sorting and compactness. Varieties of textures are recognized in our samples. Most of the samples are characterized by fine to coarse gained texture and majority of samples are sub-rounded. Degree of sorting also varies from sample to sample, some show poor sorting and other show moderate to well sorting.

Framework grains: The framework grain are non-undulatory monocrystalline quartz (Qn), undulatory monocrystalline quartz (Qu), polycrystalline quartz (Qp), K-feldspar, plagioclase and rock fragment. Quartz (most stable) is the most abundant framework grain in this sandstone constituting on average 67% of rock volume. Among quartz grains, Qn is dominant over Qu. Nevertheless, most samples have a substantial content of less stable particles; by far the most numerous are feldspar grains and small fragment of lithic grains. Other detrital grains are subsidiary. The Average Q-F-L ratio is $Q_{67}:F_6:L_3$. Most of the samples are free of matrix and on QFL diagram (Fig.4.5), the Adigrat Sandstone samples plot in the field of subarkose, Lithic subarkose and quartz arenite. The prominent cementing material is calcite with subordinate amount of clay, iron oxides and silica in some samples. The classification is broadly consistent with the geochemical data because on geochemical classification diagram, the Adigrat Sandstone samples fall in the arkose to subarkose, sublitharenite and quartzarenite fields.

Quartz

Quartz (30%–90%) includes monocrystalline and polycrystalline quartz including some grains exhibiting undulose extinction (Plate 4.1 H), incipient polygonal grains, and some form sutured grain boundaries (plate 4.1 F). Minor amount of chalcedony are also observed in some samples.

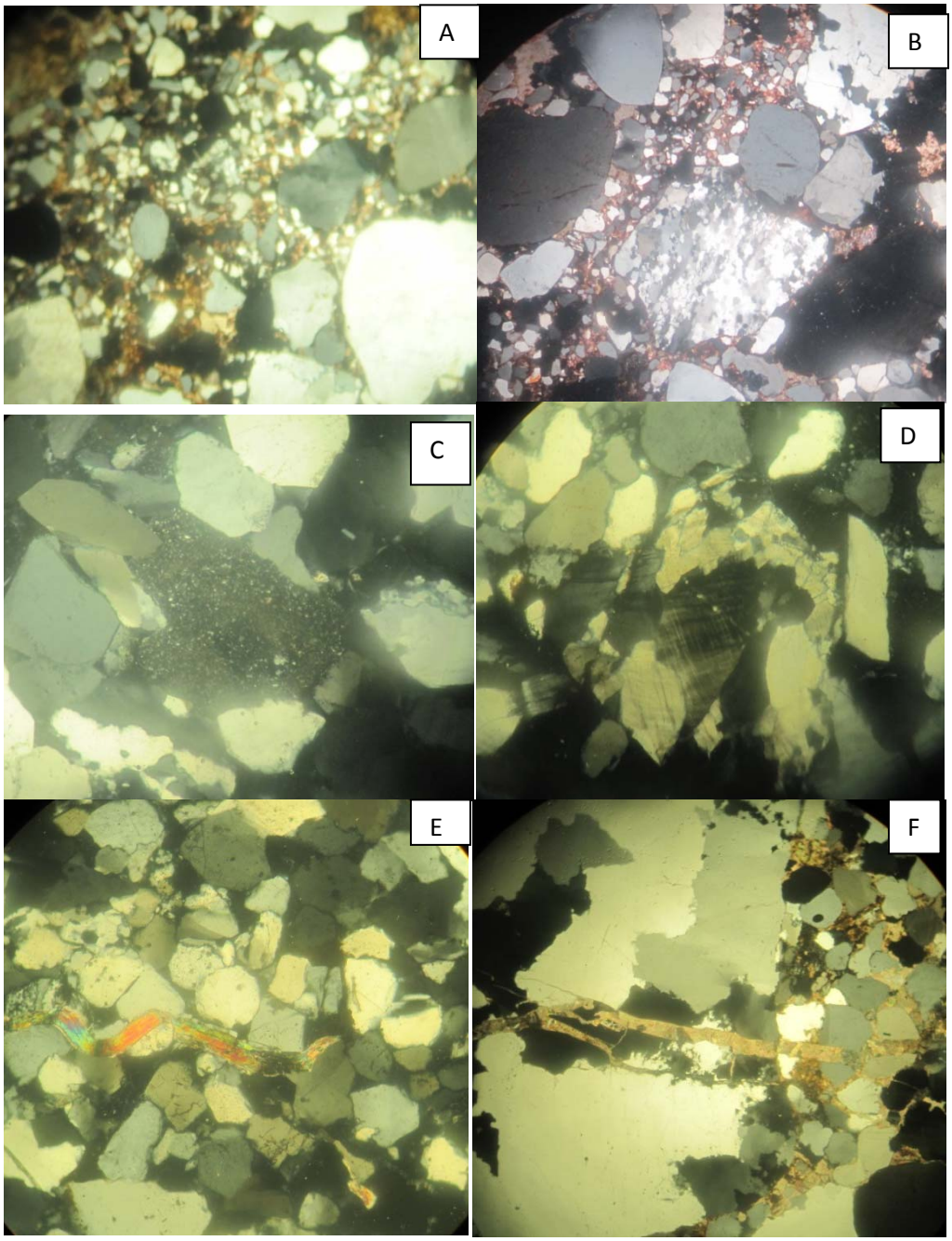

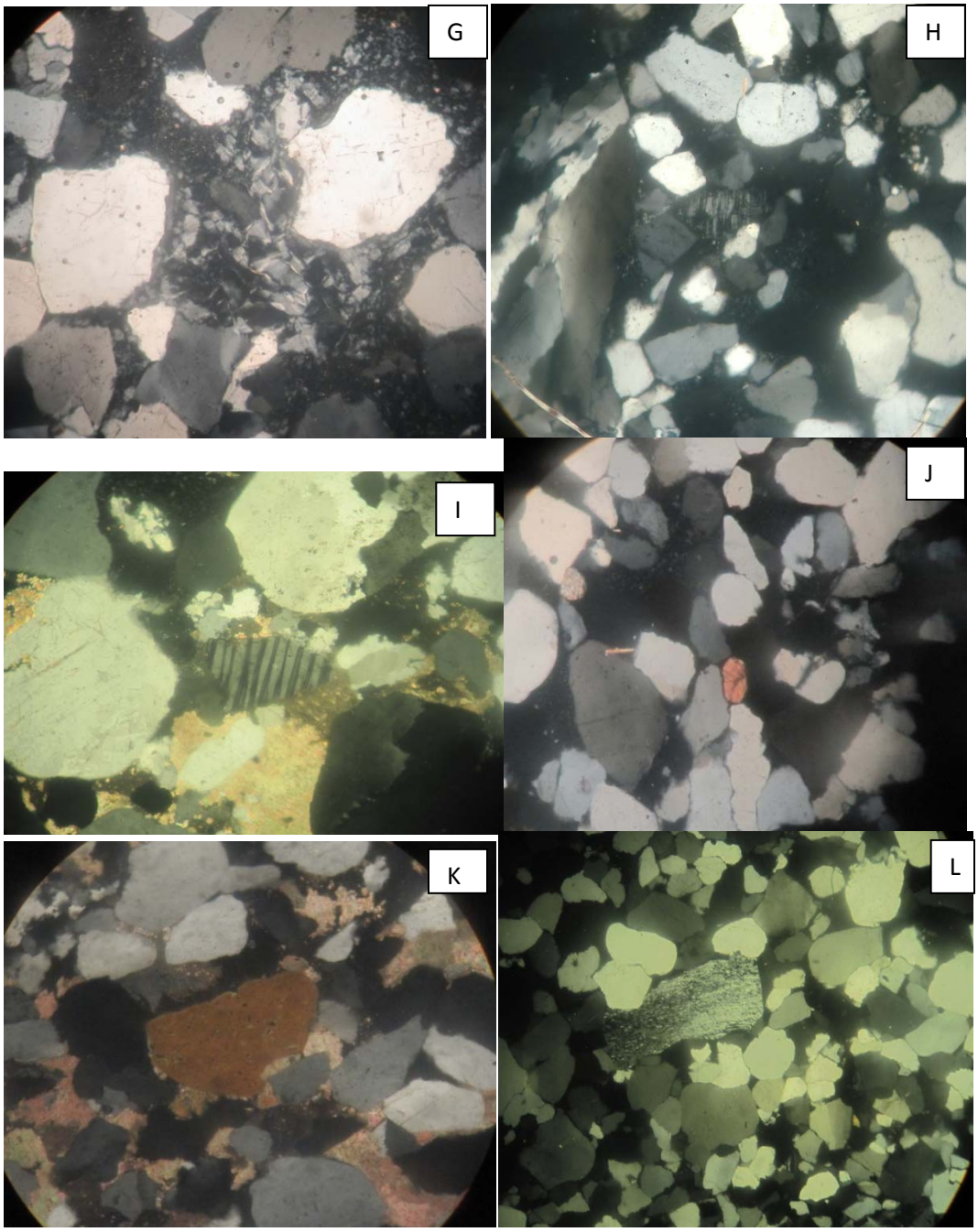

Plate 4.1 Photomicrographs of some samples (all photos are taken under XPL, and except C, G and I (which are 10x magnification) all are 4x magnification.

Feldspar

K-feldspar and the rock fragments are comparatively less abundant. However, all sandstone samples contain minor amount of feldspar grain (3%–15%) and consists mainly of alkali feldspar and minor amount of plagioclase. K-feldspar is dominantly grains of microcline which identified by distinctive cross-hatched twinning (Plate 4.1D, H).

Lithic Fragments

Lithic fragments are uncommon (0- 15%). Sedimentary lithic fragments are less abundant. Nevertheless, rare fine-grained quartzose sandstone, lithic sandstone, and quartz siltstone fragments are present. Metamorphic rock fragments are minor and are mainly metasedimentary rock fragments (Plate 4.1 L). They are also observed in some samples and are recognized by parallel alignment of grains (Plate L). In general, all sandstone samples are poor in Lithic fragment (Plate 4.1 L). Metamorphic lithic fragment are observed relatively higher than other types of lithic fragments (plate 4.1 C) in some samples.

Cementing material

Calcite (plate 4.1 A, B), clay (Plate 4.1 G), silica and opaque minerals particularly iron oxide are the main cementing materials. However, in most cases calcite cement predominates. In some samples, grain-to-grain contacts are observed where sands are essentially washed and free of clay and silt.

Opaque mineral

Iron oxide and Iron hydroxide are among opaque mineral exclusively found in our sandstone samples. Iron oxide, which exists as cementing material, is mainly of diagenetic origin and occurs as detrital grain that may had formed as bi-product of weathering of ferromagnesian minerals.

Mineral Fragments

Additional mineral fragments are relatively minor (<1%). Among mica group, flake of muscovite,(plate 4.1 E) which has been bent through compaction, is relatively observed. Others

minerals are rare and include hornblende. Very rare heavy minerals such as sphene and zircon (plate 4.1 J) are also observed almost in all samples

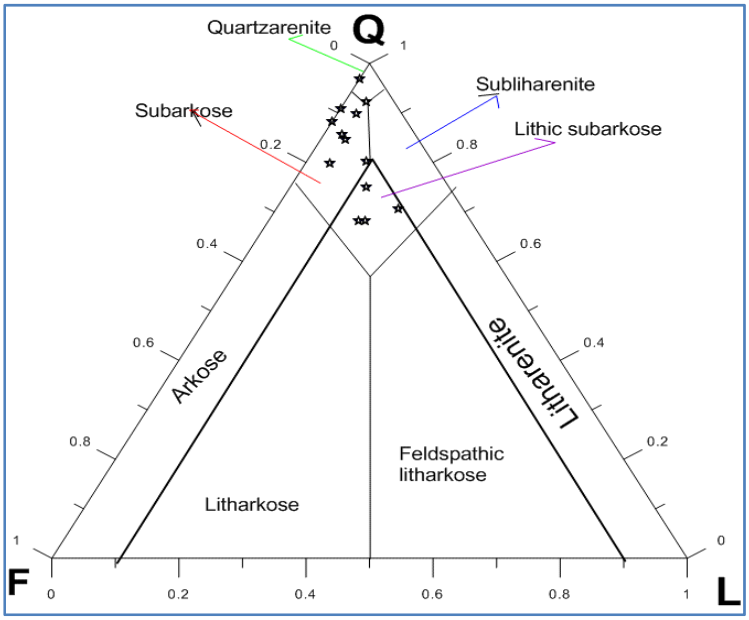

Figure 4. 5 the QFL diagram of Adigrat Sandstone from BNB (fields after Okada, 1971): Q-quartz, F-feldspar, L-lithic fragments

4.2.2 Geochemical discrimination of provenance

Prior to discussion of how the geochemical data monitor the provenance of the sandstone, better to talk which minerals control which element distribution in the analyzed samples. For instance, which mineral hosts the REE? The TiO_2 contents of the Adigrat Sandstone show strong correlation with the Al_2O_3 contents (Fig.5.6e). This correlation suggests that Ti is mainly contained in phyllosilicates (Asiedu et al., 2000; Condie *et al.,* 1992). In addition, TiO_2 is highly correlated with Fe_2O_3 but less slightly than Al_2O_3 (Fig.4.6). This however indicates the presence of iron bearing accessory minerals. It is obvious that aluminum and potassium are the two main constituents of clay minerals. A weak relationship between Al_2O_3 (R^2 = 0.408) and K_2O (R^2 = 0.000) with total REE has been observed in the Adigrat sandstone. This in turn indicates that REE chemistry of the rocks is not controlled by clay minerals. REE and Zr are not correlated (R^2=0.292) which again suggest Zircon is not responsible in hosting REE. Moderate positive

linear correlation has been observed between total REE and TiO_2 (R^2 = 0.63) than Al_2O_3 and REE (R^2=0.408), suggesting that the REE are housed in Ti bearing accessory minerals than Ti bearing phyllosilicate minerals (Taylor and McLennan 1985, Condie 1993). Perfect linear correlation between REE and P_2O_5 (R^2=0.967) are observed wich indicates that REE are mainly housed in the apatite mineral.

The Zr and Hf contents show strong correlation. Ferromagnesian trace element abundances (i.e., Cr, V, Co, and Sc) generally show poor inter-relationships. These poor inter-relationships may be the result of good mixing of the sediment prior to deposition. The Linear correlation coefficients of selected elements are reported in the appendix part. Only the linear correlations among few groups are shown below (Fig. Fig. 4.6).

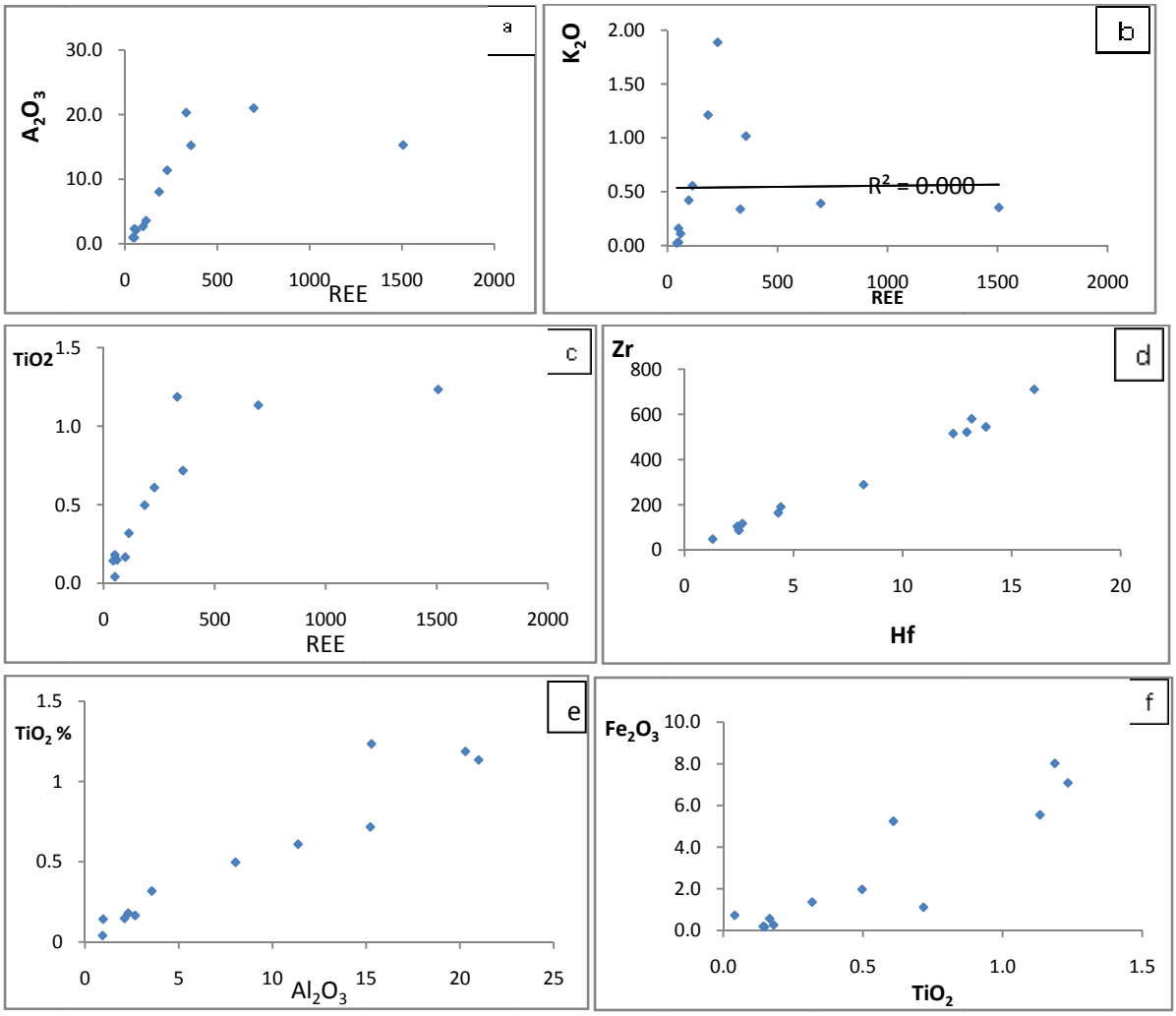

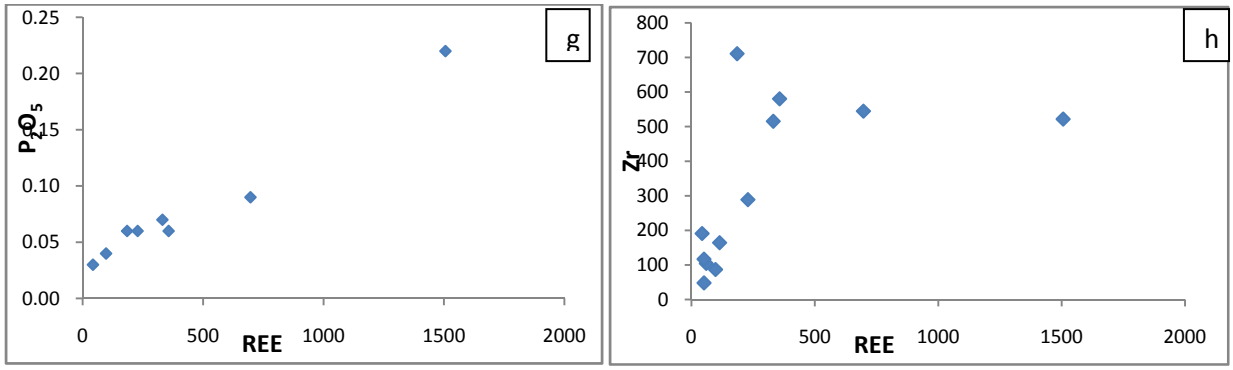

Figure 4. 6 The linear correlation plots between a) Al_2O_3 vs REE b) K_2O vs REE C) TiO_2 vs REE d) Zr vs Hf, e) Al_2O_3 vs. TiO_2 f) Fe_2O_3 and TiO_2

4.2.2.1 Major oxides

Discriminant function (DF) analysis using major element compositions is classical method for determining the provenance of sandstones (Roser and Korsch, 1988). It was designed to discriminate between four sedimentary provenance fields. These are mafic (P1); intermediate (P2); felsic (P3); and recycled (P4). There are two Discriminant function diagrams proposed by Roser and Korsch, 1988. Each of these DF diagram were briefly described in Rollinson, 1993 (Using Geochemical data). In this study, the DF diagram below is preferred due to enrichment of non-silicate CaO in some samples. When plotted on this diagram, most of the Adigrat Sandstone samples plot in the mafic provenance field, minor sample fall on intermediate igneous provenance and few samples fall in recycled sedimentary provenance (Fig.4.7).

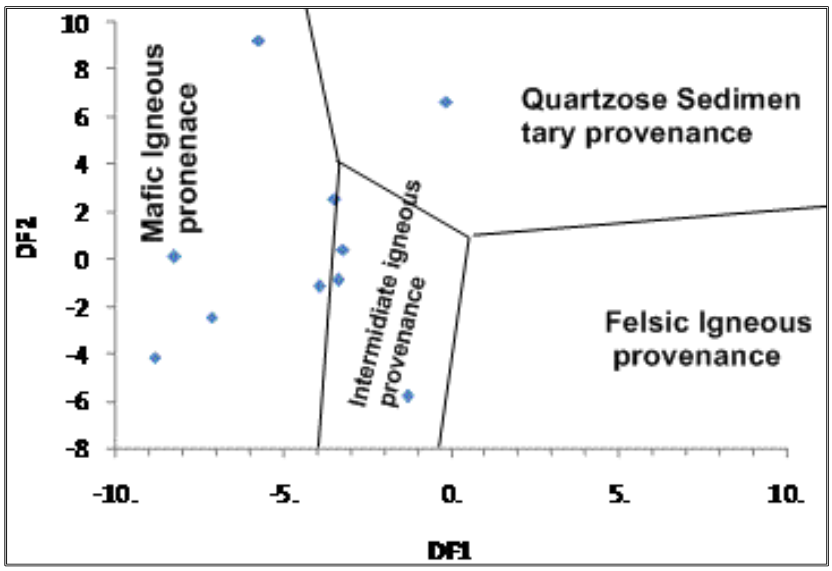

Figure 4. 7 Discriminant function (DF) diagram for the provenance signature of Adigrat sandstone (after Roser and Korsch, 1988).

4.2.2.2 Trace and REE Geochemistry

The REEs and High Field Strength Elements (HFSE, including Y, Zr, Ti, Nb, Ta), Th, Sc, Hf, and Co are the most suitable ones for provenance determination, because of their relatively low mobility during weathering, transport, diagenesis, and metamorphism (Taylor and McLennan, 1985; Fedo *et al*., 1996; Cullers and Berendsen, 1998). Ratios of both incompatible and compatible elements are useful for differentiating between felsic and mafic source components (Cullers and Graf, 1983).

Furthermore, the Eu anomaly[4] (Eu/Eu*), $(La/Lu)_N$, La/Sc, Th/Sc, Cr/Th, La/Cr, and Th/Cr, ratios of the sandstones are either similar to sediments derived from felsic source rocks or to mafic source rocks from which they may be derived (McLennan et al., 1993; Mongelli et al., 1998). Because they are significantly different in mafic and felsic source rocks and can, therefore, provide information about the provenance of sedimentary rocks (Amstrong-Altrin et al., 2004). These elements probably transferred quantitatively in to clastic material during

[4] In geochemistry, Eu anomaly is defined as the phenomenon whereby Europium (Eu) concentration is either depleted or enriched in a rock relative to the other (REEs). An Eu anomaly is said to be "negative" if Eu is depleted relative to the other REEs and is said to be "positive" if Eu is enriched relative to the other REEs and is calculated by the equation $Eu/Eu^* = Eu_{cn}/ [(Sm_{cn})(Gd_{cn})]$.

weathering and transportation, reflecting the signature of the parent materials (Armistrong-Altrin, 2004), and hence are expected to be more useful in discriminating source rocks composition than the major element (Bhatia and Crook 1986; McLennan 1989; Condie 1993). The REE and Th abundances are higher in felsic igneous rocks and in their weathering products, whereas Co, Sc, Ni, and Cr are more concentrated in mafic than in felsic igneous rocks.

Yanjing and Yongchao, 1997 based on the studies of the Early Precambrian sediments from the North China Craton, have convincingly argued that the REE patterns (including Eu anomalies) although mostly depend on their provenance, but can be controlled by fO_2 and sedimentary environment. They observed that when fO_2 is low (reducing environment), the sediments deposited in this environment should be characterized by low total REE and positive Eu anomaly. Whereas sediments deposited in oxidizing conditions (i.e. fO_2 is high) should be characterized by high total REE and Eu depletion Yanjing and Yongchao (1997). The red coloration resulted from oxidation of iron at the bottom part of Adigrat Sandstone coincides with this idea, since the lower most samples have higher REE values (Fig.4.8). However, this idea exactly corresponds with the theory of dilution by silica and is difficult to distinguish between the two effects on REE concentrations.

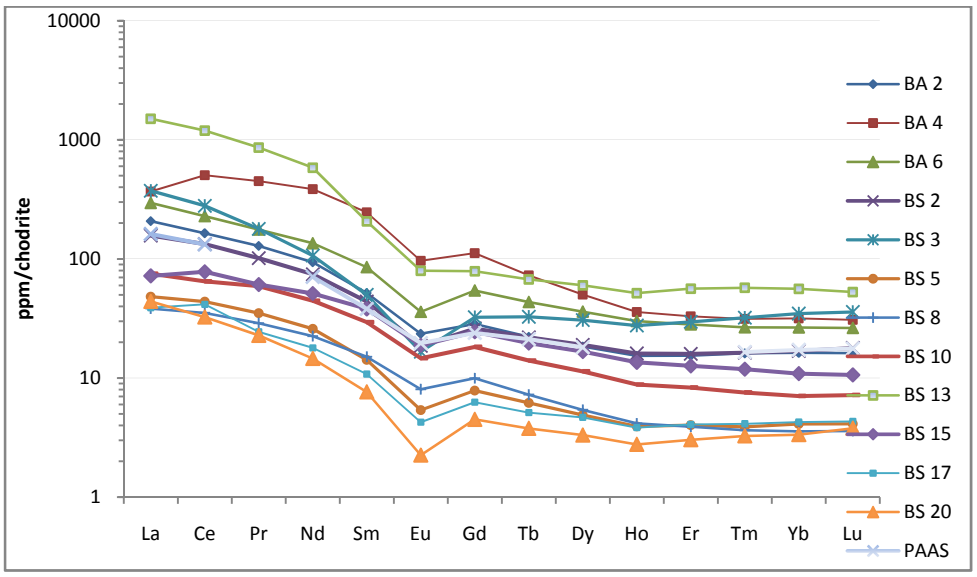

Figure 4. 8 Chondrite normalized REE plot for Adigrat Sandstone (Data of Chondrite values are from Anders and Grevesse, 1989 and PAAS from Taylor & McLennan 1985).

Ratios between incompatible-compatible elements are also proposed for provenance discriminations. High La/Cr and Th/Cr value in sandstone indicate that the sediments were derived from granitic rocks (George, *et al*., 2001). Mongelli et al., 2006, proposed Cr/V vs. Y/Ni binary diagram to discriminate source of sandstone from ultramafic to granite end member. Accordingly, the Adigrat Sandstone samples have Y/Ni and Cr/V ratios, which closely mount upneither to mafic nor to granite field, rather evenly distributed between the two end members (Fig.4.9). Ultramafic sources have very low Y/Ni and high Cr/V ratio where as granite source have high Y/Ni and very low Cr/V ratio.

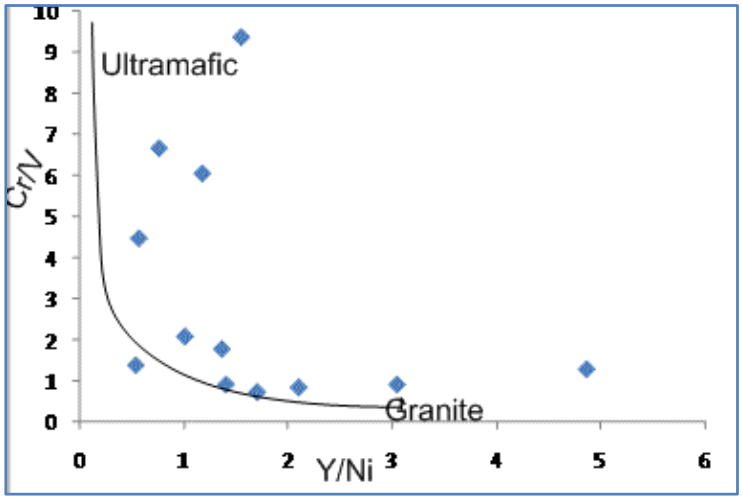

Figure 4. 9Cr/V vs. Y/Ni diagram Curve model mixing between granite and ultramafic end-members (After Mongelli et al., 2006)

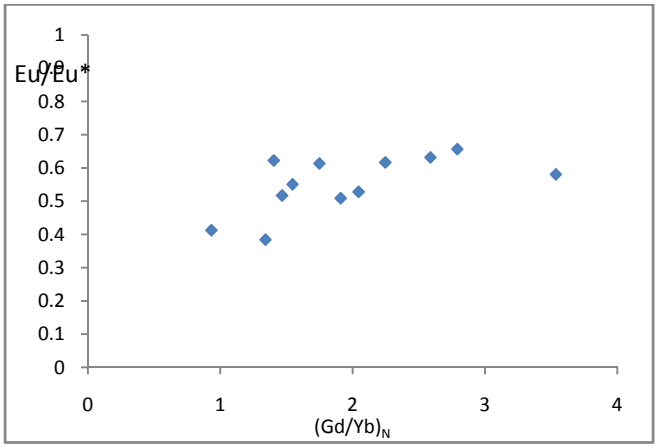

Figure 4. 10 The scatter plot of $(Eu/Eu^*)_N$ vs. $(Gd/Yb)_{cn}$ ratios

Al_2O_3/TiO_2 ratios of most clastic rocks are essentially used to infer the source rock compositions, because the Al_2O_3/TiO_2 ratio increases from **3** to **8** for mafic igneous rocks, from **8** to **21** for intermediate rocks, and from **21** to **70** for felsic igneous rocks (Hayashi *et al.*, 1997). The Al_2O_3/TiO_2 ratios for Adigrat sandstone in BNB is essentially identical and range between **6.77** to **22.87.** Thus, the Al_2O_3/TiO_2 ratio of this study suggests that mafic to intermediate granitoid rocks must be the probable source rocks for this unit. Actually these oxides are resistant to sedimentary processes, and both are fractionated together as we can observe their strong positive linear correlation (R^2 =0.922) (Fig.4.6), so that they can be a reliable provenance implication.

The REE patterns of the analyzed samples are shown in Figure 4.8. It is noteworthy that all the samples exhibit similar patterns (except sample BA4), and are characterized by moderately enriched LREE, flat HREE, and moderately negative Eu anomaly. The patterns are similar with Post Archean Australian Shale patterns (PAAS). Relatively low total REE abundances observed in the samples of Adigrat Sandstone at upper section are probably due to dilution by silica as they show negative linear correlation, (Appendix 3). The Adigrat Sandstone samples reveal moderately fractionated REE patterns (avg. La_N/Yb_N ~12.03) with lower total REE abundances. Most significant are moderate negative Eu anomalies (average value Eu/Eu* ~0.55), which are typical but slightly lower than post-Archean sediments (Eu/Eu* = 0.65 ± 0.03).

Sample	$(La/Yb)_N$	$(La/Lu)_N$	(Eu/Eu*)	$(Gd/yb)_N$
AVG	12.03	11.99	0.552	1.96
UCC	10.95	10.35	0.700	1.69
PAAS	9.396	9.149	0.65	1.39

Table 4.1 Comparisons of Chondrite normalized ratios $(La/Yb)_N$, $(La/Lu)_N$ and $(Eu/Eu^*)_N$ of AVG(Average values of Adigrat Sandstone samples) vs UCC and PAAS.

Co and Sc are among trace elements, which are considered immobile during sedimentary processes. For this reason, they are widely used in provenance discrimination. Co and Sc are enriched in mafic source rocks than felsic source rocks. Furthermore, diagrams such as Th/Co or Co/Th ratio and Th, Co, Hf are used to distinguish between felsic source and mafic source composition.

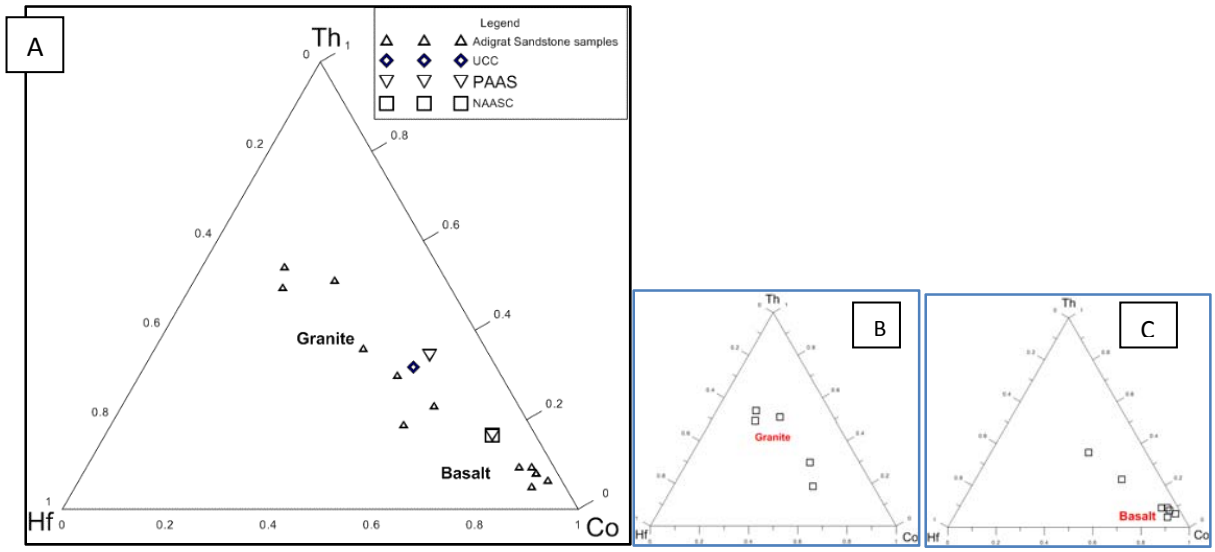

Figure 4. 11 The Th-Hf-Co ternary diagram A) all sample distribution B) lower most part fall within acidic source and C) upper part fall within mafic source, UCC, PAAS and NASC values are included for comparison (After Nath et al.,2000)

From Th-Hf-Co ternary diagram we clearly observe that Adigrat sandstone are derived from mixed source composition, where minor samples from the lower most section of Adigrat Sandstone unit fall around granite source (towards felsic field), above UCC composition and

most samples from middle and upper part of Adigrat Sandstone plot within mafic to intermediate source fields

4.3 Comparison of Adigrat Sandstone from Blue Nile (BNB) with Adigrat Sandstone from Mekele Basin5 (MB)

4.3.1 Source rocks comparisons

There are slight variation in sedimentary geochemistry of the Adigrat Sandstone in two selected localities, namely the Blue Nile Basin (BNB) and the Mekele Basin (MB). The latter has average Silica value ~ 89.64 at Agbe section, 86.42 at Mekele section, 91.95 at Wikro section and 93.32 at Chewet section, which are much greater than average silica value of Adigrat sandstone in BNB (~78.25). The total REEs concentration, nevertheless, is by far larger for Adigrat Sandstone in BNB than that of MB at all sections. The cause of the depletion of REE in MB may have at least two reasons. One may be attributed to dilutions of REEs by silica, as the silica content is higher in the MB. The second explanation is the latter removal of REE by secondary process from hosting mineral. The REE in MB show moderate correlation with K_2O and Al_2O_3 (0.68, 0.64 respectively). This suggests that REE to moderate extent is hosted by clay mineral from which latter sedimentary process can easily removes the REE. In case of BNB since the accessory mineral is the main hosting mineral (Fig. 4.6), later secondary cannot easily removes the REE.

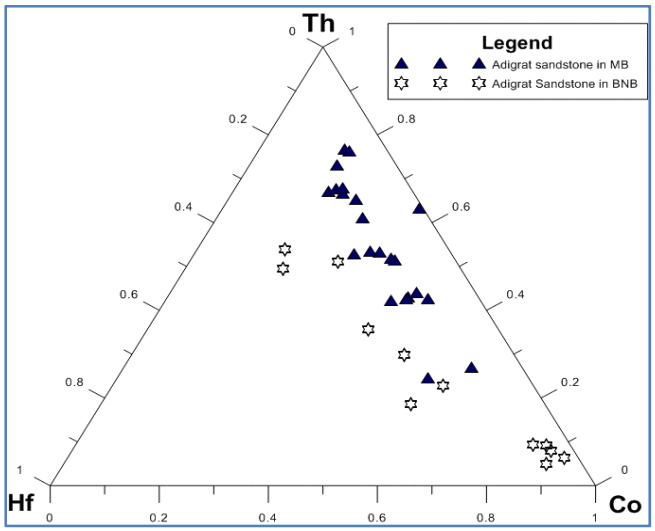

[5] Data from Worash Getaneh, 2002

Figure 4. 12 Provenance Comparisons of Adigrat sandstone in BNB vs. MB using Th-Co-Hf ternary diagram.

Significant difference in their provenance composition between Adigrat Sandstone in MB and BNB is observed easily from the comparisons diagrams (Fig. 4.12 and 4.13 a&b). On the Th-Co-Hf ternary diagram, the Adigrat Sandstone samples from MB are plotted almost above average UCC and PAAS values towards the granite source field (directed to Th apex). On the other hand, most of the Adigrat Sandstone samples from BNB are plotted within the mafic and minor samples is plotted from intermediate to granite fields. Another observation is that data point for Adigrat sandstone in BNB show little shift towards Hf apex than samples of Adigrat sandstone from MB. This is because; Zr and Hf are strongly correlated in Adigrat sandstone of BNB (Fig.4.6d) and sorted together with Zircon. High Zr enrichment in case of BNB is the result of pronounced sorting which is observed on ternary comparison diagram (Fig. 4.15).

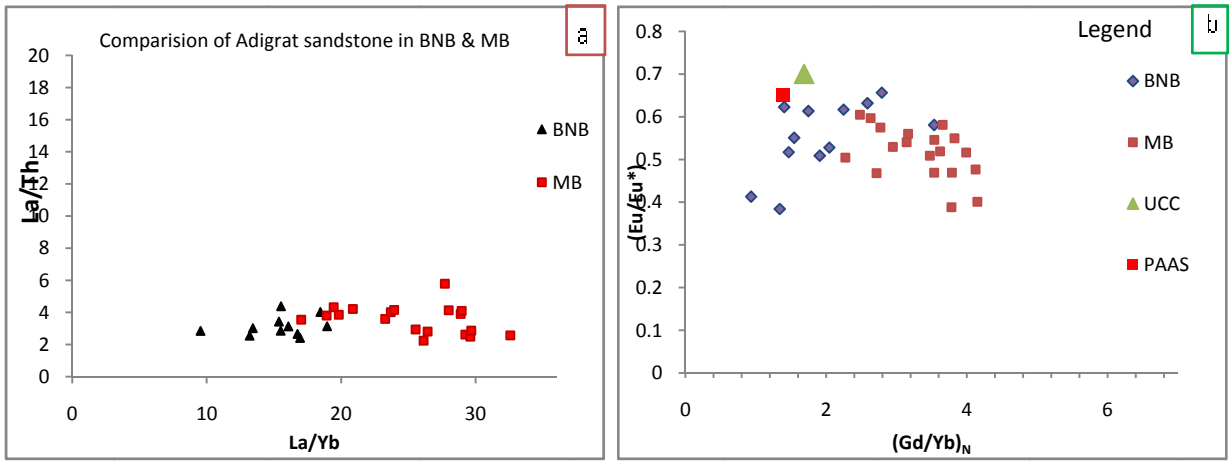

Figure 4. 13 Scatter plot for comparison of Adigrat Sandstone at BNB and MB a) La/Th vs. La/Yb b) $(Eu/Eu^*)_N$ vs $(Gd/Yb)_N$ to characterize and compare source composition.

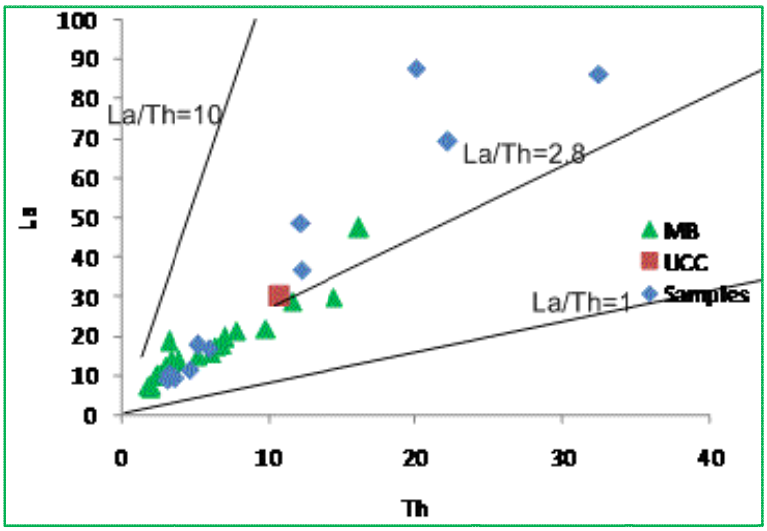

Figure 4. 14 La versus Th plot for the Adigrat sandstone samples. The La/Th = 2.8 ratio is that of upper continental crust (UCC, data from Taylor and McLennan, 1985), MB-Mekele Basin data from Worash, 2002), Samples= for BNB

On the other hand, data from the upper section of Adigrat sandstone whose depositional environment were interpreted as barrier lagoon to wave dominated shoreface by Dawit and Bussert, (2009) are plotted faithfully on the basalt field where as the lower most part are plotted in the vicinity of granite field. Similar fashions are repeated on La/Th vs. La/Yb and $(Eu/Eu^*)_N$ vs $(Gd/Yb)_N$ plots. From Fig.4.13, we can observe that the Adigrat Sandstone in MB has higher La/Yb and $(Gd/Yb)_N$ value. This indicates that source rocks for Adigrat Sandstone from MB were evolved more significantly than source rocks of Adigrat sandstone in BNB for the reason that Yb is more compatible than La and Gd. Samples from Mekele Basin are characterized by higher values of La/Yb and $(Gd/Yb)_N$ ratios. On the La/Th plot (Fig. 4.14), most of the Adigrat sandstone data significantly fails higher than the range of UCC, with small samples plotted below average UCC composition. This indicates that the sediments did not have a uniform provenance. The ratio of La to Th ranges from 2.41 to 5.48, also suggesting a mixed source of sediments.

4.3.2 Sorting recycling and transportation Effect

It is well known that recycling, transport and deposition of clastic sediments involves mechanical sorting. Its effect on the chemical composition of terrigeneous sediments is important (Mongelli *et al.,* 2006). From mineralogical analysis discussed above, samples of Adigrat Sandstone at different section show variable texture and grain morphology. These textural variations may be the result of sorting and recycling which in turn have significant effect on chemical composition and this can easily be observed either on the Upper crust-normalized spider diagrams (Fig. 5.8) or most precisely in the Al_2O_3-TiO_2 –Zr ternary diagram below. On the spider diagram fig. 4.8, samples show similar pattern. However depending on their degree of sorting and recycling slight variation in their concentration are observed. Similarly, Al_2O_3-TiO_2 –Zr ternary diagram (Fig.4.15) shows zircon addition as sediment undergoes sorting. Zr and Hf in sediments are controlled by zircon, and due to a combination of resistance to weathering and high specific gravity, this mineral suffers a sorting related fractionation (gravitative fractionation), (Taylor and McLennan, 1985). Therefore, in comparison to Adigrat Sandstone from MB, Adigrat Sandstone from BNB encountered high sorting related fractionation

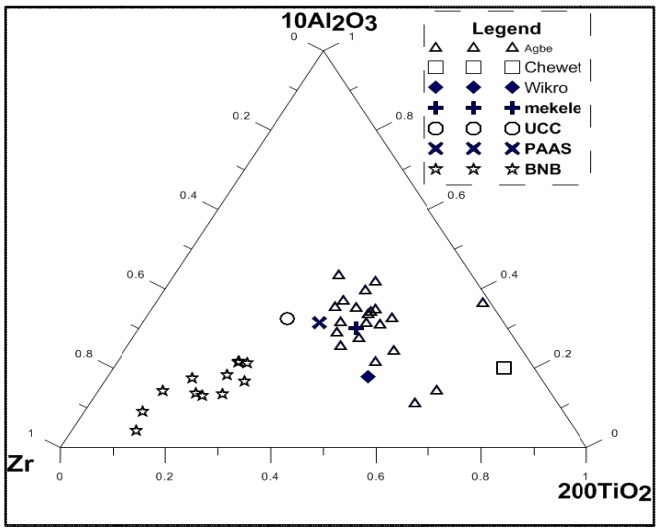

Figure 4. 15 Ternary $10Al_2O_3$-$200TiO_2$-Zr plot showing possible sorting effects (Garcia *et al*., 1991) for Comparison between Adigrat sandstone from two localities

Unless and otherwise comparatively speaking source of the Adigrat Sandstone from both regions were modified more or less by all processes (sorting, recycling and intense weathering). However, enrichment of silica values for the Adigrat Sandstone in the MB as compared to BNB is neither due to intense weathering nor due to sorting and recycling. Various weathering indexes have been calculated and all consistently show that the Adigrat Sandstone from both regions undergo intense chemical weathering. Nevertheless, source rocks of the ASSt in BNB had experienced higher intense chemical weathering as compared to that of MB. Furthermore, degree of sorting and recycling are compared using diagrams shown above (Fig. 4.12 and Fig.4.15.). These diagrams potentially suggest degree of sorting and recycling matters ASSt from BNB than that of MB. Therefore, an extreme enrichment of silica in case of MB is most probably the matter of provenance composition as exceedingly supported by ternary diagrams (Fig. 4.12) and binary diagram Fig.4.13 and Fig. 4.14.

4.4 DISCUSSION

Geochemistry and mineralogy of Adigrat sandstone from Blue Nile Basin sedimentary succession, northwestern Ethiopian plateau suggests a complex history.

Mineralogy: All the studied samples contain both strained and unstrained quartz grains. The occurrence of both strain and unstrained quartz suggest that some of the strain was inherited from the source area and, therefore, suggest a metamorphic and/ or plutonic source for the quartz grains (Young, 1976).

The relatively high proportion of strained monocrystalline quartz and strained polycrystalline quartz with sutured contacts between crystals over other types of quartz grains, coupled with the generally low content of lithic fragments may suggest their derivation from mainly plutonic/metamorphic rocks. Presence of polycrystalline quartz grains with elongate crystals and straight intercrystalline boundaries rule out significant contribution from metamorphic source rocks. However, the presence of rare rounded detrital quartz grains, sedimentary lithic fragments, such as quartz arenite, and rounded grains of zircon and sphene suggest that a component of the provenance is pre-existing sediment (reworked sediment). The high proportion of quartz (and quartzose lithic fragments), as well as the dominance of K-feldspar over the more chemically unstable plagioclase in the sandstones suggests that the source was exposed to prolonged weathering and that the sediment is at least partly multicyclic which is consistent with chemical data. Complete weathering result in the removal of clay, feldspar and lithic fragment living behind the quartz minerals at high-energy environments, which mainly characterizes the upper section of this unit.

Geochemistry: Composition of Adigrat sandstone is the complex interplay of many processes. Major oxide provenance discrimination method suggests that the Adigrat Sandstone in BNB was derived from mixed source mainly from mafic igneous, minor from intermediate contribution and very few from quartzose sedimentary provenance. Trace element ratios such as that of Mongelli *et al*., 2006, Nath et al., 2000, George *et al.,* 2001 and the Th-Co-Hf ternary diagram suggests, this Sandstone was derived from mixed sources mainly from mafic and minor contribution from intermediate to felsic source. The REE ratios and their pattern suggest the provenance composition of this sandstone is intermediate igneous rocks. The relatively enrichment of LREEs, the moderate negative Eu-anomalies and the flat HREE patterns of the

Adigrat Sandstone in the study area suggest derivation from an old upper continental crust composed chiefly of intermediate igneous rocks. However, there is a minor discrepancy between major oxides and trace element ratios with REE pattern. This discrepancy is explained as follows. There are at least two possible reasons. Although the REE are quantitatively transferred from the source to the sediment (McLennan *et al*., 1993), intense weathering produces LREE/HREE fractionation (Mongelli, 1998), possibly due to preferential HREE retention in solution (Cantrell and Byrne, 1987). Second, as trace, REE ratios and Discriminant function diagram generally suggests, there was mixing of source rocks whose compositions is variable. Therefore, mixing of different sources may result in REE pattern that is intermediate between the constituent rocks. These intricate ideas may be easily envisaged when Adigrat Sandstone from the two distinct basins are compared. The REE geochemistry, HFSE and LILE (those robust to sedimentary processes and advocated to be helpful for provenance implication) of Adigrat Sandstone from two locations is evaluated for provenance comparisons. Accordingly, the result show significant difference between them. The Chondrite normalized average Gd/Yb ratios for Adigrat Sandstone in the BNB and the MB basin (at Agbe section) are 1.96 and 6.91 respectively. Similarly, the $(La/Yb)_N$ for Adigrat Sandstone in the BNB and MB (average values 12.03 and 39.42 respectively) and the Th-La scatter plot (Fig. 4.14) show significant difference. These diagram and others all consistently suggest the same thought and demonstrate that there is remarkable difference in their source composition. The relatively low content of silica values for Adigrat sandstone from BNB than that of the Adigrat Sandstone from MB is not the effect of less weathering intensity rather attributed to provenance composition. The source rocks for Adigrat sandstone in MB experienced intense weathering but less slightly than that of the BNB as dictated by Chemical index of alteration and other weathering indexes.

5 PALEOWEATHERING AND PALEOCLIMATE SCENARIOS

5.1 Introduction

Weathering is the process by which rocks are physically and/or chemically broken down into relatively fine solids (soil or sediment particles) and dissolved components. The chemical component of weathering is more precisely described as the process by which rocks originally formed at higher temperatures come to equilibrium with water at temperatures prevailing at the surface of the earth.

Weathering plays a key role in the exogenic geochemical cycle (the cycle operating at the surface of the earth). Silicate weathering is significant buffer to acidification caused by atmospheric deposition (Driscoll et al., 1989). Atmospheric CO_2 levels have been primarily controlled by the balance between silicate weathering and the rate of volcanic input from the earth's interior (Ruddiman, 1997). These relationships convey long-term climate stability (Ruddiman, 1997).

In their model of atmospheric CO_2 levels, Berner et al., (1983) and Berner (1991) assumed that temperature is a strong control on weathering rate, and therefore there is a negative feedback that controls atmospheric CO_2 levels. The higher the global temperature, the higher the weathering rate, and therefore the higher the consumption of atmospheric CO_2. Weathering thus appears to be an important control on the concentration of atmospheric CO_2, which is in turn an important control on global temperature and climate. Hence, whatever factors control the weathering rate may also control climate.

Chemical weathering supplies both dissolved and suspended matter to rivers and seas. It is the principal reason that the ocean is salty. Weathering also supplies nutrients to the biota in form of dissolved components in the soil solution. Without weathering, terrestrial life would be far different and far more limited. Weathering can be an important source of ores, creates significant ore deposit, such as those of Al, U as well as potentially releasing high concentration of toxic trace elements such as Se, and As (Frankenberger and benson, 1994).

At larger scale observation, like any other chemical reaction, mass is conserved in weathering reactions assuming a system is *steady state*[6]. Mathematically, we may write the mass balance equation as:

Rock + climate = altered rock (sediment) + solution

Thus if the composition of the original rock, input composition , and the final water composition (the dissolved component) are known, then the gross composition of the secondary phases can be calculated. From petrographic, electron microprobe and X-ray diffraction study, Velbelos (1985a) found that the primary weathering reactions were the breakdown of biotite, garnet, and feldspar. Muscovite and quartz were not appreciably weathered and abundances of other minerals were too small to affect the mass balance. Consider, for example, weathering of feldspar

$$2NaAlSi_3O_8 + 2H_2CO_3^0 + 9H_2O\ (l) \rightarrow 2Na^+ + 2HCO_3^- + Al_2Si_2O_5(OH)_4\ (kaolinite) + 4H_4SiO_4^0$$

From thermodynamic perspectives, the Gibbs free energy change of reaction is written as:

$$\Delta_r G^0 = 2\Delta_f G_{Na+} + 2\Delta_f G_{HCO3-} + \Delta_f G_{Al2Si2O5(OH)4} + 4\Delta_f G_{H4SiO40} - (2\Delta_f G_{NaAlSi3O8} + 2\Delta_f G_{H2CO30} + 9\Delta_f G_{H2O})$$

Or in a simplified way $\Delta_r G = \sum_{products} \Delta_f G - \sum_{reactants} \Delta_f G$ ……..1

Where $\Delta_r G$) is the Gibbs free energy change of reaction and $\Delta_f G$ is Gibbs free energies change of formation. This equation tells us that when $\Delta_r G = 0$, the reaction is at equilibrium; when $\Delta_r G < 0$, the reaction will proceed to the right or favors the dissolution of feldspar; when $\Delta_r G > 0$, the dissolution of feldspar is inhibited.

The equilibrium constant for a reaction of the type is written

$$\log K_{SP} = \frac{-\Delta_r G^o}{2.303RT} \qquad \text{……..…2}$$

Where R is the gas constant and equals 8.314 J K^{-1} mol^{-1} or 1.987 cal K^{-1} mol^{-1}. The Gibbs free energies of formation ($\Delta_f G°$) of the reactants and products are quantities that determined from

[6] steady state is state in which any internal cycling will not affect the net output of the system

experiment. The $\Delta_r G°$ refers to the reaction in which reactants and products are all at STP, whereas the equilibrium constant *K* refers to the reaction in which reactants and products are in some real, non-standard state. From expression 2 above, we can easily observe that the type of mineral and T are the principal parameters in silicate weathering. Because, the K-value depends on the temperature and the Gibbs free energy change of reaction, which in turn depend on the Gibbs free energy change of formation of the mineral tends to weather and its product.

5.2 Paleoweathering and paleoclimate scenarios

Mineralogical and chemical compositions of siliciclastic deposits depend on the intensity of chemical weathering linked to the climate in provenance terrains (Nesbitt and Young, 1982; Fedo et al., 1997). Various geochemical and mineralogical climate proxies have been developed. Some of these proxies are based on dissolved loads in rivers, while others depend on solid phase. The dissolved load directly indicates weathering status at present but cannot reflect an integrated weathering history (Johnson and Stallard 1989). However, other geochemical indexes, which focus on solid phase geochemistry of sediment /sedimentary rocks, were proposed to investigate weathering history. Therefore, this thesis research is a solid phase geochemistry based relying geochemical indexes to interpret plaeoweathering and pleoclimate

5.2.1 Whole-rock geochemistry

The Appendix part lists the results of the major and trace element analyses for the Adigrat Sandstone. There is a slight variation in the major element content for all analyzed samples. For example, the SiO_2 contents range from 51.36 to 96.12 wt%, the TiO_2 content range from 0.04 to 1.23 wt%, the Al_2O_3 content range from 0.94 to 20.99 wt%, and the Fe_2O_3 content ranges from 0.17 to 8.03 wt%. Due to intense weathering, the CaO and MgO contents are low. However, an anomalously high CaO values are observed on two samples. This is most probably due to high content of calcite cement in the sample. Petrographic data supports this idea; especially in this sample, calcite veins are also observed. When the linear correlation coefficient is determined by plotting CaO values against Al_2O_3, Na_2O, K_2O, P_2O_5 and TiO_2 values, very low R^2 values (0.246, 0.088, 0.6, 0.074 and 0.201 respectively) are displayed (Fig. 4.1). This implies that large

portion of CaO in these samples is not contained in silicate minerals, rather originate from carbonate one. In another case, this high concentration of CaO has unenthusiastic profound effect on the weathering indices, i.e. lowers the values of, for example, CIA and draw out values close to CN apex on A-CN-K diagram (Fig. 5.2).

5.2.1.1 Major Oxide's climate proxies (CIA, CIW and PIA)

Silicate weathering strongly affects the major-element geochemistry and mineralogy of silicilastic sediments (Nesbitt and Young 1982; Johnsson et al., 1988; McLennan, 1993), where larger cations (Al_2O_3, Ba, Rb) remain fixed in the weathering profile preferentially over smaller cations (Ca,Na, Sr), which are selectively leached (Nesbitt et al., 1980).

The Chemical Indexes of Alteration of Nusbett and Yung (1982), the Chemical Index of Weathering of Harnois, (1988) and the Plagioclase Index of Weathering of Fedo *et al*., (1995), are among climate proxies, which rely on major oxides solid phase geochemistry. The Chemical Index of Alteration (CIA) was pioneered by Nesbitt and Young (1982), to quantitatively evaluate weathering history recorded in sediments and sedimentary rocks (McLennan, 1993; Yang *et al*., 2004, etc). Unweathered plagioclase has PIA value of 50 whereas the PAAS has PIA value of 79. The CIA values calculated for Adigrat Sandstone in the Blue Nile Basin range from 78.4 to 97.8 with average value of 88.1. The resultant CIA gives a measure of the proportion of secondary aluminous clay minerals to primary silicate minerals such as feldspars (Nesbitt and Young1982; Young et al., 1998).

CIA is defined as

$$\mathbf{CIA} = \frac{Al_2O_3}{Al2O_3 + CaO^* + Na_2O + K_2O} \times 100$$

Where oxides are in their molar contents, with CaO* being CaO content in silicate fraction of the sample. Therefore, CaO* has been corrected before calculating the weathering indices. CaO is mainly contained in the phosphate (apatite) and carbonate minerals (calcite and dolomite) except for silicate minerals.

There are two ways to correct non-silicate carbonate. One is destroying carbonaceous Ca^{2+} from the sample during sample preparation. Second, the Correction method proposed by McLennan

1983 is considered. In this research since CaO measured is total CaO, an assumption proposed by McLennan, 1983 are adopted.

First non-silicate carbonate originated from apatite is corrected according to equation proposed by McLennan (1983), $CaO^*=CaO-10/3P_2O_5$. Then CaO* has been corrected for carbonate origin. Suppose that CaO_R represents the mole fraction of remainder CaO after eliminating CaO from apatite. If $CaO_R \leq Na_2O$, then the value of CaO_R is accepted if, however, $CaO_R > Na_2O$, then $CaO^*=Na_2O$. There are two possible conditions in which carbonate mineral occur in the clastic rocks. One may be the presence of sediments of carbonate rock. Another is attributed to the leaching of upper carbonate rocks in the study area.

The calculated Chemical Index of Alteration is plotted against chronostratigraphic log of the Adigrat sandstone (Fig.5.3) to temporally calibrate the weathering intensity and the paleoclimatic scenario.

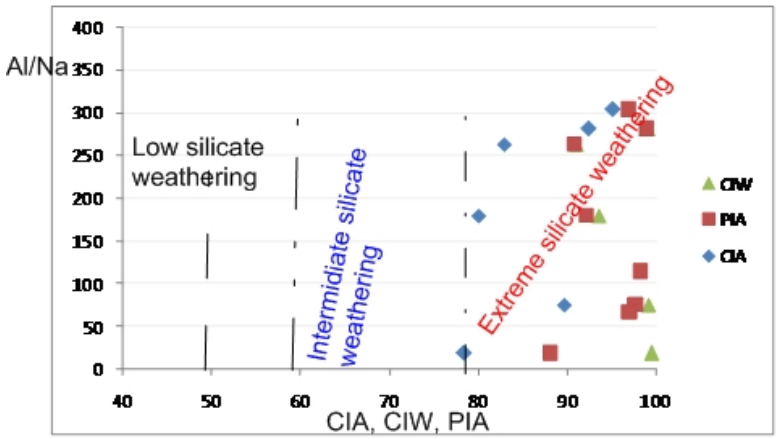

Figure 5. 1 Scatter plot of Al/Na ratio versus various Chemical Weathering Indexes (After Kandasamy and Chen-Tung Chen, 2004). Note the interrelation between all indexes, which reflects the silicate weathering intensity.

Since the CIA index is not sensitive to the weathering degree when K reintroduction occurs in the system, (but not the matter of the present case), alternative indices can be used to monitor paleo-weathering at the source. Harnois (1988) proposed the CIW index (Chemical Index of Weathering) which is not sensitive to post depositional K-enrichments.

$$\mathbf{CIW = [Al_2O_3/ (Al_2O_3 + CaO^* + Na_2O)] \times 100}$$

Similar to the CIA, it is a molecular immobile-mobile ratio, based on the assumption that Al remains in the system and accumulates in the residue while Ca and Na are leached away

Similar to CIA, CaO* is the amount of CaO incorporated in the silicate fraction only. The CIW for Adigrat sandstone in the Blue Nile Basin is calculated and ranges from 91.1 to 97.1 with average value of 97.0. Similarly PIA is also determined, the values (90.1 to 99.5) all consistent with both CIA and CIW. Large-Ion Lithophile Elements: Rb, Sr, K, and Na have also been analyzed as a weathering indices. Because increase in chemical weathering intensity rapidly leaches Sr compared to Rb (Nesbitt and Young 1982); therefore, the Rb/Sr ratio increases with increasing CIA (Ma et al. 2000). Likewise, with the increase in chemical weathering intensity, K will normally show depletion against Rb (Gronkiewicz and Condie 1989), thus leading to a lower K/Rb ratio. Rb has been considered primarily fixed in weathering residues and is less reactive than Ca, Na, and Sr (Nesbitt et al. 1980). Based on this assumption these large ion lithophile elements are used as weathering indexes. The results are all consistent with other weathering indexes. For example, the K/Rb ratio for Adigrat sandstone is calculated (avg~118) is calculated and compared with average K/Rb value of UCC (248), the values are much lower in the the Adigrat Sandstone due to preferential leaching of K over Rb because of intense weathering

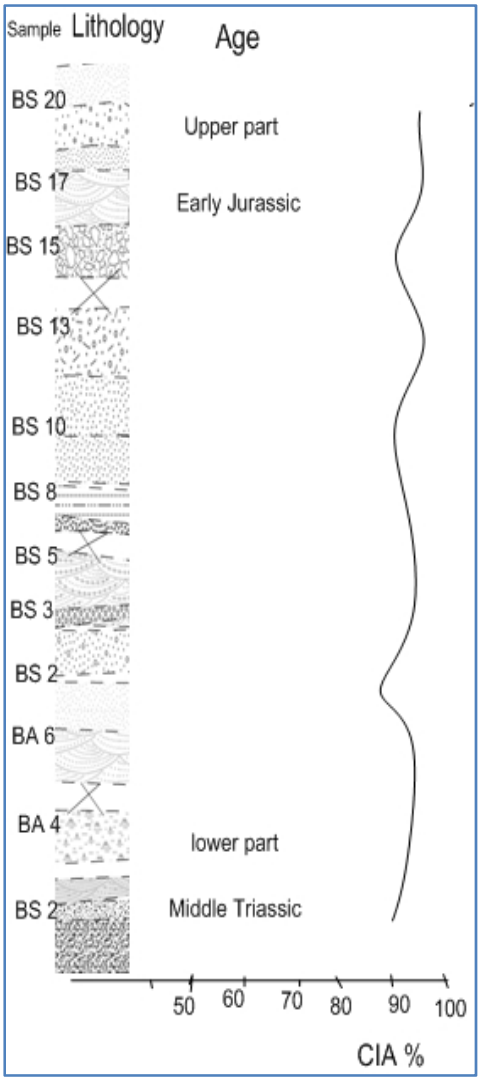

Figure 5. 2 Liotho-log vs. CIA diagram showing temporal evolution of chemical weathering depicted by the CIA as a climate proxy. (The legend for this lithologic column is described in Fig. 3. 5).

Molar ratios of Al/Na (AVG. ~148.12) of the Adigrat Sandstone are correlated well with Rb/Sr ratios as well as CIA and PIA values (Fig. 5.2). Both ratios are high enough above different shale compositions demonstrating intense silicate weathering. High K/Na and Rb/Sr ratios of sandstone indicate stronger chemical weathering at higher altitudes as well as preferential dissolution of plagioclase (Na and Sr) relative to K-feldspar during the silicate weathering process (Yang et al. 2004). The scatter plot of Al/Na ratio versus CIA (Fig.5.2) illustrates the interrelation between both indexes, which reflects the silicate weathering intensity. The diagram shows that the degree of chemical weathering was intense. This is evident by their very high Al/Na ratios (avg ~148.199) resulting from extreme dissolution of plagioclase. These inferences are consistent with their positions on the other triangular and scatter plots. In this study since major oxides are reported by their weight percent (wt %), they are converted in to their elemental concentration from weight percentage, then the concentration of an element obtained are changed to molecular value.

K/Cs McLennan et al., (1990) used the ratio of Cs and K as an indicator for climate conditions, because both elements are characteristically adsorbed on clay minerals during weathering, Cs as the larger ion is preferentially adsorbed over K. Thus, the K/Cs ratio should decrease with increasing chemical weathering. From this scatter diagram (fig .4.5). We can observe that K/Cs and CIA are negatively correlated with R^2-values about 0.74. This can be interpreted, as K- has been tending to remove preferentially to Cs as weathering intensity increase. Second, the K/Cs of our sample is very much lower than the K/Cs ratios' of UCC, which indicates intense weathering.

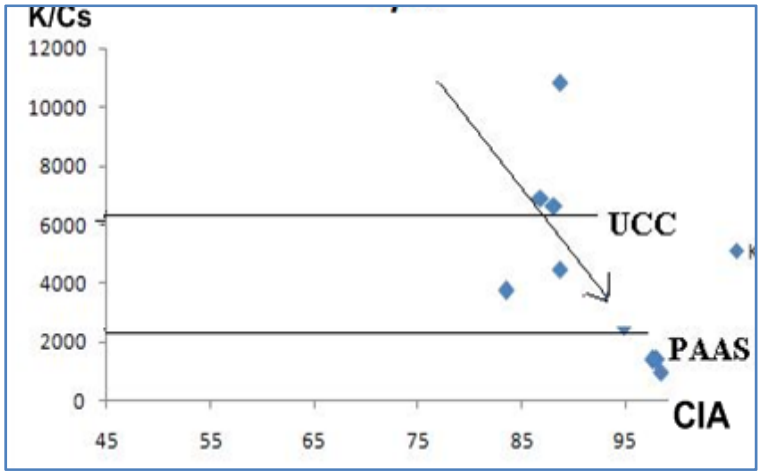

Figure 5. 3 Plot of K/Cs vs. CIA. The arrow marks the general weathering trends and shows enrichments of Cs relative to K in weathering products as weathering intensity increase. The result is compared with PAAS & UCC.

5.2.1.2 The A-CN-K diagram

Nesbett and young 1982, 1984, 1989, 1996 and Nesbett et al., 1996 used the ternary diagram Al_2O_3-(CaO + Na_2O)-K_2O (the A-CN-K), diagram and (Fe_2O_3 + MgO)-(CaO + Na_2O + K_2O)-Al_2O_3 (the A-CNK-FM, not shown to avoid redundancy), diagram to deduce weathering trends. On both diagram sandstone display an intense weathering history. The background information of this diagram is that during initial stages of weathering, Na and Ca are removed from the earlier dissolved plagioclase and those samples which have undergone weak weathering will plot close to the A–CN line. Advanced weathering results in the dissolution of K-feldspar to release K in preference to Al, so that the bulk composition trends of the residues are redirected to the Al_2O_3 apex.

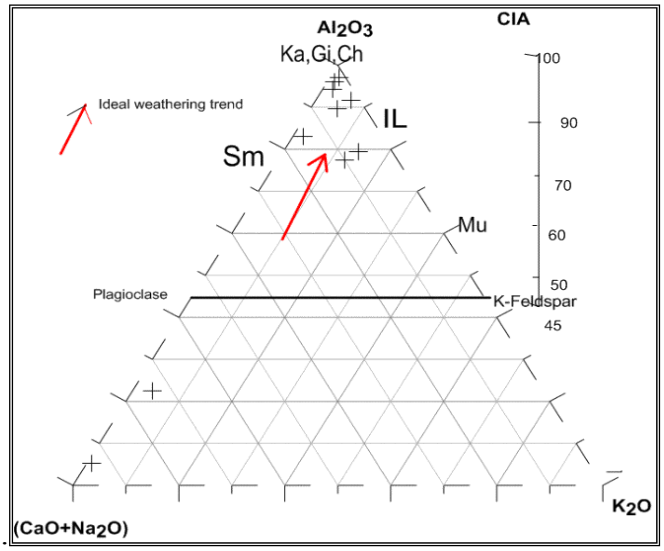

Figure 5. 4 The A-CN-K (Al_2O_3-($CaO+Na_2O$)-K_2O) ternary diagram to show weathering condition. The diagram also represents the fields of idealized minerals: Bi=biotite; Sm=smectite; Mu= muscovite; Il=illite; Ka=kaolinite; Gi=gibbsite; Ch=chlorite. Arrow indicate ideal weathering trend of fresh rocks with UCC composition.

The triangular A-CN-K diagram (Figure 5.5) allows the differentiation of compositional changes associated with chemical weathering and/or source rock composition (Fedo et al., 1997).From A-CN-K diagram we can observe that the Adigrat sandstone samples are fall with the line commensurate with the proposed ideal weathering trend of fresh rock sample with UCC composition. There is a clear observation that majority of samples are closed to Al_2O_3 apex.

5.2.1.3 Trace and Rare Earth Elements (REE)

Although the REE are quantitatively transferred from the source to the sediment (McLennan et al., 1993), intense weathering produces LREE/HREE fractionation (Mongelli, 1998), possibly due to preferential HREE retention in solution (Cantrell and Byrne, 1987). The Chondrite normalized REE plot for Adigrat sandstone is shown in Figure 5.5. To facilitate the interpretation of this sandstone other important reference REE compositions such as upper continental crust (UCC) and post- Archean shale have also been included for comparison.

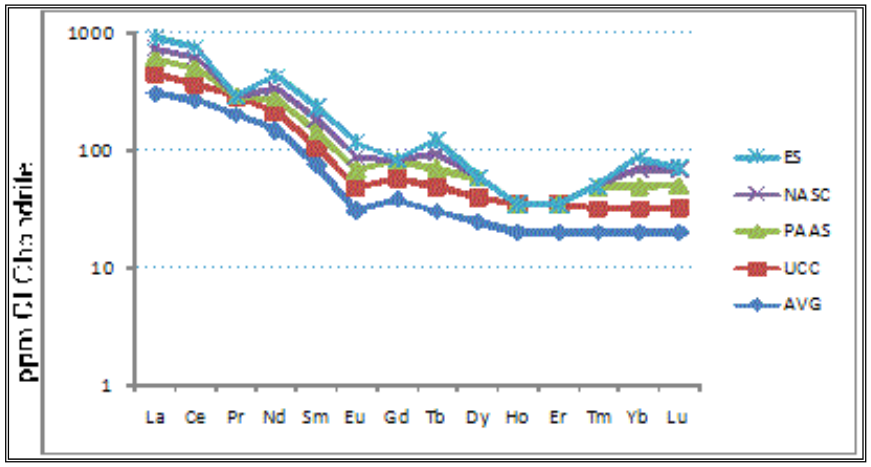

Figure 5. 5 Comparisons of the Chondrite normalized REE Plot of Average samples of Adigrat sandstone with various Post-Archean Shales and UCC. (PAAS from Taylor and McLennan 1985), and Where AVG= Average values of Adigrat sandstone, UCC=Upper Continental Crust, PAAS=post Archean Australian Shale, NASC= North American shale composite, ES=European Shale (data for Chondrite, UCC, PAAS, NASC and ES are from Anders and Grevesse (1989), Gao and Rudnick, 1998; Taylor and McLennan, 1985; Gromet et al., 1984; Haskin and Haskin, 1966 respectively).

The ratios of the light REE to relatively heavy REE for this sandstone sample are calculated and compared with the values of PAAS and UCC. The Adigrat sandstone may be recognized by higher values both by $(La/Yb)_N$ and $(La/Lu)_N$ ratio relatively to $(La/Yb)_N$ and $(La/Lu)_N$ Value of PAAS and the UCC. The evidence of intense paleoweathering at the source depicted by the $(La/Yb)_N$ and LREE/HREE fractionation is consistent with the results obtained using the weathering indices (CIW and PIA). Both CIW and PIA indices are strongly controlled by the amount of plagioclase in the rock. The significant correlations between these ratios and other major oxide weathering indices discussed above are strongly consistent.

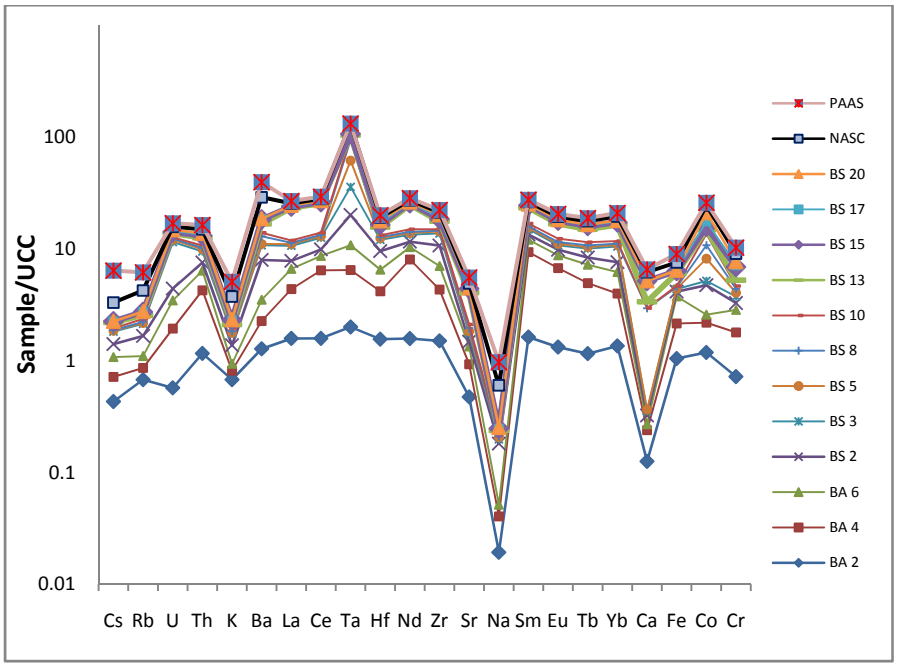

Figure 5. 6 Upper crust-normalized spider diagrams of certain elements for the Adigrat Sandstone (data for UCC from Gao and Rudnick, 1998)

The sandstone also show strongly fractionated REE patterns (avg. values of La_N/Yb_N ~12.03) with moderate negative Eu anomalies (Eu/Eu* avg ~0.55). Chondrite-normalized REE diagrams Patterns are similar to upper continental crust and typical post-Archean shales (Fig.5.6).

Upper crust-normalized spider diagrams of selected elements are also plotted (Fig. 4.6). The order of element used in the normalized diagram represents decrease of continental abundance with respect to primitive mantle of the earth or to Chondrite. The diagrams are most incompatible to the left and most compatible to the right. The patterns of all the sandstone samples are more or less similar supporting that the sedimentary mass is quite homogeneous in its composition (Taylor And McLennan, 1985). However, there is significance difference in elemental concentrations mainly due to variation in textural maturity. U show slight variation especially between upper and lower part of the Adigrat Sandstone. This is actually attributed to redox condition of the depositional environment as is manifested by oxidation of Fe in the lower most part of this lithology. Uranium depletion occurs if relatively insoluble $U^{4+}$is affected by oxidation to relatively soluble U^{6+}. The same condition affects Ce concentration. The diagram

clearly shows that mobile elements such as Na, K, Ca and Cs are strongly depleted where as immobile elements such as Ta, Sm, Ba and Co are relatively enriched.

5.3 Discussion

Major oxides and trace element geochemical paleoclimate proxies such as CIA, CIW, PIA and A-CN-K diagram have been applied on Adigrat Sandstone in the Blue Nile Basin. The average CIA, CIW and PIA values of Adigrat sandstone are 88.1, 97.0 and 95 respectively. The Adigrat Sandstone, with the exception of sample BS8 and BS15 show very uniform CIA, PIA and CIW values, and in the A-CN-K diagram form a tight array close to the A apex (Fig. 5.4) indicating that most of the mobile element was removed. This suggests intense weathering at the source area. Samples BS8 and BS15 show remarkable lower CIA, PIA and CIW values, which may be due to anomalously high CaO value and in turn high content of non-silicate CaO and not because of low weathering intensity. Non-silicate CaO correction has been made to characterize the weathering intensity according to correction method proposed by McLennan, 1985. In our sandstone samples, Potassium metasomatism is uncommon as easily observed on the A-CN-K diagram and K/Cs ratio, and therefore there is no need of K-metasomatic correction.

The REE patterns of the analyzed samples are shown in Figure 4.4 (chapter 4). It is noteworthy that all the samples exhibit similar patterns and are characterized by LREE-enriched similar with post-Archean shale patterns such as PAAS, and UCC. The $(La/Yb)_{ch}$ and $(La/Lu)_{CN}$ ratio of Adigrat Sandstone samples are relatively higher than $(La/Yb)_N$ and $(La/Lu)_{CN}$ value of the PAAS and the UCC(table 5.1). Multi-climate proxies has been applied, the result all approximately coincides. This leads as to the conclusion that Adigrat sandstone had source compositions, which were dominantly affected by chemical weathering than physical weathering. Therefore, the Adigrat Sandstone source material had experienced intense chemical weathering most likely under hot and humid conditions.

6 CONCLUSIONS AND RECOMMENDATIONS

6.1 CONCLUSIONS

The paleoweathering, paleoclimate and provenance composition of the Adigrat sandstone, BNB has been assessed using integrated petrographical and geochemical studies. Most of the samples are free of matrix and on QFL diagram; the rocks are dominantly subarkose and lithicsubarkose. The classification is broadly consistent with the geochemical data because on geochemical classification diagram, the Adigrat sandstone samples fall in the arkose to subarkose, sublitharenite and quartzarenite field. The prominent cementing material is calcite with subordinate amount of clay, iron oxides and silica in some samples. Petrographic interpretation of provenance composition indicates a provenance mixing for this sandstone. Both strain and unstrained quartz grains found in our sandstone samples. This suggests that some of the strain was inherited from the metamorphic and/ or plutonic source area. The high proportion of quartz (and quartzose lithic fragments), as well as the dominance of K-feldspar over the more chemically unstable plagioclase in the sandstones suggests that the source was exposed to prolonged weathering and the sediment is at least partly multicyclic.

Geochemically relatively immobile elements concentration, ratios and pattern have been given due attention for provenance interpretation. Relatively immobile major (Al, Ti) trace (Th, Co, Hf, , Cr, V, Y, Ni, Co) and REE element ratios, patterns, binary plots and ternary diagrams are selected for provenance interpretation. Particularly immobile element ratios preferred than their actual concentration and compared with reference Post Archean Shales and average Upper Continental Crust composition and with local and equivalent sandstone whose provenance composition were previously determined by Worash (2002). Among four sedimentary provenances distinguished by the discriminant functions diagram that were constructed from Al_2O_3, TiO_2, Fe_2O_{3T}, MgO, Na_2O, and K_2O variables, the Adigrat Sandstone plotted mainly within mafic, minor within intermediate and few samples fall within recycled sedimentary provenance. The slight enrichment of LREEs, the moderate negative Eu-anomalies and the flat HREE patterns of this Adigrat Sandstone in the study area suggest derivation from intermediate igneous rocks. Though disturbance due to weathering and recycling may have obscured the original signal of major elements, the result broadly agree with trace and REE, and all suggest the source of this sandstone were compositionally mixed between mafic and intermediate

igneous rock. The results are compared with Adigrat Sandstone in MB, which again support the above idea. High specific gravity elements that are expected to be affected by hydraulic sorting are selected to characterize degree of sorting and recycling. Accordingly, sediment of Adigrat Sandstone is remarkably affected by sorting related fractionations. Since Adigrat sandstone is deposited in complex depositional environment (Dawit, 2009), and its source was affected by multidirectional current, straightforward interpretation of paleoweathering, paleoclimate and provenance composition is not expected. Multidirectional currents are expected to bring mixed and heterogeneous sediment. Similarly, prevailing sedimentary processes affect geochemistry of this sandstone to certain extent and a great emphasis has been given in using geochemical methods for provenance interpretation.

Major oxides and trace element geochemical paleoclimate proxies such as CIA, CIW, PIA elemental ratios and A-CN-K diagram have been applied after correction of non-silicate CaO, on the Adigrat **S**andstone in the Blue Nile Basin. The calculated CIA, CIW, PIA values and the A - CN-K ternary diagram are extremely agreed and all suggest intense weathering at the source area. Therefore, humid and hot climatic condition is the inferred paleoclimate that favoring paleoweathering and sedimentation of the Adigrat Sandstone. The determined paleoclimate and paleoweathering scenarios are however the cumulative effect of all weathering cycle rather than a single episode of weathering effect as sediment were affected by high degree of sorting and recycling.

6.2 RECOMMENDATIONS

- Attempts have been made to infer paleoclimate during (Middle Triassic to Early Jurassic) sedimentation of Adigrat sandstone. However, large-scale paleoclimatic reconstruction during entire Mesozoic sedimentation in Ethiopia and BNB in particular require another work, which emphasizes on the remaining part of this sedimentary succession.
- Even though paleoredox condition is suggested by redox sensitive elements such as Fe and U where lower most part was deposited in oxic environment relative to the upper one, an additional work is required to characterize the possible cause of redox change during the deposition of this sandstone. For instance, change in PH, organic matter, organism, saturation condition, ground water level; dissolved CO_2, fO_2 etc can possibly affect redox condition so that rigorous work is needed to set the possible one.
- Dating of each section (layer) for this sandstone unit is necessary for perfect chronostraticgraphic and lithostratigraphic paleoclimate reconstructions, as I have only inferred paleoclimate at large temporal scale.
- Geochemistry's of equivalent the Adigrat Sandstone found in all basins in or outside the province are required for comparisons.
- palaeocurrent measurements, are recommended to locate the source area from which this sediment transported.

7 REFERENCES

1 Anders, E. and Grevesse, N. (1989): 'Abundances of the elements: meteoritic and solar', Geochim. Cosmochim. Acta. 53, 197 - 214.

2 Amstrong-Altrin, J. S., Lee, Y. I., Verma, S. P., and Ramasamy, S. (2004): Geochemistry of sandstones from the Upper Miocene Kudankulam Formation, southern India: implication for provenance, weathering and tectonic setting. J. Sediment. Res. **74**, 285–297.

3 Asiedu, D.K., Kutu, J.M. Manu, J. and Hayford, E.K. (2009): Geochemistry and provenance of metagreywackes from the Konongo area, southwestern Ghana. Afr. J. of Sci. and Technol (AJST) **10**, 37 – 44.

4 Asiedu, D.K., Suzuki, S., Nogami, K. and Shibata, T. (2000): Geochemistry of Lower constraints on provenance and Cretaceous sediments, Inner Zone of Southwest Japan: tectonic environment. Geochem. J., **34**, 155-173.

5 Ayalew T, Bell K, Moore JM, Parrish RR. (1990): U-Pb and Rb-Sr geochronology of the Western Ethiopian Shield. Geol. Soci. of Am. Bull. 102, 1309–1316.

6 Bauluz, B., Mayayo, M. J., Fernandez-Nieto, C., and Gonzalez Lopez, J. M. (2000): Geochemistry of Precambrian and Paleozoic siliciclastic rocks from the Iberian Range (NE Spain): implications for source-area weathering, sorting, provenance, and tectonic setting. Chemical Geology, 168, 135-150.

7 Berner, R. A., Lasaga, A. C. and Garrels, R. M. (1983): The carbonate-silicate geochemical cycle and its effect on atmospheric carbon dioxide over the last 100 million years. Am. J. Sci. 205, 641–683.

8 Berner, R.A. (1991): A model for atmospheric CO_2 over Phanerozoic time. American J. of Sci. 291, 339–376.

9 Bhatia, M. R. and Crook, K. A. W. (1986): Trace element characteristics of graywacke and tectonic setting discrimination of sedimentary basins: Contributions to Mineral. and Petrol. **92**: 181–193.

10 Bhatia, M.R. (1983): Plate tectonics and geochemical composition of sandstones. J. Geol., **91**: 611-627.

11 Blatt, H., Middleton, G.V. and Murray, R. (1980): Origin of sedimentary rocks. Englewood Cliffs, NJ, Prentice-Hall, 782p.

12 Bodo, W., Peter S., Victor, A. V., Alexander, I. and Fernando, O. (2006): Provenance ages of Late Paleozoic sandstones (Santa Rosa Formation) from the Maya Block, SE Mexico. Implications on the tectonic evolution of western Pangea. Revista Mexicana de Ciencias Geológicas, **23**, 262-276

13 Bruce, C.H. (1984): Smectite dehydration- It Is relation to structural development and hydrocarbon accumulation in northern Gulf of Mexico Basin: Am. Assoc. Petroleum Geologists Bull. **68**, 673-683.

14 Cantrell, K. J. and Byrne, R. H. (1987): Rare earth element complexation by carbonate and oxalate ions. Geochim. Cosmochim. Acta **51**, 597–605.

15 Chamley, H. (1989): Clay Sedimentology. Springer-Verlag, Heidelberg, Germany, 623 p.

16 Chao L. and Yang, S. (2010): Is Chemical Index of Alteration (CIA) a reliable proxy for chemical weathering in global drainage basin? Am. J. of Sci. **310**: 111–127.

17 Chaudhuri, S. and Cullers, R. L. (1979): The distribution of rare earth elements in deeply buried Gulf coast sediments. Chem. Geol., **24**, 327–338.

18 Coffin, M. F. & Rabinowitz, P. D. (1988): Evolution of the conjugate East African Madagaskar and the Western Sumali Basin.-Spec.Pap.Geol.Soc.Am. 226, 78p.

19 Condie, K. C. (1993): Chemical composition and evolution of the upper continental crust: Contrasting results from surface samples and shales. Chem. Geol., 104, 1–37.

20 Condie, K. C., Lee, D. and Farmer, G. L. (2001): Tectonic setting and provenance of the Neoproterozoic Uinta Mountain and Big Vottonwood groups, northern Utah: constraints from geochemistry, Nd isotopes, and detrital modes. Sediment. Geol. 443–464.

21 Condie, K. C., Noll, P. D. Jr. and Conway, C.M. (1992): Geochemical and detrital mode evidence for two sources of Early Proterozoic sedimentary rocks from the Tonto Basin. Supergroup, central Arizona. Sediment. Geo.1, **77**, 51-76.

22 Conway, D. (1997): A water model balance of the upper Blue Nile in Ethiopia. J. of hydrol., 42(2), 22p.

23 Cox, R. and Lowe, D.R. (1995): A conceptual review of regional-scale controls on the composition of clastic sediment and the co-evolution of continental blocks and their sedimentary cover: J. of Sediment. Res. **65**, 1–21.

24 Cox, R., Lowe, D.R. and Cullers, R.L. (1995): The influence of sediment recycling and basement composition on evolution of mudrock chemistry in the southwestern United States: Geochim. et Cosmochim. Acta, **59**, 2919–2940.

25 Crook, K.A.W. (1974): Lithogenesis and geotectonic: the significance of compositional variation in flysch arenites (greywackes). Soc. Econ. Paleont. Mineral. Spec. Publ. **19**, 304–310.

26 Cullers, R. L. (1994): The controls on the major and trace element variation of shales, siltstones, and sandstones Pennsylvanian-Permian age from uplifted continental blocks in Colorado to platform sediments in Kansas, USA. Geochim. Cosmochim. Acta **58**: 4955–4972.

27 Cullers, R. L. (1995): The controls on the major- and trace-element evolution of shales, siltstones, and sandstones of Ordovician to Tertiary age in the Wet Mountains region, Colorado, USA. Chem. Geol. **123**, 107–131.

28 Cullers, R. L. (2000): The geochemistry of shales, siltstones and sandstones of Pennsylvian-Permian age, Colorado, USA: implications for provenance and metamorphic studies. Lithos **51**, 181–203.

29 Cullers, R. L. and Graf, J. (1983): Rare earth elements in igneous rocks of the continental crust: intermediate and silicic rocks, ore petrogenesis. Rare-Earth Geochemistry Elsevier, Amsterdam. (Henderson, P., ed.) 275–312.

30 Cullers, R. L., Berendsen, P. (1998): The provenance and chemical variation of sandstones associated with the Midcontinent Rift System, U.S.A. Eur. J. Mineral., **10**, 987-1002.

31 Cullers, R.L., Chaudhuri, S., Kilbane, N., Koch, R. (1979): Rare-earths in size fractions and sedimentary rocks of Pennsylvanian–Permian age from the mid-continent of the USA. Geochim. Cosmochim. Acta **43**, 1285–1301.

32 Cummins, W. A. (1962): The graywacke problem: Liverpool Manchester Geological Journal, v. 3, pt. 1, p. 51-72.

33 Dalai, T.K., Krishnaswami, S. and Sarin, M.M., (2002): Major ion chemistry in the headwaters of the Yamuna River System: Chemical weathering, its temperature dependance and CO2 consumption in the Himalaya. Geochim. et Cosmochim. Acta: 66, 3397-3416.

34 Dampare, S.B., Asiedu, D.K., Osae, S., Manu, J. and Banoeng-Yakubo, B. (2004): Geochemistry of lower proterozoic greywacke from the Birm diamondiferous field, Ghana. Afr. J. of Sci. and Technol. (AJST) **5**: 9-18.

35 Daniel Gamachu, (1977): Aspects of climate and water budget in Ethiopia. Technical Monograph, Addis Ababa University Press, Addis Ababa University.

36 David A. L. (1999): An evaluation of alternative chemical classifications of sandstones. Open-file reports 99-346 electronic editions. U. S. Geological Survey, Denver, Colo., 80225, p26.

37 Dawit Enkurie (2009): Stratigraphy and Facies architecture of Adigrat Sandstone, Blue Nile Basin-Ethiopia.Zbl. Geol. plaont. Teil I, 217-232.

38 Dercourt, J., Ricou, L. E. and Vrielynck, B. (1993): Atlas Tethys Paleoenvironmental Maps. Gauthier-Villars, Paris, 307 p.

39 Detian Y., Daizhao Ch., Qingchen W., and Jianguo W. (2010): Large-scale climatic fluctuations in the latest Ordovician on the Yangtze Block, South China. **38**: 599–602.

40 Dickinson, W.R. (1970): Interpreting detrital modes of graywacke and arkose. J. Sediment. Petrol., 40, 695–707.

41 Dobrzinski N., Bahlburg H. and Strauss H. (2004): Geochemical Climate Proxies Applied to the Neoproterozoic Glacial Succession on the Yangtze Platform, South China. By the American Geophysical Union, 10, p20.

42 Driscoll, CT. Scheafer DA, Molot LA and Dillon PJ (1989): Summary of North American data. In Malanchuk JL and Nilsson J(eds) the role of nitrogen in the acidification soils and surface water. Nordic council of Ministers, Kobenhavn, Denmark, 6-45

43 Duzgoren-Aydin, N. S., Aydin, A., and Malpas, J., 2002, Re-assessment of chemical weathering indices: Case study on pyroclastic rocks of Hong Kong: Engineering Geology, 63, 99–119, doi:10.1016/S0013- 7952(01)00073-4.

44 Eman S.A., Soliman, M. A., Sayed, A., and Jeuland, M. (2009): Impact Assessment of Future Climate Change for the Blue Nile Basin, Using a RCM Nested in a GCM. Nile Basin Water Engineering Scientific Magazine, Vol.2, 16. 10-34.

45 Fedo C.M., Nesbitt H.W. and Young G.M. (1995): Unrevealing the effect of k-metasomatism in sedimentary rocks and paleosols, with implication for paleoweathering condition and provenance. Geology 23: 921-924.

46 Fedo, C.M., Eriksson, K.A. and Krogstad, E. (1996): Geochemistry of shales from the Archean (~3.0 Ga) Buhwa Greenstone Belt, Zimbabwe: implications for provenance and source-area weathering. Geochim. Cosmochim. Acta 60, 1751–1763.

47 Fedo, C.M., Young, G.M. and Nesbitt, H.W. (1997a): Paleoclimatic control on the composition of the Paleoproterozoic Serpent Formation, Huronian Super group, Canada: a greenhouse to icehouse transition. Precambrian Res. 86, 201–223.

48 Fourcade, E., Azéma, J., Bassoulet, J.-P., Cecca, F., Dercourt, J., Enay, R. and Guirard, R. (1996): Paleogeography and Paleoenvironment of the Tethyan Realm during the Jurassic Breakup of Pangea. Plenum Press, New York and London. 8, 191–214

49 Frakes, L. A., Francis, J. E. and Syktus, J. I. (1992): Climate Modes of the Phanerozoic: The History of the Earth's Climate over the Past 600 Million Years. Cambridge, Cambridge University Press, 274 p.

50 Frankenberger WT, Benson S. (1994): Selenium in the Environment. New York: Marcel Dekker.

51 Gaillardet, J., Dupre, B., Louvat, P., and Alle`gre, C. J. (1999): Global silicate weathering and CO_2 consumption rates deduced from the chemistry of large rivers. Chem. Geol. 159:3–30.

52 Gani, N. DS., Abdelsalam, M. G., Gera, S. and Gani, M. R. (2008): Stratigraphic and structural evolution of the Blue Nile Basin, Northwestern Ethiopian Plateau: www.interscience.wiley.com DOI: 10.1002/gj.1127.

53 Gazzi, P., (1966): Le arenarie del flysch sopracretaceo delrAppennino modenese; correlazioni con il flysch di Monghidoro: Mineralogica e Petrografica Acta, 12, 69-97.

54 George W., Nyakairu, A. and Koeberl, C. (2001): Mineralogical and chemical composition and distribution of rare earth elements in clay-rich sediments from central Uganda. Geochem. J. 35, 13 – 28.

55 Getaneh Assefa (1975): Stratigraphy and sedimentology of the Mesozoic sequence in the upper Abay (Blue Nile) river Valley region, Ethiopia. PH.D. thesis University of Minnesota, USA.

56 Getaneh Assefa (1981): Gohatsion formation the A new Lias –Malm lithostratigaphic unit form Abay river basin, Ethiop.-Geoscie.J.2, 63-88.

57 Getaneh Assefa (1990): Stratigraphy and sedimentation of the type Gohatsion formation (Lias-Malm): Abay river basin, -Sinet,Ethiop.J.Sci. 3, 87-110.

58 Getaneh Assefa (1991): Lithostratigraphy and environment of deposition of the Late Jurassic-Early Cretaceous sequence of the central part of the Northwestern plateau, Ethiop.-NJb.geol.**182**, 255-284.

59 Gilamichael K. (2010): Facies analysis of Middle to Upper Jurassic carbonates in eastern and north – central Ethiopia. PhD thesis; Kyushu University, Japan.

60 Golonka, J. (2000): Cambrian-Neogene Plate Tectonic Maps. Wydawnictwa Uniwersytetu Jagiello_skiego, Kraków, 125p.

61 Golonka, J. (2002): Plate-tectonic maps of the Phanerozoic: Phanerozoic Reef Patterns. SEPM (Society for Sedimentary Geology), Tulsa. Special Pub. 72, 21–75.

62 Gromet, L. P., Dymek, R. F., Haskin, L. A. and Korotev, R. L. (1984): The 'North American Shale Composite': its compilation, major, and trace element characteristics. Geochim. Cosmochim. Acta **48**, 2469– 2482.

63 Hallam, A., Grose, J.A. and Ruffell, A.H. (1991): Paleoclimatic significance of changes in clay mineralogy across the Jurassic Cretaceous boundary in England and France. Palaeogeog. Palaeoclimat., Palaeoecol. 81, 173-187.

64 Haq, B. U., Hardenbol., J., & Vail, P. R. (1987): Chronology of the fluctuating sea level since the Triassic.-Sci. 234, 1156-1167.

65 Harnois, L. (1988): The CIW index: A new chemical index of weathering. Sediment. Geol. 55, 319–322.

66 Haskin, L. A., Wildeman, T.R., Frery; F.A., Kollins, K.A.; Keedy, C.R., and Haskin, M.A. (1966): Rare earths in the sediments. J. Geophys., Res., 71: 6091-6105.

67 Haskin, M.A., and Haskin, L.A., (1966): Rare earths in European shales-A redetermination: Sci. 154, 507-509.

68 Hayashi, K., Fujisawa, H., Holland, H., Ohmoto, H., (1997): Geochemistry of ~1.9 Ga sedimentary rocks from northeastern Labrador, Canada: Geochimica et Cosmochimica Acta, 61(19), 4115-4137.

69 Herron, M.M. (1988): Geochemical classification of terrigenous sands and shales from core or log data. J. Sediment. Petrol. 58, 820–829.

70 Hofmann.C., Courtillo, V., Feaured.G, Rochette, P., Gezaheny Yirgu, Ketefo, E., & R.pik (1997): Timing of the Ethiopian flood basalt event and implication for plume birth and global change. Nature, 389, 838-841

71 Hong, H., Li, Z., Xue, H.; Zhu, Y., Zhang, K. and Xiang, S. (2007): Oligocene clay mineralogy of the Linxia basin: evidence of paleoclimatic evolution subsequent to the initial-stage uplift of the Tibetan plateau clays and clay minerals, 55, 492–505.

72 Hren, M. T., Hilley, G. E., and Chamberlain, C. P., (2007): The Relationship between tectonic uplift and chemical weathering rates in the Washington Cascades: Field measurements and model predictions: Am. J. of Sci. 307, 1041–1063

73 Huckenholz, H. G., (1963): Mineral composition and texture in graywackes from the Harz Mountains (Germany) and in arkoses from the Auvergne (France): Journal of Sediment. Petrol. 33, no. 4, p. 914-918.

74 Jebsen,D.H and Athearn, M.J.(1961): Geologic plan and section of the left bank of the Blue Nile canyon near crossing of Addis Ababa-Debre Markos road .-U.S. Dept.Interior,Ethiopia's water Res.Dept.,Addis Ababa.

75 John, A. P. (2009): Geochemical Provenance of Clastic Sedimentary Rocks in the Western Cordillera: Utah, Colorado, Wyoming, and Oregon. Unpublished MSC thesis, Utah State University, Logan, Utah.

76 Johnsson MJ, Stallard RF. (1989): Physiographic Controls On Sediments Derived From Volcanic and Sedimentary Terrains on Barro Colorado Island, Panama. *Journal of Sedimentary Petrology* **59**: 768–781

77 Johnsson, M. J. (1993): The system controlling the composition of clastic sediments, Boulder, Colorado. Geologic. Soci. of Am. Special Paper 284, 1-19.

78 Kandasamy, S. and Chen-Tung, A. C. (2006): Moderate Chemical Weathering of Subtropical Taiwan: Constraints from Solid-Phase Geochemistry of Sediments and Sedimentary Rocks. J. of Geol. University of Chicago. 114, 101–116.

79 Kazmin, V. (1995): Explanation of the Geological map of Ethiopia.-Geol. Surv. Ethiop. Bull.1: 1-14.

80 Kim, U. and Kaluarachchi, J. J. (2008). Assessment of climate change impacts on water resources of the upper Blue Nile River Basin, Ethiopia. Water Resources Management (under review).

81 Lindgreen, H. and Surlyk, F. (2000): Upper Permian–Lower Cretaceous clay mineralogy of East Greenland: provenance, palaeoclimate and volcanicity. 35, 791-806.

82 McLennan, S. M. (1989): Rare earth elements in sedimentary rocks: influence of provenance and sedimentary processes. Mineralogical Society of America, Washington, D.C., Reviews in Mineralogy 21, 169–200.

83 McLennan, S. M. (2001): Relationships between the trace element composition of sedimentary rocks and upper continental crust. Geochem. Geophys., geosyst. (G3) 2, 1–24.

84 McLennan, S. M. and Taylor, S. R. (1982): Geochemical constraints on the growth of the continental crust. J. Geol. 90, 347–361.

85 McLennan, S. M., Taylor, S. R. and Kroner, A., (1983): Geochemical evolution of Archean shales from South Africa. I. The Swaziland and Pongola Supergroups. Precambrian Res., **22**, 93–124.

86 McLennan, S.M., Taylor, S.R., McCulloch, M.T., Maynard, J.B., (1990): Geochemical and Nd–Sr isotopic composition of deep-sea turbidites: Crustal evolution and plate tectonic associations. Geochim. et Cosmochim. Acta 54, 2015–2050.

87 McLennan, S.M.; Hemming, S.; McDaniel, D.K.; Hanson, G.N. (1993): Geochemical approaches to sedimentation, provenance, and tectonics. Processes Controlling the Composition of Clastic Sediment, Geological Society of America, Colorado. Geol. Soc. Am. Spl. **284,** 21–40.

88 Middleton, G. V. (1960): Chemical composition of sandstones: Geological Society of Am. Bull. 71, 1011-1026.

89 Miller, K.G. and Snyder, S.W. (1997): Proceedings of the Ocean Drilling Program, Scientific Results, 150, 59-64.

90 Millot, G. (1970): Geology of Clays. Springer-Verlag, Berlin, 2, 345-370.

91 Mohr, P.A. (1963): Occurrence of Karoo system sediment in Ethiopia.-Nature 199:1086-1086.

92 Moll, W.F., Jr. (2001): Baseline studies of the clay minerals society source clays: Geological origin. Clays and Clay Minerals, 49, 374–380.

93 Mongelli, G., Cullers, R., Dinelli, E. and Rottura, A. (1998): Elemental mobility during the weathering of exposed lower crust: the kinzigitic paragneisses from the Serre, Calabria, and Southern Italy. Terra Nova, 10, 190–195.

94 Mongelli, G., Salvatore, C., Francesco, P., Maurizio S. and Vincenzo, P. (2006): Sedimentary recycling, provenance and paleoweathering from chemistry and mineralogy of Mesozoic continental redbed mudrocks, Peloritani Mountains, southern Italy. Geochem. J. **40**, 197-209.

95 Nath, B. N., Kunzendorf, H. and Plueger, W. L. (2000): Influ ence of Provenance, weathering, and sedimentary processes on the elemental ratios of the fine-grained fraction

of the bedload sediments from the Vembanad Lake and the adjoining continental shelf, southwest coast of India. *J. Sediment. Res*. **70**, 1081–1094.

96 Nesbitt, H. W. and Young, G. M. (1982): Early Proterozoic climates and plate motions inferred from major element chemistry of lutites. Nature, **299**, 715–717.

97 Nesbitt, H. W., and Young, G. M. (1984): Prediction of some weathering trends of plutonic and volcanic rocks based on thermodynamics and kinetic considerations. Geochim. Cosmochim. Acta, **48**: 1523–1534.

98 Nesbitt, H. W., Fedo, C. M. and Young, G. M. (1997): Quartz and feldspar stability, steady and non-steadystate weathering, and petrogenesis of siliclastic sands and muds. J. Geol. **105**, 173–191.

99 Nesbitt, H. W., Markovics, G., and Price, R. C. (1980): Chemical processes affecting alkalies and alkaline earths during continental weathering. Geochim. Cosmochim. Acta, **44**: 1659–1666.

100 Nesbitt, H.W., and Young, G.M. (1989): Formation and diagenesis of weathering profiles. J.Geol. **97**: 129-147.

101 Okada, H., (1971): Classification of sandstones: analysis and proposals. J. Geol. 79, 509–525.

102 Peters, S. C., Lockwood, R. Williamson, C. E. and Saros J. E. (2008): Using elemental ratios of calcium and strontium to track calcium availability in the freshwater zooplankton Daphnia pulicaria, J. Geophys. Res., 113, G04023, doi:10.1029/2008JG000782

103 Pettijohn, F.H., Potter, P.E., and Siever, R., (1972). Sand and sandstone. Springer-Verlag, New York, 618p.

104 Price, J. R., and Velbel, M. A., (2003): Chemical weathering indices applied to weathering profiles developed on heterogeneous felsic metamorphic parent rocks: Chem. Geol. 202, 397–416, doi:10.1016/ j.chemgeo.2002.11.001.

105 Qi, L., Hu, J. and Gregoire, D. C. (2000): Determination of trace elements in granites by inductively coupled plasma mass spectrometry. Talanta **51**, 507–513.

106 Raymo, M. E., and Ruddiman, W. F., (1992): Tectonic forcing of late Cenozoic climate: Nature, 359, 117–122.

107 Rieu, R., Allen, P.A., Plötze, M., and Pettke, T., (2007): Climatic cycles during a Neoproterozoic "snowball" glacial epoch: Geol. 35, 299–302, doi: 10.1130/G23400A.1.

108 Rollison, H. R. (1993): Using Geochemical Data: Evaluation, Presentation, and Interpretation. John Wily & Sons, New York, 352 pp.

109 Roser, B. P., and Korsch, R. J. (1986): Determination of tectonic setting of sandstones mudstones suites using SiO_2 content and K_2O/Na_2O ratio: Journal of Geology, **94**: 635-650.

110 Roser, B.P. and Korsch, R.J. (1988): Provenance signatures of sandstone–mudstone suites determined using discriminant function analysis of major-element data: Chem. Geol. 67, 119–139.

111 Ruddiman W.F. (Ed.), 1997, Tectonic uplift and Climate Change, Plenum Publishing Corporation, New York, USA, p535.

112 Rudnick R. L. and Gao S. (2003): Composition of the continental crust. In *The Crust*, Elsevier, 3, 1-64.

113 Russo, A., Grtaneh Assefa & Balemwal Atnafu (1994): Sedimentary evolution of the Abay river (Blue Nile) Basin, Ethiopia.-N.Jb.Geol.**16**: 91-107.

114 Sageman, B.B. and Lyons, T.W. (2004): Geochemistry of fine grained sediments and sedimentary rocks **29:** 116-148.

115 Seifu Kebede, Travi, Y., Alemayeh, T. and Ayenew, T. (2005): Ground water recharge circulation and geochemical evolution in source region of the Blue Nile river, Ethiopia. Applied geochem., 20(9): 1658-1676.

116 Sengör, A. M. C. (1984) The Cimmeride orogenic system and the tectonics of Eurasia. Geological Society of America Special Paper **195**, 1–82.

117 Shaik A. R. (2005): The geochemistry of Mesoproterozoic clastic sedimentary rocks from the Rautgara Formation, Kumaun Lesser Himalaya: Implications for provenance, Mineralogical control, and weathering. Current Science, 88, p11

118 Sheldon, N.D., Tabor, N.J. (2009): Quantitative paleoenvironmental and paleoclimatic reconstruction using paleosols. Earth-Sci. Rev. 6, 349-357.

119 Shiloh O., Daniel K. Asiedu, Bruce B.-Y., Christian K. and Samuel B. (2005): Provenance and tectonic setting of Late Proterozoic Buem sandstones of southeastern

Ghana (2006): Evidence from geochemistry and detrital modes, J. of Afr. Earth Sci. **44**, 85–96.

120 Soleimani, B. (2009): Paleoclimate Reconstruction during Pabdeh, Gurpi, Kazhdumi and Gadvan Formations (Cretaceous-Tertiary) Based on Clay Mineral Distribution. International Journal of Civil and Environmental Engineering 1:2, 59-63.

121 Stallard, R.F., and Edmond, J.M., (1983): Geochemistry of the Amazon 2. The influence of geology and weathering environment on the dissolved load: Journal of Geophys.Res., 88, 9671–9688.

122 Taylor, S. R. and McLennan, S. M. (1985): The Continental Crust: Its Composition and Evolution. Blackwell, Oxford. J. of Afr. Earth Sci. 44, 85–96.

123 UNESCO (2004): National Water Development Report for Ethiopia. World Water Assessment Program Report. UN-WATER/ WWAP/2006/7,

124 Vorhies, S. (2006): Provenance and tectonic setting of the paleoprotorozoic Denham formation in east central Minnesota, 161-165.

125 White, W. M. (2003): Application of Thermodynamics to the Earth: Geochemistry book, Chapter 5, 113-154.

126 Wolela, A. M, (1997): Sedimentology, Diagenesis and Hydrocarbon Potential of Sandstone in the hydrocarbon perspective rift basins (Ethiopia, UK, USA).-PHD Thesis, The Queen's Univ., Belfast, 238p.

127 Wolela, A. M. (2008): Sedimentation of the Triassic-Jurassic Adigrat sandstone formation, Blue Nile (Abay) Basin, Ethiop. **52**: 30-42.

128 Worash Getaneh (2002): Geochemistry provenance and depositional tectonic setting of the Adagrat Sandstone northern Ethiopia. J. of Afr. Earth sci. **35**, 185-198.

129 Yang, S. Y., Jung, H.-S., and Li, C. X. (2004): Two unique weathering regimes in the Changjiang and Huanghe drainage basins: geochemical evidence from river sediments. Sediment. Geol. 164, 19–34.

130 Yanjing, C. and Yongchao, Z. (1997): Geochemical characteristics and evolution of REE in the early Precambrian sediments: Evidence from the southern margin of the North China craton. Episodes, **20**, 109–116.

131 Yoshihiro K., Mukunda R. P., Takeshi M., Rie F. and Harutaka, S. (2004): Variations of paleoclimate and paleoenvironment during the last 40 recorded in clay minerals in the Kathmandu Basin sediments Himalayan. J. of Sci. 2(4), 190-191.

132 Young, G.M., Nesbitt, and H.W., (1999): Paleoclimatology and provenance of the glaciogenic Gowganda Formation (Paleoproterozoic), Ontario, Canada: a chemostratigraphic approach. Geol. Soc. Amer. Bull. **111**, 264–274.

133 Young, S.W. (1976): Petrographic textures of detrital polycrystalline quartz as an aid to interpreting crystalline source rocks. J. Sediment. Petrol. **46**, 595–603.

134 Ziegler, P.A. (1989): Evolution of Laurassia-A tudy in Late Paleozoic plate tectonics.-Kulurwer Academic,Dorderecht, p102. ANNEXES

ANNEXES

Annex 1 List of abbreviations

ASSt- Adigrat sandstone

AVG- Average values of Adigrat sandstone from BNB

BNB-Blue Nile Basin

DF –Discriminant function

ES- European Shale

F-feldspar

HFSE-High field strength elements

LILE- Large Ion lithophile elements

L-lithic fragment

ASS –Adigrat sandstone

MB- Mekele Basin

NASC-North American Shale

PAAS- average post archean Austrian

Qm –monocrystalline quartz grain

Qn-non-undlatory quartz gran

Qp –polycrystalline quartz grain

Q-quartz

Qu-Undulatory Quartz grain

REE –Rare earth elements

UCC- Average upper continental crust

Annex 2 Ratios between selected trace and REE from BNB and MB

Samples	Blue Nile Basin						
ASS	**$(La/Yb)_{CN}$**	**$(La/Lu)_{CN}$**	**La/Cr**	**Th/Cr**	La/Th	**(Gd/yb)cn**	**Eu/Eu***
BA 2	12.78167	12.82643	0.740218	0.184107	4.020593	1.748763	0.613198
BA 4	11.5992	11.91706	0.876385	0.329877	3.124436	2.045767	0.527948
BS 2	9.302423	8.779126	0.923231	0.305569	3.021346	1.545974	0.550787
BS 3	10.75226	10.42259	2.03907	0.464884	4.386193	0.93342	0.412745
BS 5	11.73303	11.72032	0.41526	0.172194	2.411589	1.910472	0.508717
BS 8	10.73836	10.68686	0.284267	0.099304	2.862608	2.79086	0.656545
BS 10	26.82557	28.53112	0.724435	0.211663	3.422584	2.587747	0.631498
BS 13	6.606884	6.778024	6.532198	0.359363	18.17714	1.405255	0.622547
BS 15	**9.137728**	**9.018516**	0.111706	0.039286	2.843434	2.247566	0.616798
BS 17	**15.13621**	**15.32912**	0.450986	0.17712	2.546214	1.468232	0.517094
BS 20			0.193325	0.06171	3.132786	1.341627	0.384076
CCU	**10.9508**	**10.35364**					**0.**700376
PAAS	**9.396494**	**9.149731**					**0.**651118

Samples	Mekele Basin[♣]			
	(La/Yb)cn	La/Th	**(Gd/yb)cn**	**Eu/Eu***
W159	23.27586	3.590426	3.163697	0.55992
w160	18.925	3.80402	2.479654	0.604837
W161	26.43243	2.810345	2.948778	0.529552
W162	26.13095	2.239796	2.715812	0.468089
W163	17.025	3.546875	2.273016	0.504186
W164	19.44444	4.320988	2.632719	0.596675
W165	19.82353	3.858779	2.771378	0.574545
W166	29.22951	2.618209	3.780456	0.387972
W167	32.58333	2.572368	4.149977	0.400734
W168	29.60825	2.493056	3.536276	0.46898
W169	23.69643	4.009063	3.143847	0.540349
W170	23.94231	4.15	3.9897	0.516439
W171	28.88889	3.903904	3.618458	0.518869
W172	28	4.13253	3.474889	0.508675
W173	29.68	2.870406	3.53764	0.545829
W174	25.53226	2.938738	4.123869	0.47664
W175	28.96154	4.092391	3.6559	0.580945
W176	27.71642	5.785047	3.824342	0.549771
W177	20.875	4.210084	3.78836	0.469171
W178	248.6667	2.072222	30.65128	0.321823
W179	178.5	2.73913	22.9368	0.447233
W180	345.6	2.7	34.88047	0.37884

[♣] Agbe section, Data from Worash Getaneh (2002)

Annex 3 calculated Discriminant function data and values

Al2O3	coff	**Fe2O3**	value	coff	**MgO**	value	COFF	**Na2O**	value	COFF	**K2O**	value	coff	**TiO2**	value	Constt	**DF1**
%		**%**			**%**			**%**			**%**			**%**			
11.36	-12.54	5.25	-5.7909	7.329	1.07	0.69	2.03	0.06	0.011	35.40	1.89	5.879	30.64	0.61	1.642	-6.38	**-3.95**
20.99	-12.54	5.55	-3.317	7.329	0.72	0.25	2.03	0.07	0.0066	35.40	0.39	0.657	30.64	1.13	1.65	-6.38	**-7.13**
20.29	-12.54	8.03	-4.960	7.329	0.37	0.13	2.03	0.04	0.0036	35.40	0.34	0.589	30.64	1.19	1.792	-6.38	**-8.82**
8.03	-12.54	1.97	-3.079	7.329	2.17	1.98	2.03	0.42	0.1069	35.40	1.21	5.343	30.64	0.50	1.896	-6.38	**-0.13**
15.22	-12.54	1.12	-0.919	7.329	0.21	0.10	2.03	0.05	0.0072	35.40	1.02	2.363	30.64	0.72	1.443	-6.38	**-3.39**
2.11	-12.54	0.17	-1.016	7.329	0.05	0.16	2.03	0.03	0.0269	35.40	0.11	1.846	30.64	0.15	2.150	-6.38	**-3.21**
2.67	-12.54	0.57	-2.66	7.329	0.09	0.26	2.03	0.03	0.0228	35.40	0.42	5.564	30.64	0.17	1.903	-6.38	**-1.30**
0.94	-12.54	0.73	-9.773	7.329	0.07	0.55	2.03	0.01	0.0303	35.40	0.16	6.00	30.64	0.04	1.339	-6.38	**-8.24**
15.28	-12.54	7.09	-5.817	7.329	6.61	3.17	2.03	0.06	0.0077	35.40	0.35	0.81	30.64	1.23	2.474	-6.38	**-5.73**
3.56	-12.54	1.36	-4.78	7.329	3.56	7.33	2.03	0.03	0.017	35.40	0.56	5.517	30.64	0.32	2.735	-6.38	**4.43**
2.30	-12.54	0.27	-1.450	7.329	0.03	0.08	2.03	< L.D.	#VA	35.40	0.03	0.461	30.64	0.18	2.39	-6.38	
0.97	-12.54	0.19	-2.446	7.329	0.00	0.01	2.03	0.02	0.033	35.40	0.02	0.803	30.64	0.14	4.521	-6.38	**-3.46**
Al2O3**%**		**Fe2O3%**		value	**MgO%**			**Na2O%**			**K2O%**			**TiO2%**		constt	**DF2**
11.36	-10.87	5.25	-5.0235	30.88	1.07	2.904	-5.40	0.06	-0.029	11.11	1.89	1.845	56.5	0.61	3.02	-3.89	**-1.165**
20.99	-10.87	5.55	-2.8776	30.88	0.72	1.055	-5.40	0.07	-0.017	11.11	0.39	0.206	56.5	1.13	3.05	-3.89	**-2.47**
20.29	-10.87	8.03	-4.3028	30.88	0.37	0.563	-5.40	0.04	-0.009	11.11	0.34	0.18	56.5	1.19	3.305	-3.89	**-4.148**
8.03	-10.87	1.97	-2.6716	30.88	2.17	8.3512	-5.40	0.42	-0.284	11.11	1.21	1.67	56.5	0.50	3.49	-3.89	**6.679**
15.22	-10.8	1.12	-0.797	30.88	0.21	0.4199	-5.40	0.05	-0.019	11.11	1.02	0.74	56.5	0.72	2.66	-3.89	**-0.88**
2.11	-10.8	0.17	-0.88	30.88	0.05	0.688	-5.40	0.03	-0.071	11.11	0.11	0.57	56.5	0.15	3.96	-3.89	**0.388**
0.94	-10.87	0.73	-8.478	30.88	0.07	2.304	-5.40	0.01	-0.080	11.11	0.16	1.88	56.5	0.04	2.46	-3.89	**-5.791**
2.67	-10.87	0.57	-2.312	30.88	0.09	1.086	-5.40	0.03	-0.060	11.11	0.42	1.746	56.5	0.17	3.510	-3.89	**0.079**
15.28	-10.87	7.09	-5.046	30.88	6.61	13.36	-5.40	0.06	-0.020	11.11	0.35	0.255	56.5	1.23	4.562	-3.89	**9.226223**
3.56	-10.87	1.36	-4.1548	30.88	3.56	30.	-5.40	0.03	-0.047	11.11	0.56	1.731	56.5	0.32	5.045	-3.89	**29.56046**
2.30	-10.87	0.27	-1.2581	30.88	0.03	0.335	-5.40	< L.D.	#VALUE	11.11	0.03	0.144	56.5	0.18	4.421	-3.89	**#VALUE!**
0.97	-10.87	0.19	-2.1219	30.88	0.00	0.05	-5.40	0.02	-0.089	11.11	0.02	0.252	56.5	0.14	8.337	-3.89	**2.540102**

DF1 and DF2 are calculated according to the following equations.

Discriminant function 1=30.638 TiO_2/Al_2O_3 -12.541Fe_2O_3/Al_2O_3+ 7.329MgO/Al_2O_3+ 2.031Na_2O/Al_2O_3 + 35.40$_2K_2O/Al_2O_3$-6.382

Discriminant function 2=56.500 TiO_2/Al_2O_3-10879Fe_2O_3T/Al_2O_3+30.875MgO/Al_2O_3-5.404Na_2O/Al_2O_3 +11.112K2O/Al203-3.89

Annex 4: Linear correlation coefficients for selected element distribution in the analyzed samples

SiO_2 – Al_2O_3	-0.710
TiO_2 – Al_2O_3	0.922
TiO_2 -Zr	0.605
TiO_2- Fe_2O_3	0.834
TiO_2-SiO_2	-0.814
V – Al2O3	0.854
Al_2O_3 – La	0.298
Al_2O_3 – Yb	0.665
Al_2O_3 – total REE	0.408
Zr – La	0.244
TiO_2 – TOTAL REE	0.627
Zr- total REEE	0.292
Zr – Yb	0.553
P_2O_5 – total REE	0.292
Zr – Hf	0.988
Cr – V	0.197
Fe_2O_3-SiO_2	-0.773
Cr – Co	0.340
V – Co	0.435

Annex 5. Ranges of estimated modal compositions Of Petrographic constituents in the Adigrat sandstones

Sample No.	Modal composition															Textural morphology					
	Qrtz	Feldspar		L.F	Cement				Opaque	Mica		Heavy mineral		Others grain	Amph.						
		microcline	Plag.		Calc.	clay	Silica	Iron oxide		Musc.	Biotite.	Sphene	Zircon	Clay	Hnb.	G. size	G. shape	compaction	Sorting	Porosity	Matrix/grain
BS4	66	7	2	3	20		-	-	2	trace	-	trace	trace		trace	Fine-medium	Sub-rounded	well	moderate		grain
BS6	45	8	3	10	20	-	-	-	-	trace	-	-	-	-	-	Fine-coarse	Sub-rounded	strong	poor		grain
BS8	59.5	5	3	2	20	-	-	-	2	0.5		-	trace			Fine-coarse	sub rounded	well	Moderate-well		grain
BS9	82	10	1	-			x		1	4			trace	1	2	Medium-coarse	Sub-angular	well	well		grain
BS10	84	2	2	3		5	x		3			trace	trace	Trace	1	Fine to medium	Sub angular	well	moderate		grain

BS11	58	8	7	12	1		x	5	7	1		trace	trace		1	Fine-coarse	Rounded-sub rounded	Well	well		Grain
BS12	63.5	10	3	3	20				0.5			1	trace	2	2	Fine-medium	sub rounded	Well	Moderate-well		grain
BS13	30	3	-	-	35	30			7							Fine-medium	sub angular	Well	poor		matrix
BS14	55	5	3	15	20				2	trace		trace	trace		trace	Fine-coarse	sub angular	well	poor		grain
BS15	75	8	5	12			x					trace	trace		trace	Medium	Sub rounded	well	well		grain
BS16	69	5	4	8		7	x	1	15	1		trace	trace	1	1	Fine-medium	sub rounded	Well	moderate		grain
BS19	90	2	1	-	-		x	4	3	-		trace	trace	5	-	Fine-coarse	Rounded Sub-rounded	well	poor		grain
BS20	88	5	2	3			x		2	trace		trace	trace		trace	Fine-medium	Rounded Sub-rounded	well	well		grain

Annex 6 Calculated CIA, CIW and PIA

samples	Al2O3	CaO	Na2O	K2O	CIAR	CaO*	CIA	CIA*	CIW	PIA
BA 2	0.210582	0.011228	0.00137	0.02413	0.011228	0.00137	0.851489	0.886837	0.987154	0.992705
BA 4	0.389047	0.010155	0.001501	0.004987	0.010155	0.001501	0.958977	0.97988	0.992345	0.996108
BA 6	0.376019	0.002769	0.000783	0.004322	0.002769	0.000783	0.979487	0.984582	0.995853	0.997898
BS 2	0.148814	0.004716	0.0092	0.015499	0.004716	0.004716	0.834964	0.834964	0.914488	0.965837
BS 3	0.282024	0.00267	0.001174	0.012992	0.00267	0.001174	0.943665	0.94841	0.99174	0.995654
BS 5	0.039085	0.001073	0.000609	0.001407	0.001073	0.000609	0.926767	0.937074	0.96978	0.984095
BS 8	0.017383	0.229591	0.000304	0.002033	0.229591	0.000304	0.069725	0.868058	0.966154	0.98055
BS 10	0.049518	0.001223	0.000652	0.005371	0.001223	0.000652	0.872351	0.881201	0.974324	0.985436
BS 13	0.283173	0.036627	0.001261	0.004501	0.036627	0.001261	0.869796	0.975795	0.991169	0.995494
BS 15	0.065993	0.159955	0.000674	0.007097	0.159955	0.000674	0.282361	0.886543	0.979977	0.988682
BS 17	0.042624	0.000848	0.0001	0.000384	0.000848	0.000848	0.969699	0.969699	0.978236	0.980313
BS 20	0.017958	0.000574	0.000348	0.000281	0.000574	0.000281	0.937208	0.951737	0.966143	0.984334
Avg.	0.160185	0.038452	0.001498	0.006917	0.038452	0.001181	0.791374	0.925398	0.983549	0.992352

Where CIA and CIA* are Uncorrected and corrected chemical index of alteration respectively and CaO* represents corrected CaO